THE UNIVERSITY OF QUEENSLAND

AUSTRALIA

Microbial electrosynthesis from carbon dioxide: performance enhancement and elucidation of mechanisms

Ludovic Jourdin

Bachelor of Chemistry

Master of Chemical Engineering

National Graduate School of Chemistry, University of Montpellier, France

A thesis submitted for the degree of Doctor of Philosophy at

The University of Queensland in 2015

School of Chemical Engineering

Advanced Water Management Centre

Abstract

Microbial electrosynthesis (MES) of organics from carbon dioxide has been recently put forward as an attractive technology for the renewable production of valuable multi-carbon reduced end-products and as a promising CO_2 transformation strategy. MES is a biocathode-driven process that relies on the conversion of electrical energy into high energy-density chemicals. However, MES remains a nascent concept and there is still limited knowledge on many aspects.

It is still unclear whether autotrophic microbial biocathode biofilms are able to self-regenerate under purely cathodic conditions without any external electron or organic carbon sources. Here we report on the successful development and long-term operation of an autotrophic biocathode whereby an electroactive biofilm was able to grow and sustain itself with CO_2 and the cathode as sole carbon and electron source, respectively, with H_2 as sole product. From a small inoculum of 15 mg_{COD} (in 250 mL), the bioelectrochemical system operating at -0.5 V vs. SHE enabled an estimated biofilm growth of 300 mg as COD over a period of 276 days.

A critical aspect is that reported performances of bioelectrosynthesis of organics are still insufficient for scaling MES to practical applications. Selective microbial consortia and biocathode material development are of paramount importance towards performance enhancement. A novel biocompatible, highly conductive three-dimensional cathode was manufactured by direct growth of flexible multiwalled carbon nanotubes on reticulated vitreous carbon (NanoWeb-RVC) by chemical vapour deposition (CVD). The results demonstrated that: (i) the high surface area to volume ratio of the macroporous RVC maximizes the available biofilm area while ensuring effective mass transfer to and from the biofilm, and (ii) the nanostructure enhances the bacteria-electrode interaction, biofilm development, microbial extracellular electron transfer, and acetate bioproduction rate.

However, for scale-up beyond certain sizes, there are some limitations with the CVD technique. We harnessed the throwing power of electrophoretic deposition technique (EPD), suitable for industrial scale production, to form multi-walled CNT coatings onto RVC to generate a new hierarchical porous structure, hereafter called EPD-3D. A very effective mixed microbial consortium was successfully enriched and transferred to EPD-3D reactors and demonstrated drastic performance enhancement reaching biocathode current density of -102 ± 1 A m^{-2} and acetate production rate of 685 ± 30 g m^{-2} day^{-1}.

An in-depth understanding on how electrons flow from the cathode to the terminal electron acceptor is still missing but crucial (e.g. for improved reactor design). High rates of acetate production by microbial electrosynthesis was shown to occur via biologically-induced hydrogen, likely through the biological synthesis of metal copper particles, with 99 ± 1% electron recovery into acetate. The acetate-producing bacteria showed the remarkable ability to consume a high H_2 flux (ca. 1.15 m^3_{H2} m^{-2} day^{-1}), without H_2 able to escape from the biofilm.

Finally, further investigation is needed towards reactor sizing and operating conditions optimization to further enhance the performance and applicability of this technology. The results demonstrated that (i) higher proton availability significantly increases the acetate production rate to 790 g m^{-2} day^{-1}, at the optimal pH of 5.2 and -0.85 V vs. SHE, which will likely suppress methanogenic activity without inhibitor addition; and (ii) that potentials as low as -1.1 V vs. SHE still achieved 99% of electron recovery in the form of acetate at a current density of around -200 A m^{-2}. These current densities are leading to an exceptional acetate production rates of up to 1330 g m^{-2} day^{-1} (133 kg m^{-3} day^{-1}) at pH 6.7. To achieve such high productivities in practice, the 3D macroporous electrode materials need to also be optimised to achieve a good balance between total surface area per volume available for biofilm formation and effective mass transfer between the bulk liquid and the electrode/biofilm surface. Using highly open, macroporous reticulated vitreous carbon electrodes with pore sizes of about 0.6 mm diameter was found to be optimal in this respect.

High product specificity and production rate are regarded as key parameters for large-scale applicability of a technology. The current density and acetate production rate reached in this study are at least an order of magnitude higher than obtained by any other group, to date. The high product specificity and product titer (11 g L^{-1}) reported are remarkable for mixed microbial cultures, which would make the product's downstream processing easier and the technology more attractive. Moreover, at zero wastage of H_2 gas, it allows superior production rates and lesser technical bottlenecks over technologies that rely on mass transfer of H_2 to microorganisms suspended in aqueous solution. Furthermore, we successfully demonstrated the use of a synthetic biogas gas mixture as cheap and readily available carbon dioxide source, yielding similarly high MES performance, which would allow this process to be used effectively for both biogas quality improvement and conversion of the available CO_2 to acetate. These findings take microbial electrosynthesis a considerable step forward towards practical implementation.

Declaration by author

This thesis is composed of my original work, and contains no material previously published or written by another person except where due reference has been made in the text. I have clearly stated the contribution by others to jointly-authored works that I have included in my thesis.

I have clearly stated the contribution of others to my thesis as a whole, including statistical assistance, survey design, data analysis, significant technical procedures, professional editorial advice, and any other original research work used or reported in my thesis. The content of my thesis is the result of work I have carried out since the commencement of my research higher degree candidature and does not include a substantial part of work that has been submitted to qualify for the award of any other degree or diploma in any university or other tertiary institution. I have clearly stated which parts of my thesis, if any, have been submitted to qualify for another award.

I acknowledge that an electronic copy of my thesis must be lodged with the University Library and, subject to the policy and procedures of The University of Queensland, the thesis be made available for research and study in accordance with the Copyright Act 1968 unless a period of embargo has been approved by the Dean of the Graduate School.

I acknowledge that copyright of all material contained in my thesis resides with the copyright holder(s) of that material. Where appropriate I have obtained copyright permission from the copyright holder to reproduce material in this thesis.

Publications during candidature

Peer-reviewed papers:

- **Ludovic Jourdin**, Stefano Freguia, Bogdan C. Donose, Jun Chen, Gordon G. Wallace, Jurg Keller, and Victoria Flexer. A novel carbon nanotube modified scaffold as an efficient biocathode material for improved microbial electrosynthesis. *J. Mater. Chem. A*, 2014, 2, 13093-13102.

- **Ludovic Jourdin**, Stefano Freguia, Bogdan C. Donose, and Jurg Keller. Autotrophic hydrogen-producing biofilm growth sustained by a cathode as the sole electron and energy source. *Bioelectrochemistry*, 2015, 102, 56-63.

- **Ludovic Jourdin,** Timothy Grieger, Juliette Monetti, Victoria Flexer, Stefano Freguia, Jun Chen, Mark Romano, Gordon G. Wallace, and Jurg Keller. Exceptional acetic acid production rate obtained by microbial electrosynthesis from carbon dioxide. *Energy and Environmental Science* (under revision), 2015.

Conference presentations:

- **Ludovic Jourdin**, Stefano Freguia, and Jurg Keller. Autotrophic biofilm growth sustained by a cathode as the sole electron source. *4th International Microbial Fuel Cell conference*, 1 to 4 September 2013, Cairns (Australia). *(platform presentation)*

- **Ludovic Jourdin**, Victoria Flexer, Jun Chen, Gordon G. Wallace, Stefano Freguia, and Jurg Keller. A novel carbon nanotube modified scaffold creates an efficient biocathode material for improved microbial electrosynthesis. *65th Annual Meeting of the International Society of Electrochemistry*, 31 August to 5 September 2014, Lausanne, Switzerland. *(platform presentation)*

- **Ludovic Jourdin**, Victoria Flexer, Jun Chen, Gordon G. Wallace, Stefano Freguia, and Jurg Keller. A novel carbon nanotube modified scaffold creates an efficient biocathode material for improved microbial electrosynthesis. *2nd European International Society for Microbial Electrochemistry and Technology Meeting*, 3 to 5 September 2014, Alcala, Spain. *(platform presentation)*

Publications included in this thesis

- **Ludovic Jourdin,** Stefano Freguia, Bogdan C. Donose, Jun Chen, Gordon G. Wallace, Jurg Keller, and Victoria Flexer. A novel carbon nanotube modified scaffold as an efficient biocathode material for improved microbial electrosynthesis. *J. Mater. Chem. A*, 2014, 2, 13093-13102.

This paper has been modified and incorporated as Chapter 6.

Contributor	Statement of contribution
Ludovic Jourdin (Candidate)	Designed experiments (60%) Conducted experiments (100%) Wrote the paper (100%)
Stefano Freguia	Designed experiments (15%) Critically reviewed the paper (15%)
Bogdan C. Donose	Performed Scanning Electron Microscopy analysis of the biofilm, Figure 3 and 4 of the published paper (100%) Critically reviewed the paper (2.5%)
Jun Chen	Provided the electrode material (NanoWeb-RVC) (50%) Performed Scanning Electron Microscopy analysis of the unmodified abiotic electrode material, Figure 3 and 4 of the published paper (100%) Critically reviewed the paper (2.5%)
Gordon G. Wallace	Provided the electrode material (NanoWeb-RVC) (50%) Critically reviewed the paper (2.5%)
Jurg Keller	Designed experiments (15%) Critically reviewed the paper (15%)
Victoria Flexer	Designed experiments (10%) Critically reviewed the paper (62.5%)

- **Ludovic Jourdin,** Stefano Freguia, Bogdan C. Donose, and Jurg Keller. Autotrophic hydrogen-producing biofilm growth sustained by a cathode as the sole electron and energy source. *Bioelectrochemistry*, 2015, 102, 56-63.

This paper has been modified and incorporated as Chapter 5.

Contributor	Statement of contribution
Ludovic Jourdin (Candidate)	Designed experiments (60%) Conducted experiments (100%) Wrote the paper (100%)
Stefano Freguia	Designed experiments (20%) Critically reviewed the paper (35%)
Bogdan C. Donose	Performed Scanning Electron Microscopy analysis, Figure 3 of the published paper (100%) Critically reviewed the paper (5%)
Jurg Keller	Designed experiments (20%) Critically reviewed the paper (60%)

- **Ludovic Jourdin,** Timothy Grieger, Juliette Monetti, Victoria Flexer, Stefano Freguia, Jun Chen, Mark Romano, Gordon G. Wallace, and Jurg Keller. Exceptional acetic acid production rate obtained by microbial electrosynthesis from carbon dioxide. Submitted to *Energy & Environmental Science*, 2015.

This paper has been modified and incorporated as Chapter 7.

Contributor	Statement of contribution
Ludovic Jourdin (Candidate)	Designed experiments (60%) Conducted experiments (34%) Wrote the paper (100%)
Timothy Grieger	Conducted experiments (33%)
Juliette Monetti	Conducted experiments (33%)
Victoria Flexer	Designed experiments (15%) Critically reviewed the paper (62.5%)
Stefano Freguia	Designed experiments (10%) Critically reviewed the paper (15%)
Jun Chen	Provided the electrode material (NanoWeb-RVC) (50%) Critically reviewed the paper (2.5%)
Mark Romano	Performed Scanning Electron Microscopy analysis of the unmodified abiotic electrode material, Figure 1 of the submitted paper (100%) Critically reviewed the paper (2.5%)
Gordon G. Wallace	Provided the electrode material (NanoWeb-RVC) (50%) Critically reviewed the paper (2.5%)
Jurg Keller	Designed experiments (15%) Critically reviewed the paper (15%)

Contributions by others to the thesis

This thesis contains the reporting of some important contributions made by another researcher, Dr Yang Lu. Dr Yang Lu, of the University of Queensland, performed fluorescence in situ hybridization analyses (FISH) and microbial community analyses, which are presented in Chapter 5 of this thesis.

Statement of parts of the thesis submitted to qualify for the award of another degree

None.

Acknowledgements

First of all, I would like to express my sincere gratitude to my advisors Prof Jurg Keller and Dr Stefano Freguia. Special thanks to Jurg for believing in me and giving me the great opportunity to join the centre and embark on this PhD journey. I would like to thank both of them for their priceless and untiring support that has helped me overcome the inevitable difficulties that I have encountered during the course of my PhD. Their critical analysis of my research plans, assistance during the writing and their constant inspiration and encouragement helped me achieve my goals. I have greatly benefited from their expertise and knowledge in a wide range of fields such as (bio)-electrochemistry, environmental (bio)-technology and chemical engineering.

Secondly, I would like to give a special thanks to my unofficial advisor and friend Dr Victoria Flexer who greatly and positively influenced my PhD. I am very grateful for the collaboration we started which really shaped my PhD, and for her tremendous efforts and critical evaluation of my papers that helped achieve higher standards in my publications.

Since this thesis is an interdisciplinary study, the job could not be done without collaborations. I am very grateful to Dr Bogdan Donose for his help and expertise with microscopy and surface chemistry analysis and Dr. Yang (Kenn) Lu for his help with microbial community and FISH analysis. I would also like to thank Assoc Prof Jun Chen and Prof Gordon Wallace for the electrode material preparation and physical characterisation and for transferring their knowledge. I am also grateful to Timothy Grieger and Juliette Monetti who helped me run my reactors, in the frame of their occupational training program, in a critical time of my PhD which allowed me to focus on other important tasks such as writing papers. I am very thankful to Dr Beatrice Keller-Lehmann and Nathan Clayton for their scientific and technical support and the administrative staff for all the support during my PhD.

I would like to acknowledge the sources of funding for my PhD. In particular, the International Postgraduate Research Scholarship from the Australian government that paid for my tuition fees and the AWMC, AWMC Top-up and CEMES that paid for my living expenses, insurance, travel cost, and supported the scientific work during my PhD.

I would like to thank all the people I have worked with or simply shared inspiring scientific discussions over the last years who made my time at the AWMC very enjoyable. There are too many people to thank so I will not mention everybody but in particular: Tim Huelsen, Ilje Pikaar,

Frauke Kracke, Nils Averesch, Elisa Sander, Bernardino Virdis, Pablo Ledezma, Igor Vassilev, Stephen Andersen, Joachim Desloover, Kun Guo, Ark Du, Elena Meija Likosova, Christy Grobbler, Mi Zhou, Guillermo Pozo Zamora, and Ampon Chumpia.

A big and very special thanks goes to all my friends that made my Australian life amazing and unforgettable; they will recognise themselves easily. Finally, I would like to thank my parents Johnny and Martine, who from France have incessantly provided me with their care and support. Thank you for believing in me throughout my studies.

Keywords

Bioelectrochemical systems, microbial electrosynthesis, cathode, carbon dioxide fixation, acetate bioproduction, enriched biofilm growth, multiwalled carbon nanotubes, three-dimensional hierarchical electrode, biohydrogen, extracellular electron transfer

Australian and New Zealand Standard Research Classifications (ANZSRC)

ANZSRC code: 090703 Environmental Technologies, 50%

ANZSRC code: 100302 Bioprocessing, Bioproduction and Bioproducts, 25%

ANZSRC code: 090401 Carbon Capture Engineering (excl. Sequestration), 25%

Fields of Research (FoR) Classification

FoR code: 0907 Environmental Engineering, 50%

FoR code: 1003 Industrial Biotechnology, 25%

FoR code: 0904 Chemical Engineering, 25%

Table of Contents

List of Figures

List of Tables

List of Abbreviations

Ag/AgCl	Silver/silver chloride
ATP	Adenosine Triphosphate
BE	Biphasic Esterification
BESs	Bioelectrochemical Systems
CE	Counter Electrode
CEM	Cation Exchange Membrane
CNTs	Carbon Nanotubes
CO_2	Carbon Dioxide
COD	Chemical Oxygen Demand
Cu	Copper
CV	Cyclic Voltammetry
CVD	Chemical Vapour Deposition
DET	Direct Electron Transfer
DO	Dissolved Oxygen
EAM	Electrochemically Active Microorganisms
E	Potential (V)
EDS	Energy Dispersive X-ray Spectroscopy
EET	Extracellular Electron Transfer
EPD	Electrophoretic Deposition
EPS	Extracellular Polymeric Substance
ET	Electron Transfer
FIA	Flow Injection Analysis
FISH	Fluorescence In-Situ Hybridization

GC	Gas Chromatography
H_2	Hydrogen
HPLC	High-Performance Liquid Chromatography
HRT	Hydraulic Retention Time
I	Current
ISISA	Ice-segregation induced self-assembly
LSV	Linear Sweep Voltammetry
ME	Membrane Electrolysis
MEC	Microbial Electrolysis Cell
MES	Microbial Electrosynthesis
MET	Mediated Electron Transfer
MFCs	Microbial Fuel Cells
mfc	Mass Flow Controller
MS	Mass Spectrometer
MWCNT	Multiwalled Carbon Nanotube
NADH	Reduced form of nicotinamide adenine dinucleotide
NR	Neutral Red
RE	Reference Electrode
RVC	Reticulated Vitreous Carbon
SEM	Scanning Electron Microscopy
SHE	Standard Hydrogen Electrode
TOGA	Titration and Off Gas Analysis
VFAs	Volatile Fatty Acids
WE	Working Electrode

1 Introduction

Bioelectrochemical systems (BESs) are emerging bioreactor technologies that have substantially expanded their scope over the last few years, from electricity generation (microbial fuel cells, MFCs) to an array of more complex processes, such as bioremediation and chemical production [1, 2]. Global concerns over CO_2 accumulation in the atmosphere, fossil resource depletion and our society's high energy and commodity chemicals demands are creating a rapidly growing demand for new, sustainable forms of fuels and chemicals. Creating novel approaches for the direct transformation of carbon dioxide into valuable end-products is very attractive [3]. Consequently, many CO_2-based production processes have been and are being investigated and developed, as recently reviewed by Mikkelsen at al. [4]. Microbial electrosynthesis (MES) is a novel and promising strategy that relies on electroactive microorganisms that are able to use electrons derived from solid-state electrodes to catalyse the reduction of carbon dioxide to generate extracellular multi-carbon organic molecules as valuable reduced end-products [2, 5, 6]. Therefore, MES allows converting electrical energy into stable, high energy-density liquid or solid products that can be easily stored, distributed and consumed on demand. In this perspective, MES might also be considered as an interesting option to capture and increase the value of the electrical energy produced from intermittent renewable sources such as solar and wind [7]. Moreover, on top of producing valuable chemicals by recycling carbon dioxide as the key carbon source, CO_2-based bioproduction presents several advantages such as independence of arable land and precious freshwater resources, limited toxicity to microorganisms, mitigation of the ever-increasing CO_2 emissions, and nearly unlimited substrate availability.

Microbial electrosynthesis remains a nascent concept with only few studies that have demonstrated the process in laboratory scale using either pure cultures [8-11] or mixed microbial consortia [12-19]. Use of mixed microbial consortia is attractive as they can be readily generated in the required quantities, are more tolerant to environmental fluctuations [20] and thus far have showed higher MES production rates than pure cultures over long term operation [14-16]. To date, mainly acetate has been sustainably produced by electroactive microorganisms using electricity and carbon dioxide as sole energy and carbon sources. Recently, however, a study has also shown the simultaneous conversion of CO_2 into a mixture of products comprising acetate, butyrate, ethanol, and butanol using mixed microbial cultures [13]. The higher market value of some of those organics (e.g. butanol) compared to acetate makes their production from CO_2 very interesting. Nevertheless,

high product specificity and production rates are regarded as key parameters that could enable large-scale applicability of such a technology.

Moreover, acetate has many potentially viable applications as a useful end-product by itself as well as a platform for further chemical transformations. Hydrogen has also been reported to be produced in most MES from CO_2 studies, concomitantly to organics. Hydrogen has been speculated to be an electron mediator from the cathode to the acetate-producing microorganisms. However, there is a clear lack of experimental evidence towards this assumption. Regardless, the efficient and sustainable production of hydrogen has also gained recognition in the last few years as a potential strategy for green energy production from renewable resources, water and biomass [21-23].

Reported performances of bioelectrosynthesis processes are still insufficient for scaling MES to practical applications. While maintaining low cost, optimizing MES relies on the enhancement of bacterial attachment, biofilm development, electron transfer rate at the cathode surface (microbes-electrode interaction), and production rate. Biocathode materials [24], selective microbial consortia and efficient reactor designs are key elements to be optimized towards that objective. A more in-depth understanding of the process and particularly on how electrons flow from the cathode to the terminal electron acceptor is also critical (e.g. for improved reactor design) and has not been investigated to date. It is also not clear from the reported results whether biocathode biofilms are able to self-regenerate under purely cathodic conditions without any organic carbon sources. The challenge is to generate a self-maintaining biocathode, with living microorganisms which are able to survive, conserve energy and grow under autotrophic conditions using carbon dioxide and electrode as sole carbon and electron source, respectively. Moreover, reactor sizing, operating conditions optimization and the need for cheap and easily usable carbon dioxide source remains to be investigated.

Firstly, this PhD aims to demonstrate that autotrophic electroactive biofilm growth can be sustained using a biocathode as the sole electron source. Secondly, this work demonstrates novel approaches leading to previously un-achieved acetate production rates from CO_2 based on the combination of well acclimatized and enriched microbial cultures and of newly synthesized three-dimensional hierarchical biocathode electrode materials. Thirdly, this PhD study aims at elucidating how the electrons flow from the cathode to the terminal electron acceptor, CO_2. Finally, reactor sizing and operational parameters are investigated towards performance enhancement for realistic practical implementation of the MES technology. MES to acetate was also investigated as a potential biogas cleaning technology when biogas was used as sole, cheap and readily available carbon dioxide source. This work should favour realistic discussions within the research community

on strategies to adopt for microbial electrosynthesis scale-up to practical implementations. Potential applications are discussed in the last chapter of this thesis, including economic feasibility study of several scenarios, based on the results obtained at lab-scale in this PhD work.

2 Literature Review

2.1. Bioelectrochemical systems – an overview

2.1.1. General principles of bioelectrochemical systems

BESs consist of two different solid-state electrodes separated with a membrane or not. One electrode, the anode, carries out the oxidation of a supplied electron donor (e.g. acetate), thus producing electrons that are transferred via an external circuit to the other electrode, the cathode, which uses them to undertake the reduction of a final electron acceptor (e.g. oxygen). At least one of these two half-reactions is biocatalysed, either by whole microbial cells, enzymes or enzyme arrays and organelles [25]. From this basic principle, a plethora of choices can be made regarding the nature of the catalysts (chemical vs. microbial), the membrane, the source of the reducing power, as summarized in Figure 1, as well as the electron donors and acceptors supplied.

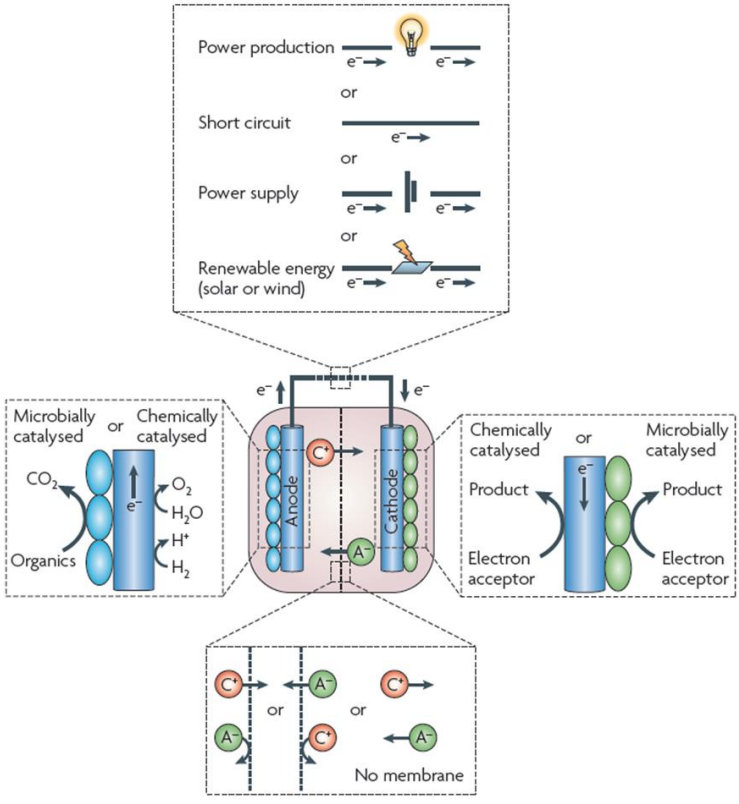

Figure 1 Bioelectrochemical system technology versatility scheme displaying the many possible choices regarding the nature of the catalysts (chemical vs. microbial), the membrane and the source of the reducing power, taken from [2].

The major expansion of the field of microbial electrochemistry was triggered by the development of microbial fuel cells (MFCs), which aim to produce electricity using electrochemically active microorganisms capable of growing on an anode electrode surface, while

using the electrode as an electron acceptor for the oxidation of organic matter. In such systems, the electrical power is harvested from the anodic reaction and the cathodic reaction occurs spontaneously (e.g. oxygen reduction). If power is added to the system the BES is said to be in microbial electrolysis cell (MEC) mode. Extra electrical power is provided to increase the kinetics of the reactions and/or drive thermodynamically unfavourable cathodic reactions (e.g. H_2 evolution reaction). Bioremediation [26-29], production of valuable chemicals [8, 9], CO_2 sequestration / fixation [30], biosensors [31-33] and water desalination [34, 35] are some examples of the versatility of BES applications (see section 2.1.3).

Microbial electrocatalysis exploits the whole catalytic machinery of living cells, which is able to perform complex or multistep transformations, whereas chemical catalysts may only perform simple reactions like one-step reduction reactions [36]. Moreover, as summarized by Rabaey and Rozendal (2010) [2], the use of whole microorganisms presents some other advantages, they are able to adapt their concentrations to the required conversion activity as well as to self-regenerate and they are flexible in substrate use. They have also been shown to decrease the overpotentials at both anodes [37] and cathodes [38], hence improving the overall performance of a BES. They are inexpensive to grow and self-sustaining and long-lived if they gain enough energy from the reaction they catalyse. However, such microorganisms cannot be considered as true catalysts as they consume part of the electrons available in the substrate or electron donor for growth and maintenance.

2.1.2. Electron transfer in BESs

In BES systems, the microbes can be present as planktonic cells and/or biofilms. Electroactive biofilms can contain both electrochemically active microorganisms (EAMs) and electrochemically inactive microorganisms. The latter may be very useful and serve functions such as the breakdown of complex substrates. EAMs' role is to enable efficient electron transfer from or toward solid state electrodes in order to maximize current densities, energy efficiencies and performance in these systems. Extracellular electron transfer (EET) has been defined as the process by which microorganisms transport electrons from or towards an insoluble electron donor or acceptor, respectively [2].

2.1.2.1. Anode electron transfer

The ability of electroactive microorganisms to directly provide electrons to electrodes has been known for over a century [39]. However, anode processes and anodic extracellular electron

transfer mechanisms have been mostly and extensively investigated in the last decade. Bond et al. (2002; 2003) [40, 41] first discovered that non-fermentable substrates, such as acetate, could also be oxidized to carbon dioxide with direct transfer of the electrons produced to the electrode. This highlighted the fact that organic matter conversions to electric current are not only due to fermentation reactions but could also be respiratory processes. This finding was an important breakthrough which stimulated the subsequent intensive research on understanding how electrons are drawn from microorganisms.

Two different EET pathways have been identified [42]. The first one involves the direct contact of electron transfer chain components of the microbes with the electrode surface and is referred to as direct electron transfer (DET). The second mechanism is called mediated electron transfer and involves electron shuttles serving as electron carriers thanks to their ability to reversibly be oxidized and reduced between the microbes and the electrodes. Mediators can either be exogenous or endogenous.

Two pathways for each of them have been proposed and are illustrated in Figure 2. The first DET occurs through membrane bound electron transport proteins such as cytochromes (Figure 2a) while the other one transports electrons from the microbes to the electrode surface along conductive pili (so-called nanowires) that are connected to the membrane bound electron transport compounds as shown in Figure 2b. The difference between both MET mechanisms is based on the location where the oxidized mediators are reduced; it could either occur in the cytoplasm (Figure 2c) or on outer cell membrane compounds such as cytochromes (Figure 2c).

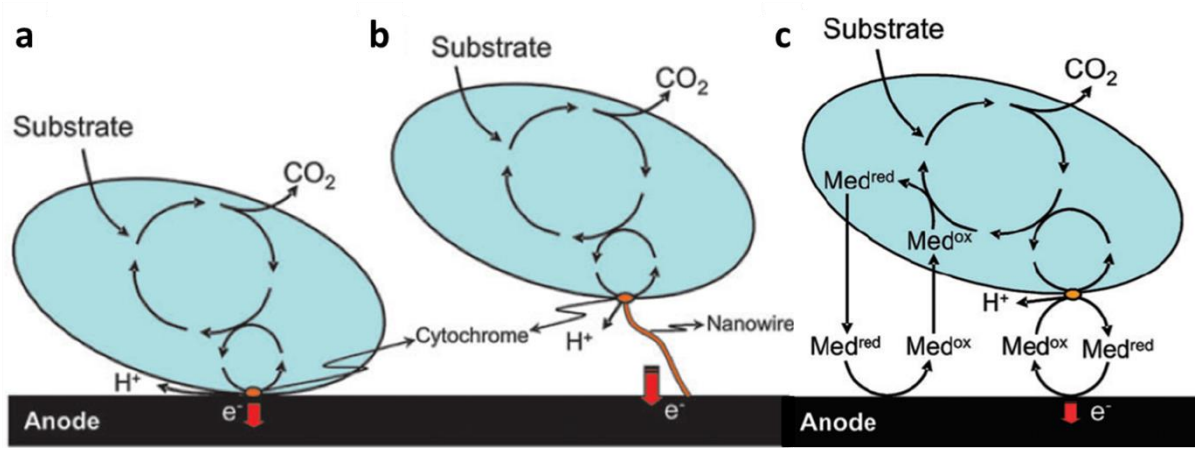

Figure 2 Mechanisms for electron transfer from microorganisms to solid-state electrodes (modified from [42]). a) Direct electron transfer through membrane bound electron transport proteins, b) direct electron transfer via conductive pili and c) mediated electron transfers occurring in the cytoplasm or on outer cell membrane compounds. Med_{red} and Med_{ox} for reduced and oxidized mediator, respectively.

Through these respiration processes and electron transfers to electrode serving as the sole electron acceptors, the ability of microorganisms to conserve energy makes it feasible for electrode-reducing populations to be self-sustaining [43]. Borole et al. (2011) [44] published a complete review on electroactive biofilms mostly focusing on anodic biofilms, though the current status of cathodic biofilms is also briefly reviewed.

2.1.2.2. Cathode electron transfer

BESs with microbial biocathodes depend upon the ability of some microorganisms to receive electrons from a solid electrode as an electron donor for the reduction of a terminal electron acceptor. Such organisms have been referred to as electrotrophs [43]. As mentioned previously, researchers have mainly focused on gathering abundant mechanistic information on the anode processes while information on the reverse process, i.e. electron flow from electrodes (cathodes) to microorganisms, is rather limited. The first report on cathodic direct electron flow appeared in 2004 [45], for nitrate to nitrite reduction from a cathode poised at approximately -0.3 V vs. SHE and enriched with sediment microbial species. Until now, the exact cathodic electron transfer pathways are still unknown. Many potential mechanisms have been proposed [2, 43, 46, 47] and are believed to be similar to the processes occurring at bioanodes, but operating at different redox potentials [47]. Rabaey and Rozendal (2010) [2] proposed some potential pathways for microbes to accept electrons from a cathode as illustrated in Figure 3.

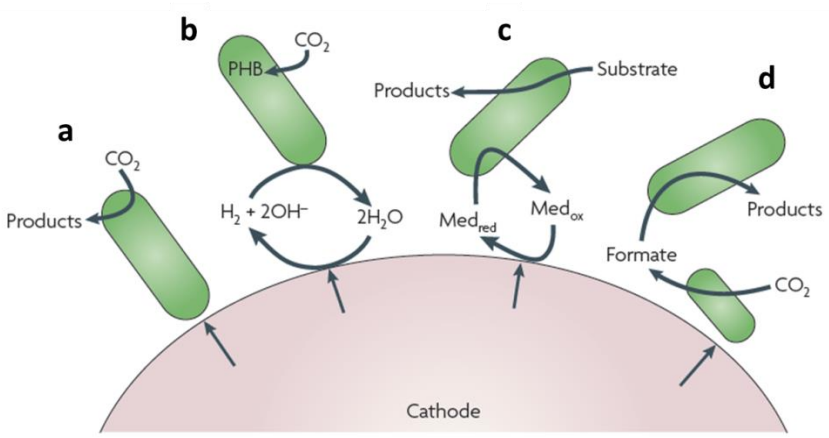

Figure 3 Proposed mechanisms for electron transfer from electrodes to microorganisms [2]. a) Direct electron transfer, b) hydrogen-mediated electron transfer, c) mediated electron transfer (Med_{red} and Med_{ox} for reduced and oxidized mediator, respectively) and d) via the formation of intermediate building blocks such as formate. PHB, poly-B-hydroxybutyrate.

It has been highlighted that DET from electrodes to microorganisms would hold most promise for microbial biocathode applications [48] (Figure 3a). It decreases overpotentials and simplifies the product recovery. The indirect means of electrons transfer via the reduction of

mediators or the production of hydrogen have some limitations for practical applications as reviewed by Trash and Coates [48] (Figure 3b and c). Finally, several microbial species may work in synergy to transfer electrons to the final products (Figure 3d). Further research needs to confirm these ET mechanisms and microbial interactions. In the context of hydrogen-producing microbial biocathodes, evidence was found for direct electron transfer from a polarized graphite cathode (-0.9 V vs. SHE) to the hydrogenase-possessing microorganism *Desulfovibrio paquesii*, which catalyses H_2 production from H^+ [49].

In addition, to the best of our knowledge, the ability of cathodic microorganisms to conserve energy and be self-sustaining with electrode and carbon dioxide as sole electron and carbon sources, respectively (i.e. without H_2 acting as an electron shuttle), have not been reported to date.

2.1.3. Applications of BESs – a brief overview

2.1.4.1. Electricity production

Even though MFCs are the pioneer of bioelectrochemical systems research and development, to date, the power generated is still too low for most applications. MFCs will likely never be used for large scale power generation and contribute to the power grid. However, MFCs could be suitable for niche applications, as power supplies for small scale systems, such as wireless sensors and telemetry systems that are not energy intensive, in remote areas. Shantaram et al. (2005) [50] developed an MFC consisting of a sacrificial anode combined with a manganese oxides cathode to power electrochemical sensors and small telemetry systems and transmit the acquired data to remote receivers. Another example is a Benthic Unattended Generator MFC that was tested to power a meteorological buoy for temperature, pressure, and humidity monitoring [51]. Urine has lately been regarded as an ideal feed for microbial electrochemical technologies given its conductivity, chemical oxygen demand and buffering capacity, and significant development towards urine utilization for electricity production has been made, with for instance the first urine-based MFC showed to power a mobile phone [52]. Biological oxygen reduction has been investigated as a cheaper cathode alternative to noble metals [53, 54]. Recently, source-separated urine using microbial electrochemical technologies for decentralized macronutrients (especially nitrogen, phosphorus, and potassium) recovery and reuse has also been proposed [55, 56].

The use of applied power in bioelectrochemical systems have only met an increasing interest within the researchers' community in the past few years. So far, microbial cathodic systems have mainly been investigated for bioremediation and bioproduction purposes, as discussed below.

2.1.4.2. Bioremediation / Removal of pollutants

BES technology is attractive for the removal of recalcitrant compounds in sediments and wastewaters. BES allows continuously providing oxidizing power and controlling the bioremediation process. For instance, inorganic compounds such as uranium [57], and sulfides [58] can be removed, and recovered using either anodic or cathodic processes, or both of them. (Bio)-cathodic processes for denitrification [26, 27, 45, 59], perchlorate reduction [29, 60] and dechlorination [28, 61, 62] are also being intensively investigated. Moreover, the transformation of strongly oxidized functional groups in persistent chemicals, such as the nitro-group of nitrobenzene [63] and the azo bond of reactive azo-dyes, using BESs is promising [64].

2.1.4.3. Production of fuels and chemicals

Using bioelectrochemical systems for the production of fuels and chemicals has gained increasing attention in the last few years and has become one of the most promising applications of BES technology. As reviewed above, power input is required to drive those thermodynamically unfavourable cathodic reactions. Therefore, the product(s) generated must be more valuable than the additional power invested for viable practical implementation. BES bioproduction cathodic processes can also be envisioned as an interesting option to capture and store harvested intermittent renewable (electrical) energy such as wind and solar energy into stable, high energy-density liquid or solid products that are easily transportable [7]. This can be interesting as off-peak energy storage. Up till now, (bio)-production of methane [65-67], hydrogen peroxide [68], sodium hydroxide [69], ethanol [70], and 1,3- or 1,2-propanediol [71] in BESs have been reported. Additionally, bioproduction of organics from carbon dioxide, referred to as microbial electrosynthesis, has received increasing interest and is extensively reviewed below, in section 2.2. Green energy generation in the form of hydrogen by (bio)-cathodic processes has also gained recognition and is reviewed in section 2.3.

2.2. Microbial electrosynthesis from CO_2 to organics

2.2.1. Microbial electrosynthesis – a promising CO_2-based technology

CO_2-based technologies present several advantages such as independence of arable land and precious freshwater resources, limited toxicity to microorganisms, mitigation of the ever-increasing CO_2 emissions, and nearly unlimited substrate availability.

Different fuel bioproduction approaches from carbon dioxide are conceivable and are depicted in Figure 4. The synthesis of target products, or fermentable substrate used in industry can then be derived from sunlight and carbon dioxide, using phototrophic cultures. Electrical energy can also be used to fix CO_2 in order to directly produce target compounds. Moreover, powered CO_2 fixation can lead to the formation of acetyl-CoA and its derivatives, via the Wood-Ljungdahl pathway, for further synthesis. It is also speculated that electrical current could drive the Calvin cycle toward the synthesis of fermentable substrate which could further be used for bioproduction purposes [6].

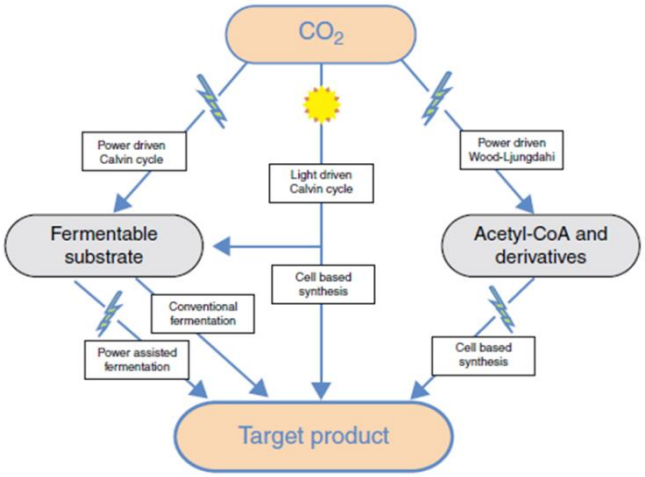

Figure 4 Overview of the different routes toward bioproduction from carbon dioxide, taken from [6]. Required inputs of solar or electrical energy are indicated. Several pathways involve MES, highlighting the potential to integrate existing approaches with this novel approach.

Microbial electrosynthesis (MES) is a biocathode-driven process in which electroactive microorganisms derive electrons from solid-state electrodes to catalyse the reduction of carbon dioxide to generate valuable extracellular multi-carbon reduced end-products [2, 5, 6], as depicted in Figure 5. In addition of the advantages of CO_2-based technologies listed above, the possibility of converting electrical energy, into high-energy density chemicals by recycling carbon dioxide as the key carbon source makes MES very attractive.

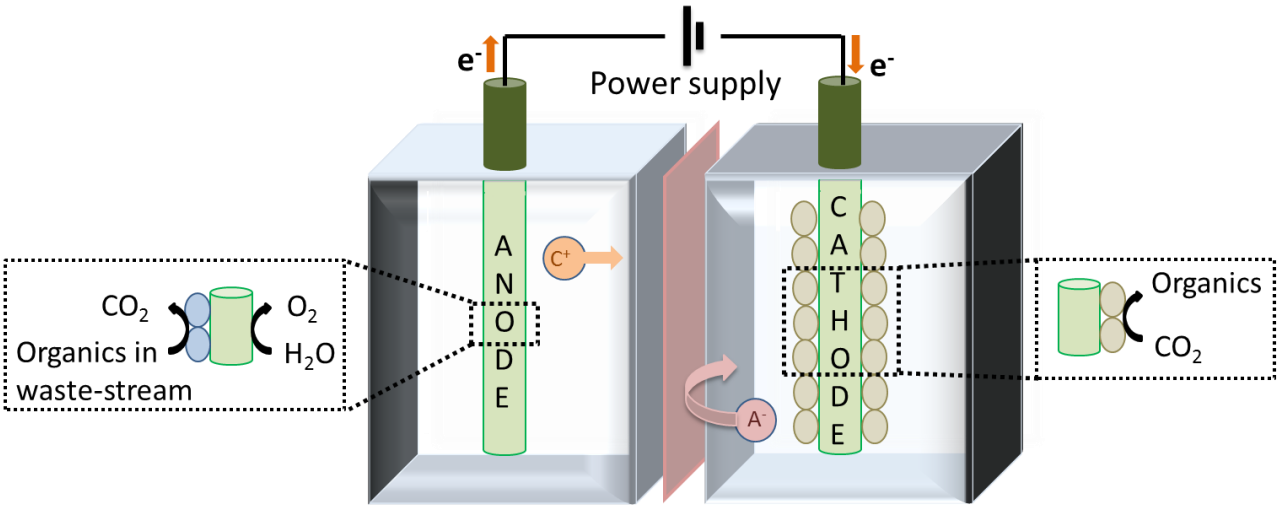

Figure 5 Microbial electrosynthesis from CO_2 scheme, with a cation exchange membrane, a biocathode for CO_2 reduction to organics and two examples of possible anodic reactions. Intermittent renewable energy (e.g. wind or solar) could be envisioned to deliver the additional power required to drive the bioproduction of high energy-density chemicals (e.g. off-peak energy storage).

Several anodic reactions could be envisioned appropriate, such as abiotic water oxidation with O_2 as sole end-product or microbial oxidation of organics from waste-stream (e.g. wastewater), with each their pros and cons, as later discussed and assessed in section 10.2. To date, investigations on MES, included this PhD work, have mainly focused on the development of the biocathode process itself without considering the anode side by using noble metal (e.g. platinum) as material for water oxidation. This is to prevent the anode side to be limiting; however, future research will need to investigate the combination of cheap and effective anode and cathode together, as discussed in Chapter 10.

Microbial electrosynthesis of organics from carbon dioxide has been recently put forward as an attractive technology for the renewable production of valuable multi-carbon reduced end-products and as a promising CO_2 transformation strategy over current techniques [4, 13]. Indeed, many CO_2-based technologies for the generation of carbon-neutral fuels and chemicals are at the research and development stage, such as chemical, photochemical, electrochemical, biological, reforming, and inorganic transformations [4, 72], as depicted in Figure 6.

CO_2 transformations			
	(1) Chemical	Non-hydrogenative	Carbonates, carbamates, etc.
		Hydrogenative	Hydrocarbons, MeOH, EtOH, etc.
	(2) Photochemical		CO, HCO_2H, CH_4
	(3) Electrochemical		CO, HCO_2H, MeOH
	(4) Biological		EtOH, Sugar, CH_3CO_2H
	(5) Reforming		CO + H_2
	(6) Inorganic		Carbonates: M_2CO_3

Figure 6 Most CO_2 transformation techniques investigated to date, apart from bioelectrochemical systems, taken from [4].

However, most of these CO_2 mitigation and conversion techniques have major drawbacks as they require the use of expensive catalysts, large amounts of electricity (energy intense processing steps), extremely large surface and volumes, and/or high consumption of hydrogen [4, 12, 13]. MES on the other hand have the advantages to use cheap and readily available (bio)catalysts, to work in ambient conditions (temperature and pressure), to potentially obtain a larger spectrum of products directly from CO_2 using the complex metabolisms of microorganisms and potentially prevent the handling of gases which is hazardous and costly. MES is also a versatile technology. Moreover, pure CO_2 may not be necessary and MES could use different sources of CO_2 as substrate without any costly pre-treatment steps (see section 10).

2.2.2. Microbial electrosynthesis from CO_2 to organics– A review

MES remains a nascent concept with only few studies that have demonstrated the process in laboratory scale using either pure cultures [8-11] or mixed microbial consortia [12-19, 73]. Microbial electrosynthesis performance can be assessed using several key parameters; these are listed in Table 1, for most MES to acetate studies reported to date. Use of mixed microbial cultures is attractive as they are readily obtainable in large quantities, are more tolerant to environmental stress and fluctuation [20] and have thus far showed higher MES performance (Table 1). Pure cultures could theoretically lead towards higher product specificity, even though, to date, similar electron recoveries into the final product(s) have been reported on both pure and mixed microbial cultures (Table 1).

Table 1 Key performance parameters of most microbial electrosynthesis to acetate studies reported to date.

Microbial inoculum (Reactor operation)	Cathode material	$E_{cathode}$ (V vs. SHE)	Current density (A m^{-2})	Acetate production (g m^{-2} day^{-1})	Max acetate titer (g L^{-1})	Electron recovery into acetate (%)	Reference
S. ovata (continuous)	Graphite rods	-0.4	-0.208	1.3	0.063	86 ± 21	Nevin et al. 2010 [9]
C. ljungdahlii (continuous)	Graphite rods	-0.4	-0.029	0.14	n.d.	72	Nevin et al. 2011 [8]
Brewery WW sludge (fed-batch)	Graphite granules	-0.590	n.d.	n.d. (8 mmol C L_{NCC}^{-1} d^{-1})	1.71	67	Marshall et al. 2012 [15]
Enriched brewery WW sludge (fed-batch)	Graphite granules	-0.590	n.d.	n.d. (34.5 mmol C L_{NCC}^{-1} d^{-1})	10.5	69	Marshall et al. 2013 [16]
Sewage treatment plant activated sludge	Carbon felt	-0.95	n.d.	0.019	n.d.	< 20	Jiang et al. 2013 [73]
Enriched WWTP sludge (fed-batch)	Carbon felt	-0.9	n.d.	34.5	n.d.	89.5	Su et al. 2013 [17]
S. ovata (continuous)	Carbon cloth-chitosan	-0.4	-0.475	2.7	0.118	86 ± 12	Zhang et al. 2013 [11]
S. ovata (continuous)	CNT-cotton CNT-polyester	-0.4	≈ -0.215	≈ 1.2	0.059	83 ± 10	Zhang et al. 2013 [11]
S. ovata (continuous)	Ni-nanowire-network-coated graphite	-0.4	≈ -0.625	3.3	n.d.	82 ± 14	Nie et al. 2013 [10]
Enriched brewery WW sludge (fed-batch)	Graphite rods	-0.6	-0.92 ± 0.12	8.56 ± 3.22	n.d.	40	LaBelle et al. 2014 [14]
Mesophilic WW anaerobic sludge (fed-batch)	Graphite felt	-1.1	≈ -2.8	10.1	1.4	65	Xafenias et al. 2014 [19]
Anaerobic digester / retention basin (continuous)	Graphite granules	-0.6	n.d. (12.3 A m_{NCC}^{-3})	n.d. (0.98 mmol C L_{NCC}^{-1} d^{-1})	n.d.	28.9 ± 6.1	Batlle-Vilanova et al. 2015 [12]

Nevin et al. (2010; 2011) [8, 9] described the first proof of concept of a biocathode-driven CO_2 reduction to acetate using pure cultures of acetogenic bacteria. In their first study [9], a culture of acetogenic microorganism *Sporomusa ovata* (gram-negative anaerobic bacteria) was grown with H_2 as the electron donor (H_2-CO_2 [80:20]). The culture was then introduced in a cathode compartment and initially bubbled with a gas mixture containing hydrogen (N_2-CO_2-H_2) as an additional electron donor to speed up the growth of a biofilm on unpolished graphite electrodes. The gas feed was then switched to N_2-CO_2 (80:20) and mainly acetate was produced as well as small amounts of 2-oxybutyrate with an electron recovery in these products of over 85%. A potential of -400 mV (versus standard hydrogen electrode) was applied to the cathode, which prevented the production of even low levels of hydrogen and hence acetate production from hydrogen by acetogens [74]. The cathode biofilms showed relatively long-term stability as after periods of more than three months their capacity for electron consumption and acetate production remained the same. However, the biofilms of acetogens remained thin, suggesting that the microorganisms gain only small amounts of energy from the reduction of carbon dioxide. Hence, actual bacterial growth on electrons from electrode and CO_2 only as energy and carbon source was not verified. After discovering the first microorganisms capable of electrosynthesis from carbon dioxide reduction in a BES, the acetogen *Sporomusa ovata*, Nevin et al. (2011) [8] aimed to determine whether a wider range of organisms was capable of electrosynthesis. To do so, several other pure acetogenic bacteria were studied according to a similar protocol. Most of them were able to accept electrons from an

electrode. The extracellular organic compound(s) produced, the electron consumption rate compared to that reported for *S. ovata* as well as the electron recovery in products determined in this study are summarized in Table 2.

Table 2 Microorganisms tested by Nevin et al. (2011) [8] for their ability to receive electrons from a solid-state electrode with carbon dioxide as the final electron acceptor.

Species	Electron consumption?	Electron consumption rate vs. *S. ovata*	Electron recovery in products	Products formed
Sporomusa ovata	Yes	100%	86% +/- 21%	Acetate + trace of 2-oxobutyrate
Sporomusa sphaeroides	Yes	5%	84% +/- 26% (n=3)	Acetate
Sporomusa silvacetica	Yes	10%	48% +/- 6%	Acetate + trace of 2-oxobutyrate + others non identified
Clostridium ljungdahli	Yes	-	82% +/- 10% (n=3)	Acetate + minor formate and 2-oxobutyrate over time
Clostridium aceticum	Yes	-	53% +/- 4% (n=2)	2-oxobutyrate and acetate as important + others non identified
Moorella thermoacetica	Yes	-	85% +/- 7% (n=3)	Acetate
Acetobacterium woodii	No	-	-	-

Among the acetogens tested, *A. woodi* was the only one that appeared unable to receive electrons from an electrode. The low electron recoveries in identified products found for *S. silvacetica* and *C. aceticum* were attributed to the presence of other products detected on the HPLC chromatograms but not yet identified. Gram-negative (*Sporomusa* species) as well as Gram-positive (*Clostridium* species) bacteria were shown capable of establishing electrical connections with electrodes. In previous studies, Gram-negative species such as Geobacter [45, 57, 62, 75] and Anaeromyxobacter [76] have shown this capacity but Gram-positive species were only shown with the capacity of giving electrons to an electrode. Therefore, they demonstrated that a wide diversity of organisms is able to derive electrons from an electrode in order to reduce carbon dioxide to organic compounds. From the same research group, Lovley et al. (2013) [10, 11] further investigated a number of modified electrode materials for the improvement of microbial electrosynthesis of acetate from CO_2 by pure cultures of *Sporomusa ovata*, as discussed below in more details (section 2.4.2).

Subsequent studies by Marshall et al. (2012; 2013) demonstrated for the first time the ability of mixed cultures to perform MES of acetate from CO_2 [15, 16]. They reported simultaneous production of methane, acetate and hydrogen using a mixed microbial community originating from brewery wastewater anaerobic sludge selected on granular graphite cathode poised at – 0.59 V vs. SHE [15]. Methane was found to be the dominant product with production rates of up to 7 mM

day^{-1}. When methanogenesis was inhibited following the addition of specific chemical inhibitor, 2-bromoethanesulfonate, acetate production rate increased up to 4 mM day^{-1} and hydrogen production up to 11 mM day^{-1}. A maximum titer of about 1.71 g L^{-1} of acetate was achieved in this study. They further demonstrated improved performance over long-term operation (over 150 days) of the established acetogenic biocathode aforementioned [16]. Acetate production rates reached a maximum of 17.25 mM day^{-1} with a high titer of 10.5 g L^{-1} accumulated over 20 days. Hydrogen was also found to be simultaneously produced at high rates, reaching 100 mM day^{-1}. In both studies, the active electrosynthetic microbiome revealed a similar community structure, with *Acetobacterium* spp. found to be dominant, which were speculated primarily responsible for electroacetogenesis in the MESs. Also prevalent were *Sulfurospirillum* spp. and an unclassified *Rhodobacteraceae,* although their roles were not clear. Both direct electron transfer and H_2-mediated electron transfer from the cathode to the acetate-producers were speculated [16]. Few other studies have also reported biocathodic concomitant production of acetate, methane and hydrogen by mixed microbial consortia on graphite or carbon felt [17, 19, 73]. Jiang et al. (2012) showed that the metabolic pathway and end-products spectrum was dependent on the applied cathode potentials [73]. They reported methane and H_2 production only at set potentials between -0.65 and -0.75 V vs. SHE while methane was also produced at potentials more negative than -0.75 V vs. SHE. It was also highlighted that cathode potential was a critical factor that affected MES performance with acetate production rate increasing from 0.38 mM day^{-1} and 53.6 % electron recovery into acetate at -0.7 V vs. SHE to 2.35 mM day^{-1} and 89.5 % electron recovery at -0.9 V vs. SHE [17]. The pH was also shown to have some influence on microbial electrosynthesis rates [12, 14]. Lowering the pH from near neutral to 5 was shown by LaBelle et al. (2014) [14] not to affect acetate production while concomitant H_2 production significantly increased. Further decrease of the pH below 5 was found detrimental to acetate production, while electrohydrogenesis rates further increased [14]. Controlling the pH slightly acidic (ca. 5.8) was shown to enhance acetate production in another study, as either a direct effect of the low pH or due to the indirect increase of substrate availability [12].

It appears clear that when using mixed microbial consortia, concomitant methane production was also observed in most MES to organics studies. Bioelectrochemical systems for primary methane production from CO_2 have also been investigated [65-67, 77-79]. However, in the frame of organics production, methane is regarded as an undesired product, which formation redirects the carbon flow and ultimately decreases the carbon and electron recoveries into the targeted product (e.g. acetate). Therefore, preventing methane production in these systems is of paramount

importance. To date in MES to organics studies, methanogenesis has been inhibited by adding a chemical inhibitor, 2-bromoethanesulfonate (BrES). BrES has been shown to be a specific inhibitor towards methanogens while non-methanogenic organisms in pure cultures as well as in more complex environments, even at high BrES concentrations, were not affected [80-87]. Adding external chemicals is suitable for lab-scale fundamental research. However it will become more problematic for larger-scale applications, from both technical and economic point of view. Further research will need to investigate other means of effective methanogenesis inhibition.

Initially, only acetate could be produced by MES from CO_2, however, a recent study has showed the simultaneous conversion of CO_2 into a mixture of products composed of acetate, butyrate, ethanol, and butanol [13].Acetate was first produced and subsequent mechanisms of formations of butyrate and alcohols were not clear. Direct CO_2 reduction and chain elongation reactions from the combination of acetate and ethanol were proposed as potential mechanisms for butyrate production. A maximum butyrate production rate of 1.82 mMC day^{-1} was achieved. The higher market value of some of those organics (e.g. butanol) compared to acetate makes their direct production from CO_2 very interesting. Nevertheless, high product specificity and production rates are regarded as key parameters that could enable large-scale applicability of such a technology. One of the main challenges in large scale chemical production is the product separation / extraction, which is often regarded as one of the major cost [88]. For instance, industrial fermentation products separation can reach up to 50-60% of the total plant costs [89].

Low-cost technologies are being investigated. On-line liquid/liquid extraction using membranes was reported as one possibility to remove acetate from engineered systems (e.g. fermenters) [90]. Membrane Electrolysis (ME) was also showed successful for the extraction of carboxylates from cathode to anode compartment, combined with Biphasic Esterification (BE) for the production of fine chemicals [91]; similar concept could be coupled to microbial electrosynthesis of acetate from CO_2.

Acetate can be an important end-product as well as a platform for further chemical syntheses [88, 92]. Agler et al. (2011) reviewed a range of processes for the production of higher value compounds (e.g. alcohols and long chain fatty acids) from short-chain carboxylates described as “the carboxylate platform” [88]. Short-chain carboxylates can be further processed by secondary fermentation reactions and/or with separate post-processing steps (e.g. bio/chemical, electrochemical and/or thermochemical steps). Carbonyls, esters, alcohols and alkanes are examples of high-value end-products generated through such reactions, producing directly usable fuels and/or industrial solvents [88]. Liu et al. (2015) very recently described a new direct solar-powered process

for the production of acetate from CO_2 coupled with the biosynthesis of complex organic molecules from acetate, such as n-butanol, PHB biopolymer and isoprenoid compounds using genetically engineered *E. coli*, in a separate vessel [92]. Acetate itself is also widely used as carbon substrate for industrial and/or environmental biological processes such as denitrification or biological phosphorus removal. In this context, microbial electrosynthesis could be an interesting option for on-site production of organics for such processes at a wastewater treatment plant. However, reported performances of bioelectrosynthesis processes are still insufficient for scaling MES to practical applications (Table 1). Moreover, considerable further process development of all these options is required to maximise the production rates and yields and to identify the most valuable utilisation of acetate, or other organics, generated by MES (see Chapter 10 for potential practical implementations and economic feasibility studies).

2.3. Microbial electrolysis for H_2 production

As seen above, hydrogen has been regularly reported as a co-product of microbial electrosynthesis from CO_2. H_2 is also regarded as a valuable fuel. The efficient and sustainable production of hydrogen in a microbial electrolysis cell (MEC) is a potential strategy for green energy production from renewable resources, water and biomass, which has gained recognition in the last few years [21-23]. Conventionally, expensive materials such as platinum were used as cathode catalyst for hydrogen production in MEC, but were shown to be not economically viable [93]. Nickel and stainless steel have also been investigated due to their stability, reduced cost, and low overpotentials, and comparative efficiency with platinum catalyst for hydrogen evolution [23, 93-95]. Microbial biocathodes have been developed as promising alternatives, due to their low cost (for both electrode material and catalyst) and low overpotentials. Immobilized hydrogenases that catalyse the reversible reaction $2H^+ + 2e^- \leftrightarrow H_2$ on carbon electrodes were first shown to successfully catalyse hydrogen production [96-101]. However, enzymatic biocathodes are not self-regenerating, are unstable and lose their catalytic activity over time. Therefore, whole cells of pure cultures of hydrogenase-possessing microorganisms, such as *Desulfovibrio* sp., have been immobilized with methyl viologen as a redox mediator, and were reportedly successful in catalysing hydrogen production [102, 103]. Nevertheless, from an economical and technical point of view, mediator-less mixed culture microbial biocathodes would be much more desirable in respect to the stability of operation of the BES [104]. In this perspective, hydrogen-producing microbial biocathodes based on naturally selected mixed cultures were investigated and showed bioelectrocatalytic activity for enhanced hydrogen production [104-108]. In all these studies,

electrochemically active biofilms were grown on anodes with acetate and/or hydrogen as electron donor and then, the polarity of the electrode was reversed to biocathode mode for hydrogen production [104-106, 108]. Alternatively, the inocula used in biocathodes were pre-enriched as bioanodes with acetate as electron source [107]. It is not clear from the reported results whether these H_2-producing biofilms are able to self-regenerate under purely cathodic conditions without any organic carbon sources and hydrogen as electron donor.

2.4. Prospective biocompatible electrode materials

Practical implementation of BESs has previously been discussed [109-111] and some scale-up attempts have been made, especially of microbial fuel cells and microbial electrolysis cells [112-114]. Extensive reviews of the processes have identified the main challenges for the industrial implementation of BES systems to include the low productivity, low growth rates of the biocatalyst and limited product specificity [6, 109]. To address these challenges, it has been proposed to focus the research efforts on: an optimized electrode surface to volume ratio, biocompatible, high-current density surfaces allowing enhanced interaction with the microorganisms, scalable designs and electrodes, low-cost and long-term stability of all components, and avoiding or minimising chemical/consumables inputs [109].

2.4.1. Bioanode electrode materials – a brief overview

Until very recently, research on prospective electrode materials for BESs was only focused on the anodic processes. Several approaches have been reported for enhanced biofilm formation and improved MFC performance. Until very recently, anode materials were almost exclusively commercially available carbonaceous materials, due to their excellent electrical conductivity and chemical stability [115, 116]. These include graphite granules and rods, carbon paper, carbon cloth, graphite felt, reticulated vitreous carbon and glassy carbon. Lately, some novel, purposefully synthesized materials have been presented for MFC application [117-123] as detailed in section 2.4.3.

An alternative strategy to improve biofilm formation and bacteria-electrode interaction is to apply some type of pre-treatment to the electrodes before exposing them to MFC operation and biofilm development [124]. Biofilm formation is an extremely complicated process which is affected by several factors including electrode surface hydrophobicity, charge and topography in addition of environmental factors and bacterial properties [125].

Contradictory opinions exist on the relationships between bacterial adhesion and surface hydrophobicity. While several authors claim that hydrophilic surface will accelerate bacterial adhesion, others claim exactly the opposite [124, 126, 127]. Many argue that the preference towards one or the other types of surface will depend on the bacterial species under consideration [124]. However, others found that bacterial cell hydrophobicity have much less influence on bacterial adhesion than material surface hydrophobicity [128].

Some pre-treatment techniques proposed aim at modifying the electrode surface with different redox molecules that will mediate the electron transfer from microorganism to electrode [129-132]. For instance, neutral red (NR), a known mediator, was bound to a woven graphite electrode and increased power 450 times compared to the same electrode lacking the mediator, using a pure culture of *Shewanella putrefaciens* and lactate as substrate. Later on, a simple and novel method to covalently graft NR onto carbon surfaces with spontaneous reduction of in situ generated NR diazonium salts was developed and also showed current density enhancement [129].

Another possibility to improve bacterial attachment, in turn related to the bacteria-electrode electron transfer process, is to activate the electrode surface while keeping the inherent extracellular bacterial electron transfer mechanism, i.e. without the addition of exogenous mediators [124]. The electron transfer potential is thus maintained at the enzyme redox potential, instead of the mediator potential. For instance, pre-treating anodes with ammonia gas at 700ºC [133], with nitric acid and ethylenediamine [134], with HNO_3 and quinone/quinoids [135], or HNO_3 and hydrazine [136] all showed successful at enhancing the current density at anodes of microbial fuel cells. Zhou et al. (2012) also proposed electrochemical oxidation in different concentrated electrolytes as a new method [137]. The trend that positively-charged anode surface allows for better bacterial attachment and biofilm activity (by increasing the rate of electron transfer) has been supported by several studies [124, 133, 138-140]. This observation goes with the fact that bacterial surfaces in aqueous suspension are typically negatively charged, hence more attracted by positively charged surfaces [125]. Ammonia treatment was shown to increase the positive surface charge of carbon cloth from 0.38 to 3.99 meq m^{-2} which in turn reduced microbial acclimation time by 50% and increased maximal power density [133]. Reduction of the activation energy threshold for electron transfer from microorganisms to electrodes was shown by applying metal catalysts [115, 141-143].

Finally, material surface topography was shown to significantly influence bacterial adhesion to anode surface. Bacteria were shown to more easily adhere and colonize porous, grooved or braided surfaces than smooth surfaces [144, 145]. Roughened surfaces offer greater surface and provide more favourable sites for colonization. Increasing the available surface area for biofilm

growth by using rough or porous materials is a well-proven strategy for MFC performance enhancement [116, 117, 127, 146-148].

2.4.2. Biocathode electrode materials for MES

Optimizing and scaling microbial electrosynthesis, and biocathode processes, to practical applications relies on performance improvements while maintaining low costs. Enhancement of bacterial attachment, biofilm development, electron transfer rate at the cathode surface (microorganism-electrode interaction), and chemical production rate requires optimization of several key elements, particularly improved cathode materials, selective microbial consortia and efficient reactor designs. Moreover, the electrode material must be scalable, highly conductive and cost effective.

Despite the large number of reports on new electrode materials and surface modification strategies for the improvement of anodic processes, there is hardly any work reported on new electrodes materials for cathodes. This is not surprising, since there is now quite a general agreement that bacteria-electrode electron transfer processes are most probably following different routes during an anodic or cathodic process [2, 6]. Therefore, it is not straightforward to predict that a given electrode material yielding good results as a microbial anode will perform equally well as a cathode.

To the best of our knowledge, only Lovley et al. (2013) [10, 11] have very recently proposed a number of modified electrode materials for the improvement of cathodic processes. Their work focuses on the improvement of microbial electrosynthesis of acetate from CO_2 by pure cultures of *Sporomusa ovata* by modifying cathode surfaces following strategies tested for bioanode electrodes, for the same reasons as discussed above. Using different treatments, they altered the surface chemistry of carbon cloth by the immobilization of positively charged molecules, or by treating it with metal nanoparticles, in the aim of enhancing microbe-electrode interactions. Moreover, they tried depositing carbon nanotubes on non-conductive textile composites. Both current density and acetate production rate obtained on each modified electrode, compared to untreated carbon cloth can be seen in Table 3 [11].

Table 3 Carbon cloth cathode treatments tested, average current consumption and acetate production rate obtained on each, taken from [11].

Carbon cloth cathode treatment	Average current consumption density[a] (mA m^{-2})	Acetate[a] (mM m^{-2} day^{-1})	Coulombic efficiency[a]
Carbon cloth	−71 ± 11	30 ± 7	76 ± 14
Chitosan	−475 ± 18	229 ± 56	86 ± 12
Cyanuric chloride	−451 ± 79	205 ± 50	81 ± 16
3-Aminopropyltriethoxysilane	−206 ± 11	95 ± 20	82 ± 11
Polyaniline	−189 ± 18	90 ± 22	85 ± 7
Melamine	−69 ± 9	31 ± 8	80 ± 15
Ammonia	−60 ± 21	28 ± 14	82 ± 8
Au	−388 ± 43	181 ± 44	83 ± 14
Pd	−320 ± 64	141 ± 35	79 ± 16
Ni	−302 ± 48	136 ± 33	80 ± 15
CNT–cotton	−220 ± 1	102 ± 25	83 ± 10
CNT–polyester	−210 ± 13	96 ± 24	82 ± 8

[a] Each value is the mean and standard deviation of three replicates.

The pure culture under investigation, *S. ovata*, has a negative outer-surface charge. The first six of those treatments (Table 3) aimed at conferring positive surface charge to the carbon cloth. The best results were obtained by cathode functionalization with chitosan and cyanuric chloride, with 6-7 fold higher production rates (ca. 0.02 mM cm^{-2} day^{-1}) and highest current density of 0.0475 mA cm^{-2} reached with a chitosan modified electrode. However, not all surface treatments increasing the positive charge were found to be successful. Rates obtained on melamine and ammonia-treated electrode were found similar than those on unmodified carbon cloth, suggesting that surface charge alone might not be sufficient to enhance bacterial attachment and in turn biofilm development, electrode-microbe electron transfer rate and maximal achievable production rate. It was concluded that other features of the cathode modifications designed to provide a positive charge may be critical [11].

Another strategy tested, with the objective of enhancing electrode-microbe electron exchange rate, was applying nanoparticles of metals, Au, Pd or Ni, onto the surface of carbon cloth, by physical deposition [11]. Those metal nanoparticles have been reported to be biocompatible, have excellent catalytic activity and high active surface area and were all showed in this study to increase acetate microbial electrosynthesis by factors of 4.5 to 6 versus the untreated control (Table 3) [11].

A novel cathode using nickel nanowires anchored to graphite was also developed and tested in a similar set-up than above, using *S. ovata* for the reduction of CO_2 to acetate [10]. Around 282 mM m^{-2} day^{-1} of acetate was produced, 2.3 fold higher rate than obtained on an untreated

graphite electrode. The porous nickel-nanowire-network was argued to increase the interfacial area and enhance interactions between the cathode surface and the microbial biofilm [10].

Even though most of these material modification strategies showed successful at increasing microbial electrosynthesis rates over carbon cloth or graphite control, performance remains insufficient for potential practical implementation of MES process (Table 1) and other approaches are required.

2.4.3. Three-dimensional hierarchical electrodes

Maximal current densities obtainable on bioanodes were shown to be limited by the transfer of substrates and products to and from the electrode surface at flat and rough electrodes [42, 149]. To remedy this issue, a novel approach was recently proposed which consists of using three-dimensional and purposefully synthesized materials as bioanode electrodes. We refer here to porous three-dimensional materials, where microorganisms can develop in the whole volume of the electrode, as opposed to rough or dense fibrous materials. For example, on graphite felt a biofilm is only developed in the outer layers of the fibre mat, but not 2-3 mm from the surface in the deepest core of the electrode. In the last five years, several authors reported current generation enhancement in MFC mode using such 3D electrodes as bioanode material [117-123].

Three-dimensional microchanneled nanocomposite electrodes were fabricated by ice-segregation induced self-assembly (ISISA) of chitosan-dispersed multiwalled carbon nanotubes [122]. The hierarchical structure was shown to provide a conductive scaffold available for *G. sulfurreducens* colonization and achieve high current production as acetate-oxidizing bioanodes. High current densities as high as 24.5 A m^{-2}, corresponding to a volumetric current density of 19 kA m^{-3} were obtained in flow-through configuration. High performance was attributed to the successful bacterial colonization throughout the 3D surface area and to the effective mass transport of nutrients and products, while the CNT provided a high surface area [122]. ISISA technique was also used to manufacture a novel hierarchically porous structure consisting of biocompatible chitosan and vacuum-stripped graphene (CHI/VSG) [121]. CHI/VSG was shown promising as bioanode material, with a maximum power density of 1.53 W m^{-2} obtained in a mediator-less MFC. The higher surface area available for bacteria immobilization and the biocompatible characteristic of VSG were argued to improve the electron transfer processes [121]. Three-dimensional carbon fibre electrodes prepared by electrospinning and solution blowing were also shown promising with current densities up to 30 A m^{-2} reported in MFC configuration [118]. Coating a sponge with carbon nanotubes offered an electrode with low internal resistance, great stability, tuneable and uniform

macroporous structure (pores up to 1 mm in diameter), and good mechanical properties [119]. The 3D scaffold was shown highly biocompatible with microbial colonization throughout the structure. Power density of 1.24 W m^{-2} was achieved using a fed-batch H-shaped MFC outfitted with CNT-sponge electrodes when treating domestic wastewater [119]. Novel reticulated carbon foam electrodes was prepared by direct carbonization of the sponge-like natural product, Pomelo peel, and used as low-cost, sustainable and eco-friendly bioanode electrode in MFC. High projected current density of over 40 A m^{-2} were obtained and attributed to the wrinkled electrode surface, large pore size and high porosity of over 97 % in the carbon foam [120].

Reticulated vitreous carbon (RVC) is a rather cheap and commercially available open-pore foam material of honeycomb structure that has also been used in few microbial fuel cell studies [116, 146-148]. RVC has a number of advantages for bioelectrochemical systems such as a very high surface area to volume ratio, high electrical conductivity, strong chemical and heat resistance and minimal reactivity over a wide range of conditions [150]. However, they have also been found not to have the most favourable surface characteristics for microbial attachment and electron transfer [120, 146].

Carbon nanotube-based (CNT) electrode materials have become extremely attractive for application in BES. Indeed, CNTs have large aspect ratios, high surface area, and an exceptional electric conductivity along their length [151]. Moreover, their mechanical strength and chemical stability are excellent. CNTs were also described as being highly biocompatible allowing for bacteria immobilization and proliferation [122, 146, 152]. So far, most studies were carried out in MFC configuration; electrodes were coated with CNT inks and produced promising current densities [119, 122, 138, 153, 154]. CNT ink deposition on cotton and polyester fabrics also yielded biocathodes with up to 3 times higher current density (0.021 mA cm^{-2}) and acetate bioelectrosynthesis rates (0.010 mM day^{-1} cm^{-2}) than unmodified carbon cloth control [11] (Table 3).

To enable a good connection of the CNT to the substrate, a new CNT growth technique has been developed, chemical vapour deposition, which achieves CNT development directly on any type of surface, including conductive substrates [155]. This approach was used to synthesize a new biocompatible, highly conductive three-dimensional microbial bioelectrode, with a hierarchical porous structure, by direct growth of multiwalled carbon nanotubes on reticulated vitreous carbon, called NanoWeb-RVC [146]. The NanoWeb-RVC showed excellent performance as bioanode material for power production, with one of the highest current density of 68 A m^{-2} ever recorded [146]. This electrode structure benefits from all the advantages of both RVC and CNT mentioned

above. The macrostructure enhances the mass transfer to and from the electrode surface while the nanostructure improves bacterial attachment to the electrode and increases the extracellular electron transfer rate from the microorganisms to the electrode. To the best of our knowledge, only two studies have reported similar or higher performance. Schröder et al. (2012) [117] reported a higher current density, using a layered corrugated carbon microbial electrode, with 70 A m^{-2} for their basic electrode configuration, and up to 400 A m^{-2} when several electrodes were stacked together. Ketep et al. (2014) [156] reported current densities in the range of 60-80 A m^{-2} at -0.2 V vs. SHE and more than 100 A m^{-2} at 0 V vs. SHE by using stainless steel foams.

From these bioanode studies, the general rule for high performance electrode material would be (a) self-supported reticulated macroporous architecture, (b) rough surface, (c) good hydrophilicity and (d) high biocompatibility for good biofilm attachment and development. Mass transfer of substrates and products to and from the electrode surface also need to be taken into consideration, with reported limitation when electrode thickness increases or pore size decreases [120]. The dimension selection is thus important for practical implementation of 3D macroporous electrodes.

In similar fashion, 3D macroporous electrode could significantly enhance biocathode processes as well and microbial electrosynthesis in particular, but has not been investigated to date, to the best of our knowledge.

3 Thesis Overview

3.1. Research questions

Research question 1: Are mixed microbial cultures able to self-regenerate and grow using the cathode as the sole electron donor and carbon dioxide as the sole carbon source?

While anodic microorganisms consume part of the electrons available in the organic substrate for growth and maintenance with an electrode serving as the sole electron acceptor, cell growth and energy conservation with an electrode serving as the sole electron donor remains to be shown. Contradictory opinions exist on whether effective growth can be sustained at biocathodes. It was suggested that, due to their redox potentials, the electron transfer chain components within the cells may not necessarily lead to energy conservation for the microorganisms [47] and that a lithoheterotrophic metabolism would be required for cathodic growth [38, 157]. However, cathodic growth is theoretically possible when the final electron acceptors are reduced in the cytoplasm or within the inner membrane [43]. Lovley et al. (2011) argued that protons will be consumed for the production of the reduced end-product. Therefore, if the reduction of these electron acceptors occurs within the cytoplasm, this will result in a proton gradient across the inner membrane leading to ATP formation [43]. In the context of bioproduction, autotrophic growth solely using electrical current has been very challenging and only pre-grown biofilms (using e.g. acetate or hydrogen as electron donor) have been obtained thus far [8-11, 45, 104]. The challenge is to generate a self-maintaining biocathode, with living microorganisms which are able to survive, conserve energy and grow for continuous bioproduction under autotrophic conditions using carbon dioxide as the sole carbon source. In this PhD work, autotrophic biomass growth and bioproduction with the electrode as sole electron donor, was investigated on graphite plates by applying high cathodic potential at which abiotic hydrogen is not produced, (see Chapter 5).

Research question 2: How can advanced three-dimensional hierarchical electrodes influence the performance of microbial electrosynthesis by mixed microbial cultures from carbon dioxide to organics? To what end-products do they direct the electron flow and what are the achievable yields and production rates from CO_2?

As developed in sections 2.2 and 2.4, reported performance of bioelectrosynthesis of organics processes are still insufficient for scaling MES to practical applications. Biocathode material development is of paramount importance towards performance enhancement. Optimizing

the electrode material can enhance bacterial attachment, biofilm development, interaction with the microbes and ultimately electron transfer and organics production rates. It can be predicted that transfer of substrate and products to and from the electrode surface, can limit the current density of biocathodes and production rate for microbial electrosynthesis at flat and rough electrodes, in a similar fashion as it has already been described for anodic biofilms (section 2.4.3). 'True' three-dimensional cathodes with macropores at least in the hundreds of micrometer scale in all three geometric directions could overcome those limitations and allow for efficient mass transfer towards and from the electroactive biofilm [146]. Moreover, a high surface-to-volume ratio, as is typical for three-dimensional electrodes, will provide a large surface area and therefore could increase the active biomass and the maximum electron consumption per given volume unit. As seen for bioanodes, a certain surface roughness could be necessary to enhance biocompatibility, bacterial attachment, biofilm development and electrode-microbe electron transfer rate as well. Therefore, in this PhD thesis, we evaluated the performance of a novel biocathode electrode material manufactured by direct growth of flexible multiwalled carbon nanotubes on reticulated vitreous carbon, by chemical vapour deposition (NanoWeb-RVC), for microbial electrosynthesis from carbon dioxide, with mixed cultures (see Chapter 6).

- *Sub-research question 2a*: Can carbon nanotubes be deposited on three-dimensional scaffold by a simple and scalable technique and what microbial electrosynthesis performance is achievable? Can the acclimatized and enriched microbial consortium be successfully transferred?

Chemical Vapour Deposition (CVD) technique is a great tool for novel material synthesis, which is suitable for lab-scale demonstration. However, for scale-up beyond certain sizes, there are some limitations with the CVD technique. Indeed, the requirement of specialised equipment and the complexity of the CVD process make this method unsuitable both for production of large size samples, and large scale production. Therefore, we investigated a novel method to deposit multiwalled carbon nanotubes onto three-dimensional scaffold, which has not been reported to date. We harnessed the throwing power of electrophoretic deposition technique (EPD) to form multiwalled CNT coatings onto RVC to generate a new hierarchical porous structure, hereafter called EPD-3D, which we used as biocathode electrode. The simplicity of the equipment required for EPD and short deposition time make this method suitable and very attractive for industrial large scale production of EPD-3D [158]. The newly synthesized material was found to be significantly different than NanoWeb-RVC and lab-scale MES performance on EPD-3D was investigated in this work (see Chapter 7).

Moreover, the successful transfer of an enriched microbial culture to achieve a rapid colonisation and electrosynthesis activity in new reactors is an important demonstration for a successful start-up strategy for larger scale reactors. In this PhD thesis we investigated this feature by inoculating new reactors with enriched culture that showed capable of microbial electrosynthesis from CO_2.

- *Sub-research question 2b*: How do the macropores size of three-dimensional scaffold electrode affect microbial electrosynthesis performance?

Mass transfer of substrates and/or products through the 3D macroporous structure itself and/or within the biofilm can limit the maximal performance achievable (electron consumption and organics production rates). Larger pores are hypothesized to favour the flow through the 3D structure, thus maximising the production rates when normalized to the total surface area available to microorganisms. However, from a large-scale implementation point of view, the higher the total surface area per volume unit the better, to maximize production rate per volume unit. Nevertheless, it is hypothesized that too small pore diameter (very high surface per volume ratio) may also negatively impact MES performance. We investigated in this PhD thesis the effect of three different EPD-3D electrode pore sizes on MES performance from CO_2 to organics, from both intrinsic and engineering performance perspective (Chapter 9).

Research question 3: How are electrons transferred from the electrode to the final electron acceptor, CO_2? What are the dominant strains in the cathodic bacterial communities? What is the respective importance of both biofilm and planktonic cells on the microbial electrosynthesis performance?

A more in-depth understanding of the process and particularly on how electrons flow from the cathode to the terminal electron acceptor can be of paramount importance, not only for fundamental knowledge but also for actual MES technology scale up to practical implementation (e.g. for improved reactor design). As developed in sections 2.1.2 and 2.2, electron transfer pathways occurring in biocathodes, particularly in MES, are still unknown and potential pathways have been proposed (section 2.1.2.2). Based on literature, both direct and hydrogen-mediated electron transfers to organics-producing microorganism were hypothesized at the start of this PhD. Electron fluxes were thus investigated in this PhD work. In addition, microorganisms involved in the process were identified and relative importance to the process performance of both biofilm and planktonic cells was attributed (see Chapter 8).

Research question 4: How do operating conditions impact microbial electrosynthesis performance? Can biogas be directly used as substrate for microbial electrosynthesis of organics?

Further investigation is needed towards operating conditions optimization and the need for cheap and easily usable carbon dioxide source. Protons are required for the CO_2 reduction reaction to organics. High proton availability could hypothetically enhance the conversion rate, to a certain extent that is driven by biological response (activity) to lower pH. Moreover, higher energy of electrons (lower reductive potentials) could enhance production rate. However, high product specificity needs to be still achieved. We investigated in this PhD thesis the effects of pH and applied potentials on MES performance. Additional insights on the process mechanisms were obtained.

Another key consideration for potential practical applications is the source of carbon dioxide. Several options are available, but not all of them are attractive for MES applications to produce relatively low-value end-products such as acetate. Therefore, a cheap and readily available carbon dioxide source would be favoured, which would likely be in a mixed gas situation. Biogas could be regarded as an interesting option in this context as it is primarily composed of methane (CH_4) and carbon dioxide. Biogas is produced during anaerobic digestion and can be used on-site for power generation but could also be more economically used as a transport fuel for buses/cars etc. For the latter application the CO_2 fraction needs to be removed to improve gas compression/storage and combustion efficiency. Therefore, an MES process to convert the CO_2 fraction to organics could be perfectly suitable for such a biogas 'cleaning' operation. This option could then be both environmentally and economically attractive for both applications, organics production and biogas utilisation as fuel. Consequently, a synthetic biogas mixture, CH_4-CO_2 (70%:30% v/v), was fed to an MES reactor and performance assessed (see Chapter 9).

3.2. Thesis structure

From this point onwards, the thesis is structured by chapters as follows. Firstly, Chapter 4 gathers together all the experimental materials and methods used in this work. Secondly, Chapters 5 to 9 presents the research outcomes based on the research questions listed above. Chapters 5, 6, and 7 correspond to the research outcome sections, modified for incorporation in this thesis, of the peer-reviewed papers published (Chapter 5 and 6) or currently under revision (Chapter 7). Chapters 8 and 9 are the research outcome sections, modified for incorporation in this thesis, of two papers (see below) that have been fully written, internally peer-reviewed and ready for submission upon

receiving comments from the paper already submitted to Energy & Environmental Science (Chapter 7).

- **Ludovic Jourdin,** Yang Lu, Victoria Flexer, Jurg Keller, and Stefano Freguia. Biologically-induced hydrogen production drives high rate / high efficiency microbial electrosynthesis of acetate from carbon dioxide. To be submitted to *Energy & Environmental Science*, 2015.

This paper has been modified and incorporated as Chapter 8.

- **Ludovic Jourdin,** Stefano Freguia, Victoria Flexer, and Jurg Keller. Bringing high-rate, CO_2-based microbial electrosynthesis closer to practical implementation through improved design and operating conditions. To be submitted to *Environmental Science & Technology*, 2015.

This paper has been modified and incorporated as Chapter 9.

Finally, Chapter 10 gives an overview of the main conclusions of this thesis as well as perspectives and recommendations for future research and development towards practical implementation of microbial electrosynthesis. This latter section includes economic feasibility studies of several potential practical implementations of MES.

4 Research materials and methods

Electrode materials, electrode preparations and characteristics, bioelectrochemical reactor setup and operations, electrochemical experiments, analytical methods, titration and off-gas analyses, biofilm analysis techniques and microbial community analysis are described in this Chapter.

4.1. Electrode preparations

4.1.1. Preparation of graphite plates

Graphite plates (50 mm x 19.3 mm x 4 mm; Morgan AM&T, Sydney, NSW, Australia) were used as cathode electrodes for the autotrophic growth study presented in Chapter 5, and as a control electrode for microbial electrosynthesis of organics from CO_2 presented in Chapter 6. They were specifically modified by making 1.4 mm deep grooves on each side, in order to obtain 8 easily detachable 8.5 mm^2 squares per electrode, for further analysis (Figure 7). The total surface area of the modified plates was calculated to be 29 cm^2. The graphite electrodes were washed with 1 M hydrochloric acid, 1 M sodium hydroxide (24 hours in each), and deionized water in succession to remove organic and metal contamination prior use in BES.

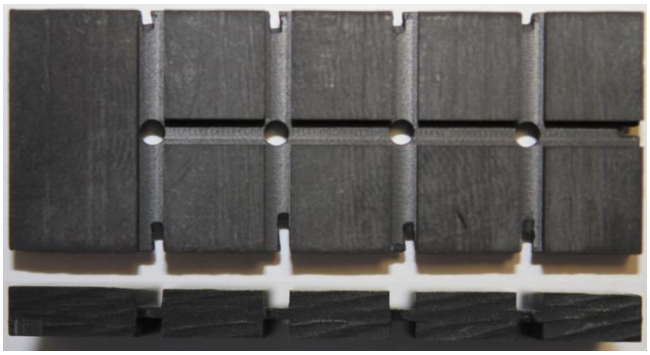

Figure 7 Specifically modified graphite plate.

4.1.2. Preparation of NanoWeb-RVC – Chemical Vapour Deposition technique

Synthesis of NanoWeb-RVC has previously been reported [146, 155]. CNT NanoWeb was grown using chemical vapour deposition (CVD) onto reticulated vitreous carbon (45 pores per inch (ppi), Duocel, ERG Materials and Aerospace Corporation), which was first coated with a thin layer of catalyst solution consisting of 10% (w/w) iron(III) *para*-toluenesulfonate (Baytron) in ethanol. Substrates were briefly immersed in the 10% (w/w) catalyst solution before being removed, shaken

to remove excess solution, and then allowed to dry until all the excess oxidant had drained. The solvent was then removed using a 100 ºC oven. CVD growth of the NanoWeb material was achieved using a Thermal CVD system (Atomate). Initially the system was flushed with Ar (200 mL min^{-1}) for 30 minutes, after which the furnace temperature was increased to 600 ºC whilst a mixture of Ar (150 mL min^{-1}) and H_2 (20 mL min^{-1}) was passed through the furnace. The furnace temperature was then maintained at 600 ºC for 10 minutes, resulting in reduction of the iron (III) catalyst to iron nanoparticles. Growth of the NanoWeb was then initiated by ramping the temperature up to 800 ºC at which point acetylene gas (10 mL min^{-1}) was passed through the furnace whilst maintaining a constant flow of Ar (200 mL min^{-1}) and H_2 (3 mL min^{-1}). Synthesis of the NanoWeb was complete after 30 minutes, at which point the furnace, acetylene and H_2 were turned off, and the system flushed continuously with Ar (150 mL min^{-1}) until the temperature was less than 100 ºC. Electrochemical characterisation with a classical reversible redox couple, ferrycianide 10 mM, of both NanoWeb-RVC and Unmodified RVC was carried out in a standard three-electrode cell with a 0.1 M $NaNO_3$ solution containing at a scan rate of 5 mV s^{-1}. MES to organics performance on NanoWeb-RVC was studied and outcomes are presented in Chapter 6.

4.1.3. Preparation of EPD-3D – Electrophoretic Deposition technique

We harnessed the throwing power of electrophoretic deposition to form multiwalled CNT coatings onto RVC to generate a new hierarchical porous structure, hereafter called EPD-3D, which we used as biocathode electrode for microbial electrosynthesis of organics from CO_2. EPD-3D electrodes were used to answer several research questions as presented in Chapters 7, 8 and 9.

Reticulated vitreous carbon foam was activated by immersion in 2 M HNO_3 overnight. The RVC was then cleaned by washing with Milli-Q water after which it was oven dried for 3 hours. A wire was attached to the RVC using silver paste to ensure good electrical conductivity.

Multiwalled carbon nanotubes (MWCNT) were oxidised to facilitate dispersion in water. This was done by first plasma treating the MWCNT in air for 30 seconds. The MWCNT were then dispersed in a 1:1 mixture of 3 M H_2SO_4 and 3 M HNO_3 using a Branson B1500R-MT bath sonicator for 2 hours. The dispersion was then centrifuged at 4400 rpm for 30 minutes using an Eppendorf Centrifuge 5415 D. The solids were collected and washed with water after which centrifugation was repeated. This washing step was done four times; the solids were then collected and oven dried. The MWCNT were then dispersed in Milli-Q water at a concentration of 0.1 mg/ml using a Branson S450-D 400 watt Sonifier. A 1/8 inch tapered microtip was used during sonication with 20 % amplitude for 1 hour.

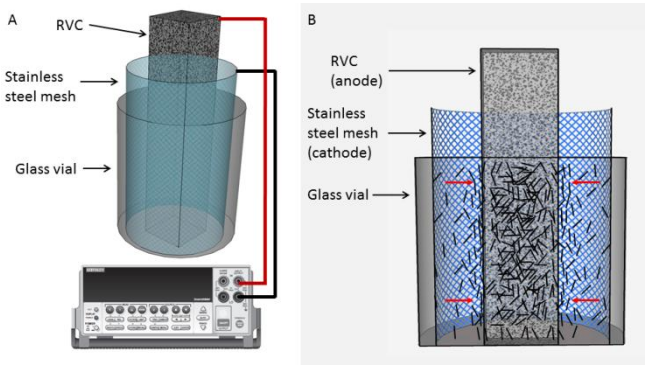

Schematic 1 Illustration of (a) System set-up for EPD process; and (B) Cell-set-up for EPD deposition of MWNT.

The MWCNT dispersion was then added after which electrophoretic deposition (EPD) was carried out using a Keithley 2400 sourcemeter wherein 10 V was applied for 10 minutes. The negative terminal of the sourcemeter was connected to stainless steel mesh bent in a cylinder and placed in a vial (See Schematic 1). The RVC was connected to the positive terminal of the sourcemeter and positioned in the centre of the stainless steel mesh cylinder. This was done to ensure uniform deposition on the RVC.

4.1.4. Current collector and plasma treatment

All the electrodes (graphite plates, unmodified RVC, NanoWeb-RVC, EPD-3D) used in this PhD work were pierced with a 0.5 mm thick Ti wire that acted as a current collector. The electrical connection was reinforced by means of conductive carbon paint that was left to dry for 3 days. Epoxy glue was also applied on the immersed surface of the Ti wire to avoid any contribution of the Ti wire to the electrochemical performance.

All electrodes were pre-treated in a N_2 plasma for 20 minutes before being introduced in the reactor, in order to remove surface contamination and render the surface hydrophilic [124].

4.1.5. Electrode's projected surface area vs. total surface area

When using structured 3D electrodes as an electrode in bioelectrochemical systems, it is important to understand the difference between normalizing performance to projected or total surface area. The projected surface area of the electrodes refers to the maximal footprint of the electrode (the area of the base of the electrode, irrespectively whether it is a 3D or a flat electrode) [146] as described by the following equation:

$$Projected\ surface\ area = (l \times w) - x(l \times w)$$

where (l) and (w) represent the length and the width of the electrode, respectively (the thickness being the shortest of the three dimensions is not considered here), and (x) the percentage of the surface (pores) blocked by the carbon paint used to strengthen the electrical contact, which depends on the size of the departing electrode.

The projected surface area is of particular interest from an engineering perspective as it determines the size of a bioelectrochemical reactor for large scale applications. The total surface area refers to the area within the RVC scaffold before CNT deposition. This means we are considering the total surface area available for bacteria immobilization, i.e. including the surface area of the macropores within the scaffold. As reported previously [146, 155], as well as in this PhD work, the pores created within the carbon nanotube web are 100 nm or smaller (see Figure 19 and 22), i.e. they are at least one order of magnitude smaller than typical bacterial sizes (about 1 µm length, see Figure 19 and 27). Therefore, the additional nano-porous surface area created by the CNT deposition does not create more available surface area for bacterial immobilization, and hence is not considered as part of the 'total surface area'. The total (biofilm accessible) surface area of the electrode is being used to assess the intrinsic performance of the electrode materials. The total surface area for the macroporous RVC foam is therefore much higher than the projected surface area of the electrode. For a 45 ppi RVC scaffold, a value of 26.2 cm^{-2} cm^{-3} is given by the RVC manufacturer using the multipoint BET method by the adsorption of Krypton gas at cryogenic temperatures and is confirmed by Friedrich et al. (2004) [159]. Using the same references, values of 6.1 and 39.02 cm^{-2} cm^{-3} are found for 10 ppi and 60 ppi RVC scaffolds, respectively. Photographs of each RVC type can be seen in Figure 8. Since the carbon paint blocked a few of the pores, the surface area and the volume values used for normalization do not consider this area/volume.

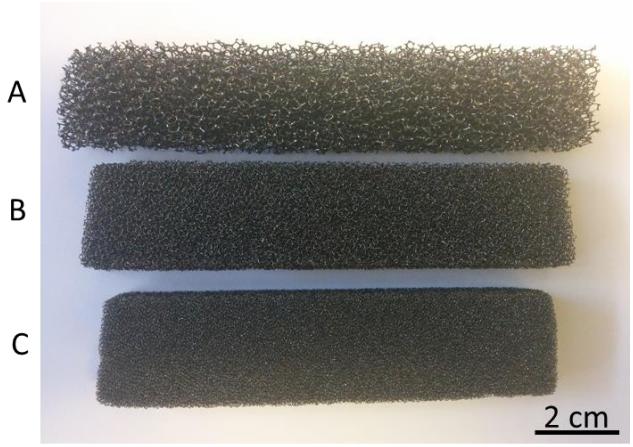

Figure 8 Photographs of three types of unmodified reticulated vitreous carbon A) 10 ppi, B) 45 ppi, and C) 60 ppi.

Both NanoWeb-RVC and EPD-3D electrodes as well as three pore sizes (10, 45 and 60 ppi) have been studied and the characteristics of each 3D RVC-based electrodes used in the frame of this PhD work can be found in Table 4 below.

Table 4 List of each electrode used in the frame of this PhD work, their geometrical characteristics and dimensions and the thesis chapter they are referred to in.

Thesis Chapter	Electrode type (electrode #)	RVC foam characteristic (ppi)	Average pore diameter (mm)	Dimension (mm x mm x mm)	Projected surface area (cm^2)	Total surface area (cm^2)
6	Unmodified-RVC (1 and 2)	45	0.56	1.6 x 1.25 x 0.46	1.85	24.9
6	NanoWeb-RVC (3 and 4)			0.6 x 0.6 x 0.6	0.32	4.1
7 and 9	EPD-3D (5)			1.21 x 1.19 x 1.03	1.36	36.9
7, 8 and 9	EPD-3D (6)			1.21 x 1.19 x 1.03	1.36	36.9
8 and 9	EPD-3D (7)	60	0.42	1.02 x 1.01 x 0.96	0.98	36.9
9	EPD-3D (8)	10	2.54	1.21 x 1.13 x 1.03	1.30	8.14
9	EPD-3D (9)			1.09 x 0.99 x 0.90	1.02	5.37

To assess performance from an engineering perspective, performance has also been normalized to the volume of the cathode electrode, taking into account its 3D nature and the total electrode surface available for biofilm development per unit volume. This would also correspond to an extrapolation of the performance normalized to the volume of a theoretical cathode chamber that would be completely filled with the 3D electrode of the same volume.

4.2. Source of microorganisms

A mixed microbial consortia from natural environments (stormwater pond sediments, located on the University of Queensland St Lucia campus, latitude -27.500373, longitude 153.015062) and engineered anaerobic systems (from the Luggage Point Waste Water Treatment Plant anaerobic digester, Brisbane, Australia) were combined. It was added as such to a final concentration of 60 mg L^{-1}, as chemical oxygen demand (COD), in the reactors described in Chapters 5 and 6. This amount of inoculum was very small compared to previous biocathode studies in order to easily monitor the actual growth of the microorganisms (Chapter 5). For the studies presented in Chapters 7, 8, and 9, planktonic cells from parent reactors that showed capable of microbial electrosynthesis were collected, centrifuged, resuspended in fresh catholyte and used as

inoculum for the MESs described. Therefore, we did not introduce any organics in the new reactors. The enriched inoculum was added to a final concentration of about 200 mg_{COD} L^{-1} in those reactors.

4.3. Fed-batch electrochemical experiments

All fed-batch bioelectrochemical experiments were carried out under strictly anaerobic conditions, at ambient temperature (ca. 24 +/- 1ºC) for the autotrophic biomass growth study (Chapter 5) and at 35 ºC for the MES to organics studies (Chapters 6 to 9), in three-electrode/two-chamber systems. All experiments were carried out under dark conditions to avoid phototrophic activity. Glass bottles were specifically designed, with a cathode chamber volume of approximately 300 mL. A 1 cm diameter, 15 cm long glass tube was inserted through the bottle top and served as the anode chamber, with platinum wire as counter electrode (purity 99.95%, temper hard, 0.50 mm diameter x 50 mm long, Advent Research Material Ltd, Oxford, England). The chambers were separated by a cation exchange membrane (Ultrex CM17000, Membranes International Inc., NJ, USA). Two ports were equipped with rubber septa to take samples from both the liquid phase and the headspace. A custom-made KCl saturated Ag/AgCl reference electrode was inserted into the bottle in proximity of the cathode. All potentials are reported in this PhD thesis versus Standard Hydrogen Electrode (SHE). A gas bag (Flexfoil plus, Air-Met Scientific Pty Ltd, QLD, Australia), specified for collection of CO_2, H_2 and CH_4, was connected to the reactor to measure gas composition and production rate and avoid pressure increase within the cathode chamber. A schematic and photographs of the BES reactor setup can be seen in Figure 9.

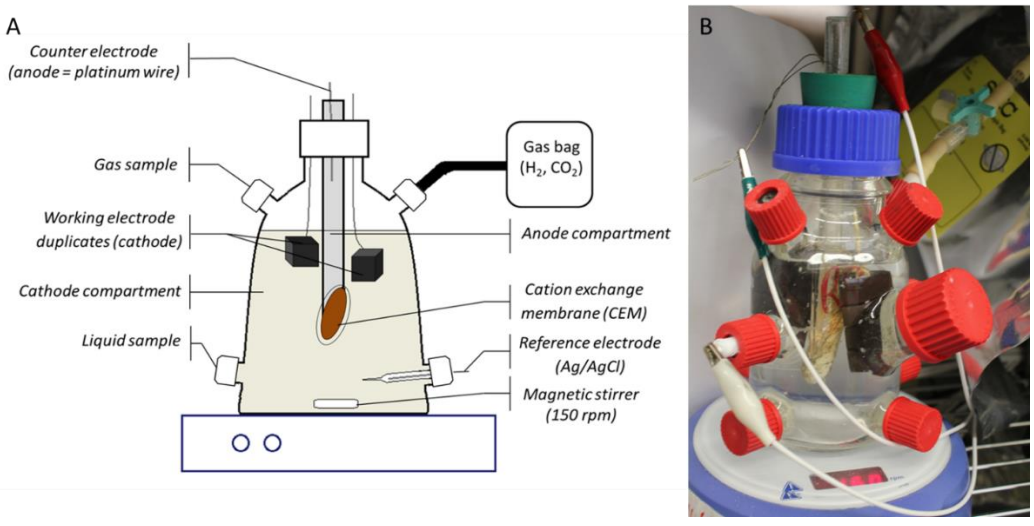

Figure 9 A) schematic and B) photograph of the bioelectrochemical system reactor set-up

The cathode chamber was filled with 250 mL of a medium containing: 0.2 g L^{-1} NH_4Cl, 0.04 g L^{-1} $MgCl_2.6H_2O$, 0.015 g L^{-1} $CaCl_2$, 6 g L^{-1} Na_2HPO_4, 3 g L^{-1} KH_2PO_4 and 1 mL L^{-1} of a mixed

trace element solution. $NaHCO_3$ to a final concentration of 0.5 to 4 g L^{-1} was added periodically as sole carbon source. The trace element solution contained 1.5 g L^{-1} $FeCl_3.6H_20$, 0.15 g L^{-1} H_3BO_3, 0.03 g L^{-1} $CuSO_4.5H_2O$, 0.18 g L^{-1} KI, 0.12 g L^{-1} $MnCl_2.4H_2O$, 0.06 g L^{-1} $Na_2MoO_4.2H_2O$, 0.12 g L^{-1} $ZnSO_4.7H_2O$, 0.15 g L^{-1} $CoCl_2.6H_2O$, 0.023 g L^{-1} $NiCl_2.6H_2O$ and 10 g L^{-1} EDTA. The medium was prepared under anaerobic conditions (flushed with 100% N_2) and introduced into the cathode compartment inside an anaerobic chamber. The anolyte used contained 6 g L^{-1} Na_2HPO_4 and 3 mg L^{-1} KH_2PO_4.

The BESs were operated in fed-batch mode. A multi-channel potentiostat (CH Instruments, Austin, TX, USA or VMP-3, Bio-Logic SAS, France) was used for all experiments. During all chronoamperometry experiments, the cathode was poised at either -0.5 V (Chapter 5) or -0.85 V vs. SHE (Chapters 6 to 9). The total charge (Coulomb) consumed was calculated by integrating the area under the current versus time curve (i-t curve). The pH was either controlled at 7 (Chapters 5 and 6) or at 6.7 (Chapters 7 to 9) by dosing 1M HCl as needed.

Periodically, cathodes were subjected to cyclic voltammetry (CV) and linear sweep voltammetry (LSV) for the identification of any catalytic effects. The scan range and scan rate used varied and are specified in each case.

4.4. Titration and off-gas analysis (TOGA)

4.4.1. TOGA sensor

The titration and off-gas analysis sensor developed by Gapes et al. (2001) [160] and Pratt et al. (2002) [161] for the study of wastewater treatment systems was modified for this study and is shown in Schematic 2. A pH probe (pH/ORP sensors, Endress + Hauser, Australia) was inserted in the BES reactor and a pH controller (Liquisys M, Endress + Hauser, Australia) was used to control the pH of the cathode. The cathode medium was recirculated through a smaller bottle (ca. 100 mL liquid volume) using a recirculation pump (Monarch Alloy, TECO Australia Pty Ltd, Australia) with a flow rate of ca. 200 mL min^{-1}. The reactor was additionally stirred with a magnetic stirrer to ensure thorough mixing. Liquid temperature was also measured using the same probe (pH/ORP sensors, Endress + Hauser, Australia). Both the BES reactor and the recirculation bottle were wrapped with flexible tubing through which water flowed from and to a water bath for the purpose of temperature control. The temperature was controlled at 31 ± 1 ºC throughout all the tests. Both the reactor and the recirculation bottle were wrapped in cotton to make temperature control easier

and constant throughout the day and all tubing were wrapped in aluminium foil to avoid illumination of light and phototrophic activity development.

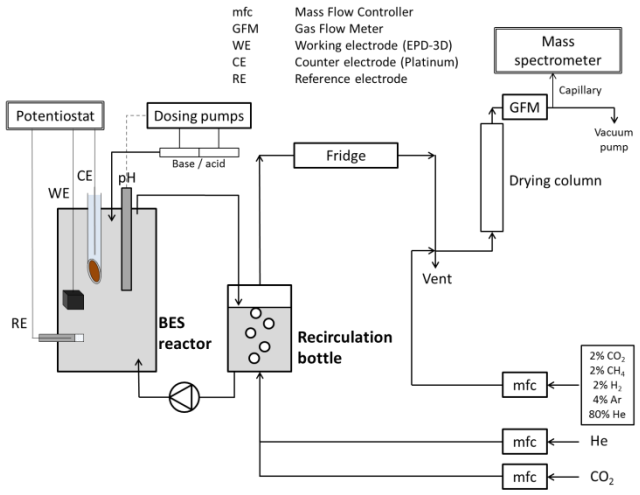

Schematic 2. Schematic of the TOGA sensor experimental apparatus. Briefly, gases (carrier gas and possibly CO_2) are sparged through a BES recirculation bottle, dried off afterwards and targeted gases (H_2, CO_2 and CH_4) are detected online by a mass spectrometer.

The off-gas measurement technique relies on the use of a quadrupole mass spectrometer (OmniStar, Balzers AG, Liechtenstein) in conjunction with a number of in-line mass flow controllers (MFC) (Bronkhorst Hi-tech, EI-Flow, Netherlands) [160, 161]. Helium (Ultra high purity, BOC, Australia) was used as carrier gas and supplied to the reactor via one mass flow controller (mfc) at a flow rate of 200 mL min^{-1} for each test. Carbon dioxide flow was controlled by another mfc and mixed with the helium flow before being introduced into the reactor for turnover condition tests. The last mfc was used to control calibration gas flow, which by-passes the reactor and was used for both the calibration of the mass spectrometer and as a baseline during experiments. This premixed gas was supplied from a cylinder (BOC, Australia), and had a defined composition of 2% CO_2, 2% CH_4, 2% H_2, 4% Ar and 90% He. The carrier gas was controlled (200 mL min^{-1}) to provide sufficient stripping driving force, and so that the mass spectrometric intensity signal for the targeted off-gas components (in this case, H_2, CO_2 and CH_4) could be maintained within a narrow range throughout the experiment [160]. During experiments, gas was fed to the recirculation bottle to avoid any disturbance of the cathode electrode in the BES reactor itself. As previously described, humidity was removed from the gas emerging from the recirculation bottle by passing it through a water trap after cooling down the gas through a 4 m copper coiled tube immersed in an cold water bath [160]. The gas was further dried through a drying column where dry air was used to drive moisture out of the gas across a membrane, prior to sampling by the mass spectrometer. The majority of the off-gas was vented prior to measurement, reducing pressure fluctuations at the mass spectrometer capillary inlet [160].

For the calibration of the mass spectrometer, the carrier gas (with or without CO_2 depending on whether it was used for the test) was sparged, at the same flows as used for the experiment (200 mL min^{-1}), through a calibration bottle instead, which had the same volume than the recirculation bottle and was filled with the same catholyte solution as described above. Different flows of the calibration gas were used to obtain regression lines for each targeted gas. Deviation of the signals over the time of the experiment was taken into account by performing a calibration before and after each experiment. Argon, an inert gas, was used as an internal standard. The flow rates of the targeted gases (H_2, CH_4, CO_2) were then determined by measuring the change in their concentration relative to the argon gas [161].

The measured flow-rates of H_2 in mL min^{-1} were converted in mol of H_2 using the ideal gas law and further converted in mA (i.e. current assimilated into H_2) using Faraday's law, which is the final H_2 form plotted and referred to in the research outcome chapters 8 and 9. H_2 that might have been produced but consumed within the biofilm, and hence not detected by the TOGA sensor, is not taken into account by the parameter "current assimilated into H_2".

4.4.2. Electrochemical-TOGA tests (related to work presented in Chapter 8)

After the reactor (electrode 6) was installed on the TOGA sensor setup, cathode potential of -0.85 V vs. SHE was applied over a period of about 87 days (current density evolution can be seen in Figure 28) and only momentarily stopped, as indicated in the text, to perform linear sweep voltammetry tests. It has to be stressed here that the TOGA sensor could not be used at all times for online gas measurement, but the same recirculation setup was used at all times nevertheless. For each turnover condition test that was performed, CO_2 was mixed with the carrier gas at a flow rate of 70 mL min^{-1}.

- Electron flux investigation

To investigate the electron fluxes and elucidate possible syntrophic interactions within the cathodic microbial community, different tests were performed with the TOGA sensor on EPD-3D reactors (electrodes 6 and 7). Chronoamperometry experiments with the cathode potential poised at -0.85 V vs. SHE in both turnover and non-turnover conditions (i.e. with or without carbon dioxide, respectively) were performed, at constant pH of 6.7. Liquid samples for VFA analysis were taken at the beginning and at the end of each test. Additionally, linear sweep voltammetry (LSV) at pH 6.7 in both turnover and non-turnover conditions as well were performed around day 30 to 35. The potential was scanned from 0 to -1.0 V vs. SHE, unless otherwise specified, at a slow scan rate

of 0.1 mV s^{-1}. Chronoamperometry and LSV tests with the TOGA sensor and in the exact same conditions were also carried out on an abiotic control equipped with the same cathode material (EPD-3D-45 ppi), without an inoculum addition, for comparison with biocathode performance.

- Biofilm / planktonic cells relative importance to MES performance

The respective importance of both biofilm and planktonic cells on organics production rate was assessed by replacing the whole of the cathode medium with fresh cell-free medium, and performing chronoamperometry at -0.85 V vs. SHE; liquid samples were taken at the start and end of each test.

- Biofilm removal

We further investigated the role of the biofilm on the MES performance. To do so, the system underwent several extreme conditions in order to remove the biofilm. Firstly, the pH was decreased to 2 for 2-3 hours, then the reactor and recirculation bottle were autoclaved while the rest of the setup was sterilized with EtOH, and finally, the electrode was taken out and air-dried for a week. After each treatment, the electrode was reconnected and current recorded at the same applied potential of -0.85 V vs. SHE. The duplicate reactor (electrode 7) underwent the low pH and autoclave treatment only.

4.4.3. Electrochemical-TOGA tests (related to work presented in Chapter 9)

Linear sweep voltammetry (LSV) experiments from 0 to -1.1 V vs. SHE (unidirectional) at a scan rate of 0.1 mV s^{-1} and pH 6.7 using CO_2 were performed using the TOGA sensor to investigate the effect of applied potential on MES performance (electrode 6). Chronoamperometry tests at -0.85 V vs. SHE while screening pH from 6.7 to 3 using the TOGA sensor were also performed to assess the effect of pH on MES performance (electrodes 6 and 7).

Finally, chronoamperometry tests at -0.85 V vs. SHE cathode applied potential at pH 6.7 using biogas-like gas mixture (CH_4-CO_2 70:30) as sole carbon source (instead of feeding pure CO_2) were performed with the TOGA sensor. This experiment was performed on the MES reactor described above (electrode 6) after the current had decreased to about -30-35 A m^{-2}, possibly due to a large number of LSV experiments conducted on this reactor that may have affected the performance of this biocathode (Figure 28). Without using the TOGA sensor but the same reactor setup described above, the biogas mixture was sparged in the recirculation bottle at a flow rate of 35 mL min^{-1} for about 13 days and the current and VFA production were followed while a cathode

potential of -0.85 V vs. SHE was applied at pH 6.7. Chronoamperometry tests using the TOGA sensor were carried out on both days 4 and 7 (refer to Chapter 9), as described above.

4.5. Characterisations

4.5.1. Scanning Electron Microscopy (SEM) - Energy-Dispersive X-ray Spectroscopy (EDS)

Scanning electron microscope images of the bare RVC-CNT electrodes, before being used in BESs, showed in Chapters 6 and 7, were obtained using a JEOL JSM 7500FA cold-field-gun field emission microscope.

Biocathode electrode samples (Chapters 6, 7, and 8) were fixed in 5% glutaraldehyde for 2 h. The samples then underwent a MQ water postfix wash. Dehydrated (<24 h in a high vacuum desiccator) and subsequently carbon coated (QT150TS Turbo-pumped coater, Argon purged) samples were imaged in secondary electron mode employing a XL30 Philips conventional (LaB6 source electron gun) Scanning Electron Microscope. Samples were imaged at 10-20 kV acceleration, 8-12 mm working distance and 5-6 spot size. EDS data (Chapter 8) was collected employing the same XL30 Philips conventional SEM.

4.5.2. Fluorescent In Situ Hybridization (FISH)

Scratched biofilm were first fixed with 4% PFA for two hours and then washed with phosphate buffered saline (PBS, 130mM sodium chloride, 10mM sodium phosphate buffer, pH 7.2) and stored at 1:1 100% ethanol: PBS. FISH was performed according to the protocol described by Manz et al. (1993) [162]. Details of the oligonucleotides FISH probes used in each chapter (5 and 8) are listed. The slides were viewed under Zeiss Axioscope LSM510 confocal microscope (Zeiss, Germany).

Table 5 Details of oligonucleotide probes used for FISH in Chapter 5.

Target population(s)	FISH probe – fluorochrome	Probe sequences (5'-3')	References
Bacteria	EUB338 – Cy3	GCT GCC TCC CGT AGG AGT	Amann et al. [163]
	EUB338II – Cy3	GCA GCC ACC CGT AGG TGT	Daims et al. [164]
	EUB338III – Cy3	GCT GCC ACC CGT AGG TGT	Daims et al. [164]
Betaproteobacteria	Bet42a – Cy5	GCC TTC CCA CTT CGT TT	Manz et al. [165]

Table 6 Details of oligonucleotide probes used for FISH in Chapter 8.

Target population(s)	FISH probe – fluorochrome	Probe sequences (5'-3')	References
Bacteria	EUB338 – Cy3	GCT GCC TCC CGT AGG AGT	Amann et al. [163]
	EUB338II – Cy3	GCA GCC ACC CGT AGG TGT	Daims et al. [164]
	EUB338III – Cy3	GCT GCC ACC CGT AGG TGT	Daims et al. [164]
Betaproteobacteria	BET42A – Cy5	GCC TTC CCA CTT CGT TT	Manz et al. [165]
Firmicutes	SRB 385 – Cy5	CGG CGT CGC TGC GTC AGG	Amann et al. [163]

4.6. Microbial community analysis

4.6.1. Community analysis presented in Chapter 5

In a sterile fumehood, cathode graphite squares were placed in a minimum volume of DNA-free water in a petri-dish and the biofilm was scraped off with a sterile disposable knife to suspend the cells in solution. DNA was extracted by using a PowerSoil DNA isolation kit (MO BIO Laboratories) according to the manufacturer's instructions.

DNA was then amplified by PCR using universal primers pyroLSSU926F and pyroLSSU1392wR [166]. The PCR products were then quantified on a TapeStation, gel extracted, and amplified by emulsion PCR before sequencing on a GS FLX pyrosequencing platform

(Hoffmann-La Roche Ltd). The nucleotide collection (nr/nt) of the National Center for Biotechnology Information (http://www.ncbi.nlm.nih.gob/BLAST/) was searched by using the BLASTn algorithm to analyse the sequences. MEGA 5.2.2 was used to align these sequences.

4.6.2. Community analysis presented in Chapter 8

Biofilm and planktonic cells were collected from two replicate biocathodes (electrodes 6 and 7) under steady MES performance. Those reactors were started using the same inoculum and electrode materials as described above and reached the same performance (data not shown). Genomic DNA was separately extracted with FastDNA SPIN Kit for Soil (MP Biomedicals, Santa Ana, California, US) according to manufacturer's protocol. 300 ng DNA of each sample were provided to Australian Centre for Ecogenomics (ACE) for 16S rRNA Amplicon paired-end sequencing by Illumina Miseq Platform using 926F (5'-AAACTYAAAKGAATTGACGG-3') and 1392wR (5'-ACGGGCGGTGWGTRC-3') primer set [167].

Raw paired reads was first trimmed by Trimmomatic [168] to remove short reads (less than 190bp) and low quality (lower than Phred-33 of 20). The trimmed paired reads was then assembled by Pandaseq [169] with default parameters. The adapter sequences were removed by FASTQ Clipper of FASTX-Toolkit [170]. The joined high quality sequences was analysed by QIIME v1.8.0 [171] using open-reference OTU picking strategy by uclust [172] at 1% phylogenetic distance and assigned taxonomy by uclust against greengenes database (13_05 release [173, 174]). OTUs with only one read were filtered from the OTUs table by command filter_otus_from_otu_table.py in QIIME. In house script "Normaliser" (https://github.com/minillinim/Normaliser) was used to find a centroid normalized OTUs table with 40000 reads per sample. The normalized OTU table was imported into R, version 3.0.1 (R Development Core Team, 2012) to generate heatmap with function pheatmap in Package "pheatmap" (http://cran.r-project.org/web/packages/pheatmap/pheatmap.pdf).

4.7. Analytical methods

Liquid samples (11.5 mL) were taken out of the cathode compartment through a rubber stopper using a 15 mL syringe equipped with a sterile needle, and were immediately filtered through a 0.22 µm filter.

Volatile fatty acids were measured using a gas chromatography (GC) apparatus (Agilent Technologies 7890A GC System) equipped with a flame ionisation detector (FID; 10 mL min^{-1} N_2;

250ºC) and a polar capillary column (DB-FFAP 15 m x 0.53 mm x 1.0 µm). High purity helium flowing with an initial flow of 12.5 mL min^{-1} was used as carrier gas. 0.9 mL sample was added to 0.1 mL of 10% formic acid solution and 0.5 µL of this mixture were injected in pulsed splitless at 220ºC. The detection limit of this method was about 2 ppm.

Analytik Jena multi N/C 2100S Total Organic Carbon Analyser was used for the total inorganic carbon (TIC) analysis and followed the bicarbonate consumption. 250 µL samples were injected into a 2.6 M phosphoric acid solution and the resulting carbon dioxide was stripped of the solution and into the near infrared detector with a stream of oxygen.

Gas samples of 5 mL were taken from the reactor headspace using a gas tight syringe. Beforehand, the gas bag was disconnected from the reactor and the volume of gas produced between two sampling steps was assessed and a N_2-full gas bag was connected to the reactor. Methane, hydrogen and carbon dioxide gases were measured on a gas chromatography-Thermal Conductivity Detection (GC-TCD). The system was a Perkin Elmer auto system GC-TCD with a 2.44 m stainless steel column packed with Haysep (80/100 mesh). The GC was fitted with a GC Plus Data station, Model 1022 (Perkin Elmer, Waltham, MA, USA). High purity nitrogen (99.99%) was used as carrier gas at a flow rate of 24.3 mL/min and a pressure of 380 kPa. The injection port, oven and detector were operated at 75 ºC, 40 ºC and 100 ºC, respectively. The detection limit for that technique was of about 2% content for each gas.

Chemical Oxygen Demand (COD) was determined by the dichromate method [175] with level of detection of 25 mg_{COD} L^{-1}.

Optical density of non-filtered samples was assessed using a UV-visible spectrophotometer (Varian, Cary 50 Conc UV-Visible Spectrophotometer, California, USA) at 660 nm.

5 Autotrophic hydrogen-producing biofilm growth sustained by a cathode as the sole electron and energy source[1]

As discussed above in sections 2.3 and 3.1, contradictory opinions exist on whether effective growth can be sustained at biocathodes. Here we report the generation of a microbial biocathode with living cells, which are able to self-regenerate and grow using the cathode as the sole electron donor and CO_2 as the only carbon source, for long-term sustained hydrogen production. This study also highlights a new H_2-producing electroactive microorganism enrichment method using CO_2 while avoiding archaea and methanogen development as well as any other H_2-consuming species (e.g. acetogens). This study shows that autotrophic electroactive biofilm growth can be sustained using a biocathode as the sole electron source for proton reduction to hydrogen.

Two bioelectrochemical reactors were filled with 0.25 L of inorganic medium that contained bicarbonate as sole carbon source. Each was equipped with two 29 cm^2 graphite plate electrodes (connected together) and polarized at -0.5 V vs SHE. Small current of about 2 $\mu A\ cm^{-2}$ was recorded before inoculation. Inoculum was added to both on day 0. Reported in the text are the values obtained on one of the two reactors (the 'main' reactor) unless otherwise specified. The results obtained on the duplicate reactor are also plotted below and were in close accordance with the main reactor.

CO_2 and electron consumption without soluble organic carbon production or planktonic cells

The development of the inorganic carbon and electron consumption during chronoamperometry at applied potentials of -0.5 V vs. SHE is shown in Figure 10.

[1] This chapter has been published and modified for incorporation in this thesis: **Ludovic Jourdin**, Stefano Freguia, Bogdan C. Donose, and Jurg Keller. Autotrophic hydrogen-producing biofilm growth sustained by a cathode as the sole electron and energy source. *Bioelectrochemistry*, 2015, 102, 56-63.

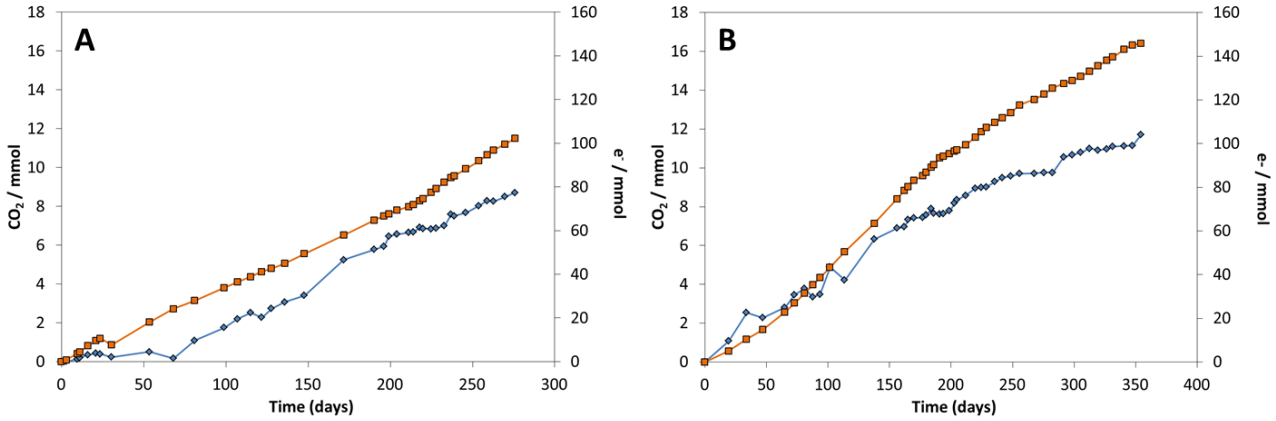

Figure 10 Carbon dioxide (diamond) and electron (square) consumptions development during chronoamperometry at applied potentials of -0.5 V vs. SHE on both A) the main reactor and B) the replicate reactor.

An exponential increase of the cathodic current in the first 25 days following the addition of the inoculum was observed. This can also been seen on the actual current evolution over time in Figure 11A. Once stable performance was reached, a nearly constant carbon dioxide and electron consumption (averaged with the duplicate reactor) of about 0.036 ± 0.007 mmol day^{-1} and 0.40 ± 0.04 mmol day^{-1} (7.7 ± 0.7 μA cm^{-2}), respectively, was recorded. Those rates for the duplicate experiment were within 15-20% (Figure 11B). During the same period, no planktonic cell development was observed with both optical density and chemical oxygen demand (COD) in the solution remaining equal to zero and below the level of detection (<25 mg_{COD}/L), respectively. Similarly, neither soluble organics nor gaseous methane production was detected over the course of the experiment.

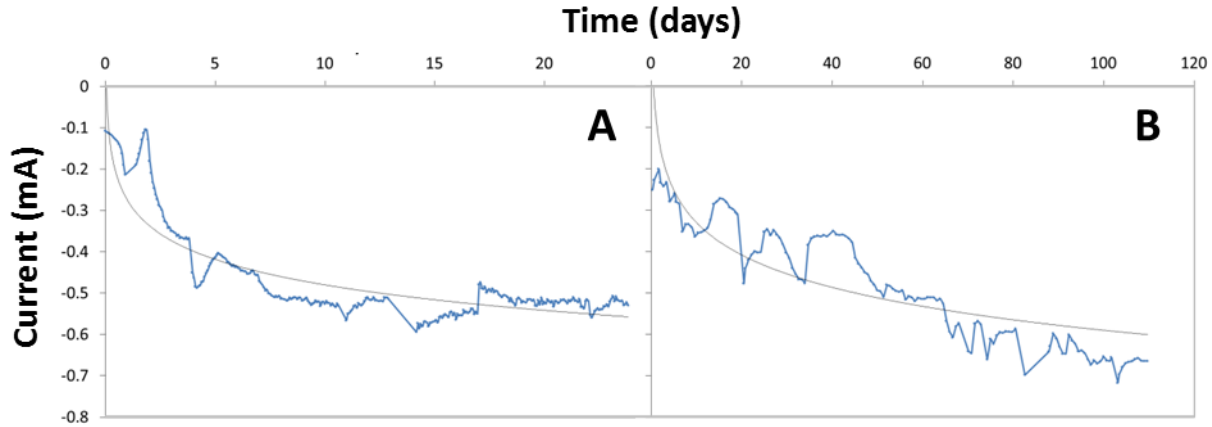

Figure 11 Cathodic current evolution in the first days following the addition of the inoculum until stable performance was reached on A) the 'main' reactor and B) the replicate reactor.

Bioelectrocatalytic activity is sustained for a long period of time

The electrochemical performance of the biocathode, on days 200 and 275, was compared to that of the abiotic control electrode on the basis of cyclic voltammograms recorded at pH 7 (Figure

12A). Higher current was generated by the biocathode compared to the control electrode over the complete measuring range of the CVs. Remarkably, a clear shift of the reductive wave onset can be noticed towards higher potentials (ca. -0.60 V vs. SHE) compared to the onset of current in the abiotic reactor (-0.83 V vs. SHE). This may be an indication of biological catalytic activity on the surface of the electrode [15, 104], which in this case is sustained for a long period of time. Furthermore, while the reductive wave onset remained constant around the same potential when the reactor was run chronoamperometrically at -0.5 V vs. SHE until day 276, a further shift to higher potential was observed on the CV recorded 91 days after the potential was decreased to -0.75 V vs. SHE. This increase in putative biological catalytic activity may be due to an increase of the biomass on the electrode following a period of higher activity. Similar trends were observed on the duplicate reactor (Figure 12 B).

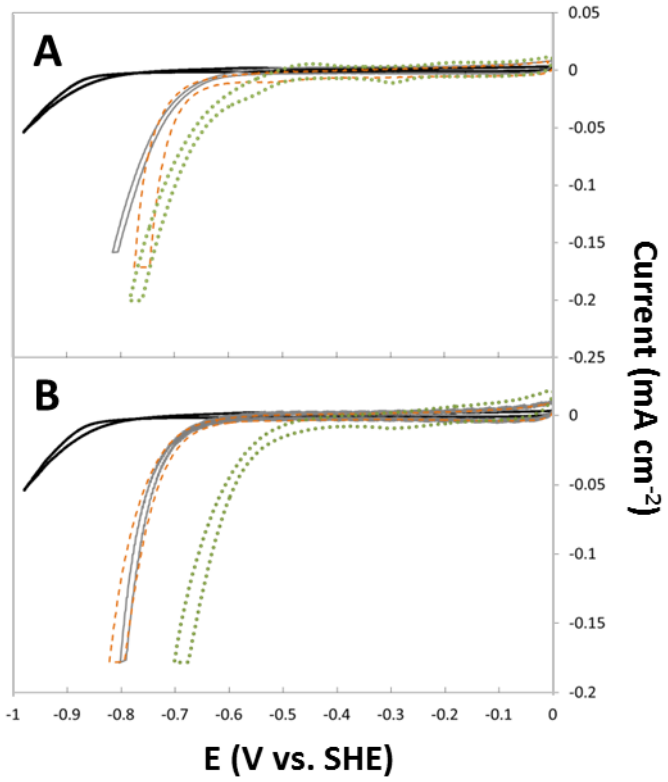

Figure 12 Cyclic voltammetry on abiotic reactor (black solid line) and biotic BES over time after inoculation; A) after 200 days (grey solid line), 275 days (dashed line) and 367 days (i.e. 91 days after switching cathode applied potential to -0.75 V vs. SHE; dotted line) on the 'main' reactor, and B) after 172 days (grey solid line), 242 days (dashed line) and 371 days (i.e. 15 days after switching cathode applied potential to -0.75 V vs. SHE; dotted line) on the replicate reactor. Scan rate, 1 mV s^{-1}.

Evidence of biofilm development

- Scanning electron microscopy and FISH

SEM was used to visualize both the control electrode and the inoculated electrode (Figure 13A-C). The SEM images reveal that, at day 352, the surface was covered by irregular structures

which are a further indication of a likely development of a biofilm with uniform cathode coverage, whereas the control electrode appeared smooth with some minor grooves (likely pores in the graphite material). The hypothesis that these structures represent a biofilm is corroborated by the catalytic current observed from the CVs, as well as the observation of general bacteria and betaproteobacteria on the biocathode surface analyzed by FISH (Figure 13D-E). As the amount of biomass initially inoculated was extremely small, the uniform biofilm coverage over the whole electrode surface suggests that microorganisms grew and developed using CO_2 as the sole carbon source.

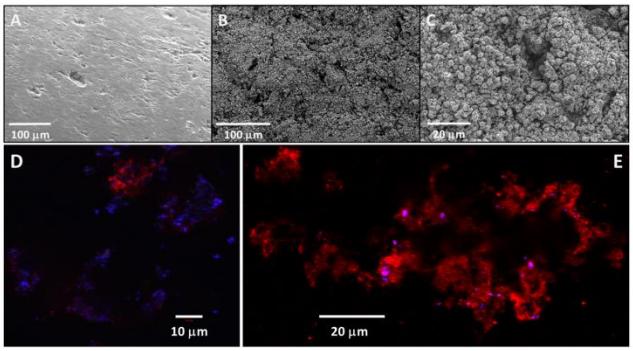

Figure 13 Scanning electron micrographs of the control electrode (A) and of the microbial biocathode biofilm (B-C), and confocal laser scanning micrographs of biocathode biofilm samples dual hybridized with EUB mix (Cy3 labelled - red) and Bet42a (Cy5 labelled - purple) probes (D-E), 352 days after inoculation at different magnifications. (For interpretation of the references to color in this figure legend, the reader is referred to the web version of this article.)

- Microbial community analysis

To confirm that the electrode was indeed covered with a biofilm and to assess the microbial community composition of such an autotrophic electroactive biofilm, DNA was extracted from the electrode scrapings taken at day 352 and the 16S rRNA genes were amplified for pyrosequencing. Similarly, the microbial community composition of the initial inoculum was also determined. Both phylum distribution and percent abundance of 16S rRNA of the initial inoculum and the biocathode biofilm can be seen in Figure 14 and 15, respectively. A dramatic change in the population composition was observed. From an inoculum containing 30.3 % of Archaea, the BES operated in these experimental conditions allowed for an enrichment of bacteria only, hence avoiding any methane-producing archaea to proliferate (Archaea fraction in biofilm <0.1%). Moreover, a considerable shift in the bacterial population groups occurred. Overall, the predominant bacterial phyla enriched after 392 days were *Proteobacteria* (57.3%), *Firmicutes* (12.4%), *Bacteroidetes* (11.6%) and *Actinobacteria* (1.1%). This major change in the bacterial community structure is a further strong indication that there has been a selective enrichment and growth of certain groups, while others have not been able to maintain their initial population fractions.

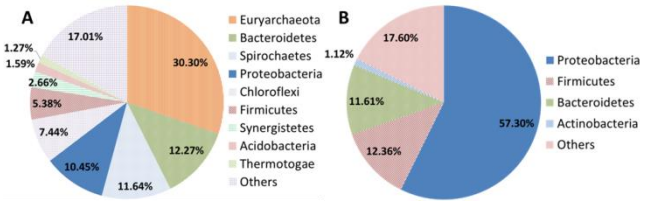

Figure 14 Phylum distribution of both the initial inoculum (A) and the biocathode biofilm on day 352 (B). Fractions shown as "Others" consist of phylogenetic groups with <1% abundance each and/or no blast hit.

Similar microbial communities were observed, by several research groups, on microbial biocathodes that catalyzed hydrogen production [176]. However, as mentioned above in the introduction, these systems were firstly enriched using acetate and autotrophic biofilm growth on biocathodes for sole proton reduction to hydrogen has not been demonstrated so far. Moreover, electron transfer and ATP generation mechanisms are yet to be identified. The first report on microbial electrocatalysis for H_2 production in naturally selected mixed-culture biocathodes was published by Rozendal et al. in 2008 [104], but only in 2011 Croese et al. (2011) identified the microbial population of this MEC [176]. Their bacterial population was very similar to the one determined in this work, and consisted of 46% *Proteobacteria*, 25% *Firmicutes*, 17% *Bacteroidetes*, and 12% related to other phyla, with *Desulfovibrio vulgaris* the dominant ribotype. In our study, the dominant ribotype (35%) was an uncultured species of *Rhodocyclaceae*. Using MEGA 5.2.2 and a BLAST search result (nearest match), 19 bacterium clones with >99% identity were found. Among them, 10 were previously found either in MFC or MEC for hydrogen production [177-179].

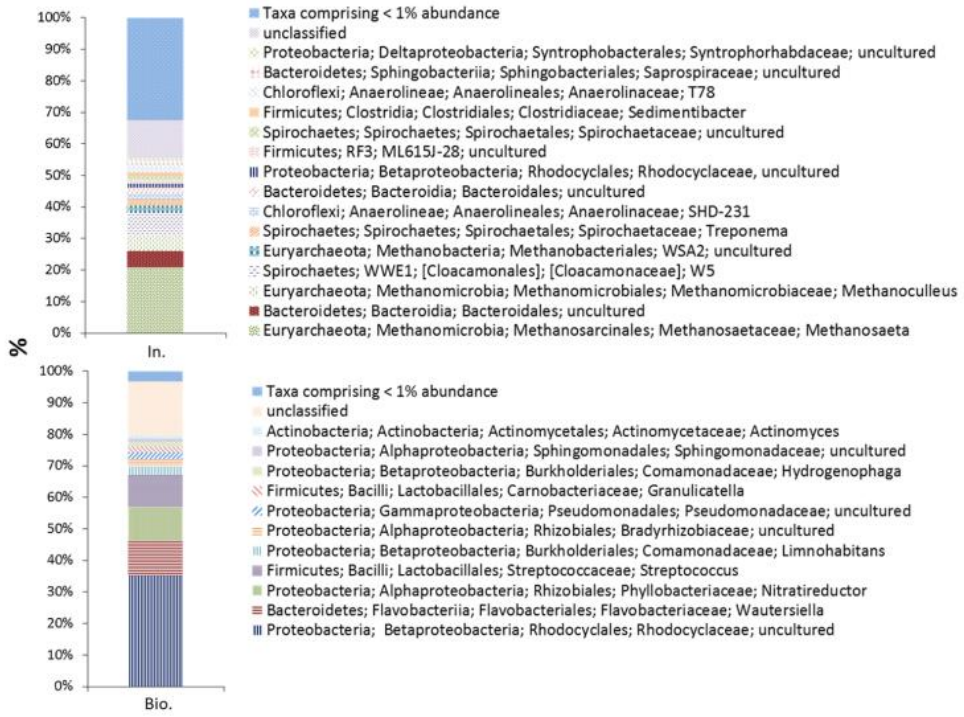

Figure 15 Percent abundance of 16S rRNA from both the initial inoculum (In.) and the biocathode biofilm (Bio.) on day 352.

Recently, some microorganisms have been reported to be able to conserve energy and grow through the sole reduction of protons to hydrogen, involving either an energy conserving hydrogenase or a hydrogenase with its proton-consuming-H_2-generating enzyme complex located at the cytoplasmic side of the cell membrane [180-182]. This was shown on microorganisms using formate as electron donor for the production of hydrogen in methanogenic systems. It was hypothesized that a membrane-integrated formate dehydrogenase oxidizes formate to bicarbonate and proton at the outside of the membrane, which is then coupled to proton translocation through the cell membrane via a membrane-integrated ATP synthase. Both the electrons from formate oxidation and the translocated protons are then consumed by a hydrogenase within the cytoplasm for hydrogen production [180]. *Desulfovibrio G11* was shown to gain energy and grow on formate from production of H_2 while in co-culture with *Methanobrevibacter arboriphilus AZ* as a hydrogen sink [180].

It has been suggested that H_2-producing microorganisms could conserve energy in a similar fashion by directly deriving electrons from a cathode [176, 183]. Both major classes of hydrogenases, the [Fe]-hydrogenases and the [NiFe]-hydrogenases, and whole cells containing these hydrogenases such as *Desulfovibrio vulgaris* were successfully immobilized on carbon electrodes for the production of H_2 using direct electron transfer [101, 102, 184, 185]. In all these studies, energy conservation was not assessed. However, Geelhoed et al. (2010) [183] and Croese et al. (2011) [176] calculated that the energy applied to MEC systems, taking into account energy losses and overpotential in the system, is enough to allow energy conservation and growth, assuming that the correct growth conditions (e.g. pH and temperature) are met and that a carbon source for growth is provided.

Hydrogen production coupled to energy conservation would allow for growing and self-regenerating biocathodes and may therefore enable a continuous catalytic activity [176]. Thus far, autotrophic microbial growth on such biocathodes for long-term continuous hydrogen production alone have not been experimentally proven and reported. Previously experiments were conducted only with heterotrophically grown biocathodes, demonstrating hydrogen-producing activity for up to two-month periods [104, 186].

Hydrogen yield tests

Hydrogen production was not accurately measurable at -0.5 V vs. SHE. We speculate that hydrogen production at this high potential, even though possibly enhanced by microbial catalysis, would be too small (max. 4.5 mL day^{-1} based on current) and the amount produced may diffuse out

of the reactor through the membrane and/or rubber stoppers and tubing. Similar diffusion losses have been reported by others [22, 23, 104, 186]. To increase the H_2 production rate and promote better detection, the applied potential was decreased to -0.75 V vs. SHE at day 276 and maintained for 100 days. The abiotic control BES was also run in the same conditions for comparison. Current densities and hydrogen production rates in both cases are reported in Table 7. Averages and standard errors were calculated between both microbial biocathode replicates. After the applied potential was decreased to -0.75 V vs. SHE, the current density immediately increased up to 0.188 +/- 0.002 mA cm^{-2}. Likewise, the carbon dioxide consumption rapidly increased about 2.2-fold up to 0.09 mmol day^{-1}. It should also be stressed here that throughout the 100-days test at lower potential, no soluble COD, VFA, and gaseous methane was measurable and the optical density remained equal to zero. It was also ruled out that potential planktonic cells could be all washed out due to sampling. Indeed, as mentioned in the materials and methods section 2.4, 11.5 mL sample were taken every 7 days, which would translate in a hydraulic retention time of about 152 days.

Table 7 Current densities and H_2 production rates of both microbial biocathode (averaged between both duplicates) and the abiotic control at -0.75 V.

	Current density (mA cm^{-2})	Measured hydrogen production rate (L H_2 m^{-2} day^{-1})
Abiotic cathode	0.0231 ± 0.0002	0.091 ± 0.004
Microbial biocathode	0.188 ± 0.002	9.2 ± 1.3

Higher current density (8-fold) and measured hydrogen production rate (100-fold) were recorded in the microbial biocathode versus the abiotic control. It seems that both abiotic and biological cathodes had H_2 diffusion losses. Indeed, electron recoveries as hydrogen were only 5.4% in the abiotic case and 39.4% in the biocathode. The fraction of hydrogen loss was higher for the low-current reactor, as would be expected. This suggests, along with population composition and bioelectrocatalytic activity assessed by CV that the extra hydrogen produced over long periods of time (>100 days) in the biocathode was from microbial origin. Moreover, no planktonic cell growth developed over the course of the experiment and a uniform biofilm was observed over the surface of the electrode; these observations are in line with what would be expected from a growing, adapting, and self-maintaining consortium of electrochemically active H_2-producing microorganisms.

Carbon and nitrogen consumption over time

To further demonstrate the growth of a biofilm on the surface of the electrode for proton reduction alone, both carbon dioxide and ammonium consumption over time were followed from day 100 to the end of the chronoamperometry experiment at -0.5 V vs. SHE (day 276) and are shown in Figure 16 A. The same representation for the duplicate is shown in Figure 16 B.

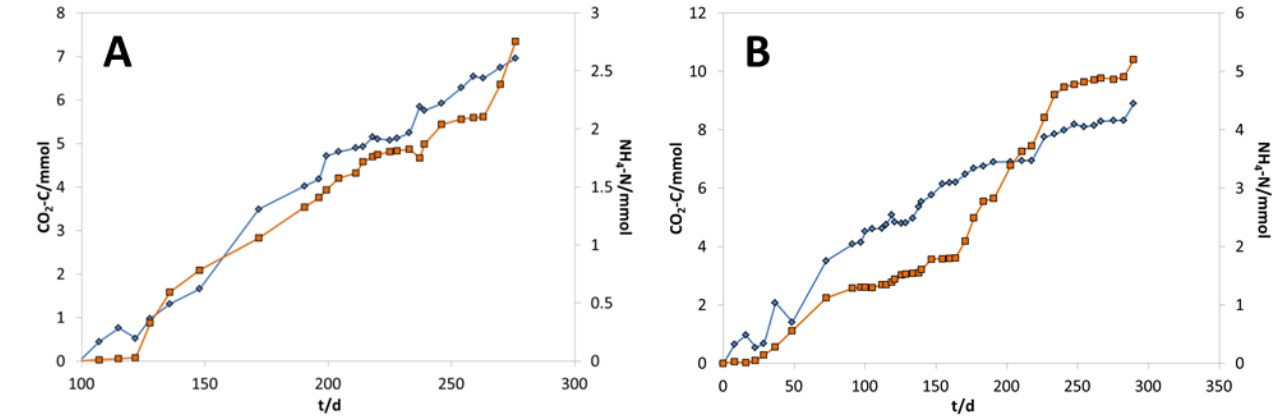

Figure 16 Linear carbon dioxide-C (diamond) and ammonium-N (square) consumption over time at -0.5 V applied cathode potential on the A) main reactor and B) replicate reactor.

As mentioned above, no extracellular carbon compounds (measured as soluble COD or gaseous CH_4) were produced in the cathode over time. However, continuous and largely constant inorganic carbon (CO_2) and nitrogen (NH_4^+) consumption was observed throughout the experiment. Based on this data, the average carbon to nitrogen consumption ratio, calculated point by point and then averaged, was 5.16 to 1. A very similar ratio of 5.3 to 1 was obtained on the microbial biocathode duplicate (Figure 16 B). The typically used 'generic' biomass composition formula of $CH_{1.8}O_{0.5}N_{0.2}$ has indeed a C:N ratio of 5:1 [187]. Additionally, we confirmed that neither carbon dioxide nor nitrogen were diffusing out of the cathode chamber as the concentrations of CO_2 and NH_4^+ were constant over time in the abiotic control (data not shown). Therefore, the carbon and nitrogen uptake ratio is consistent with previous observations for assimilation into biomass [188, 189].

These combined observations strongly suggest that a cathodic biofilm was growing and self-regenerating for over 1 year, while continuously producing hydrogen as the only metabolic product, using carbon dioxide and the electrode as sole carbon and energy sources, respectively. An approximate biomass formula $CH_{1.8}O_{0.5}N_{0.19}$ can be estimated from these results. Using the postulated biomass formula to convert the carbon uptake into biomass-COD, it can be calculated that after 276 days, about 0.3 g_{COD} of biomass had accumulated in the biofilm, a 20-fold increase from the initial inoculum of 15mg_{COD} used to seed the reactor. The evidence collected from the

literature suggests a possible catabolic reaction for ATP generation through proton translocation into the cells coupled to proton reduction to hydrogen by energy-conserving hydrogenase located at the cytoplasmic side of the cell membrane, using electrons transferred from the electrode [176, 183], as illustrated in Schematic 3. The ATP produced by ATP synthase through this pathway would be used for anabolic processes and thus growth. However, further investigation would need to be carried out to ascertain if this is indeed the metabolic pathway utilized by these electroactive microorganisms. The mechanism of electron transfer also needs to be elucidated.

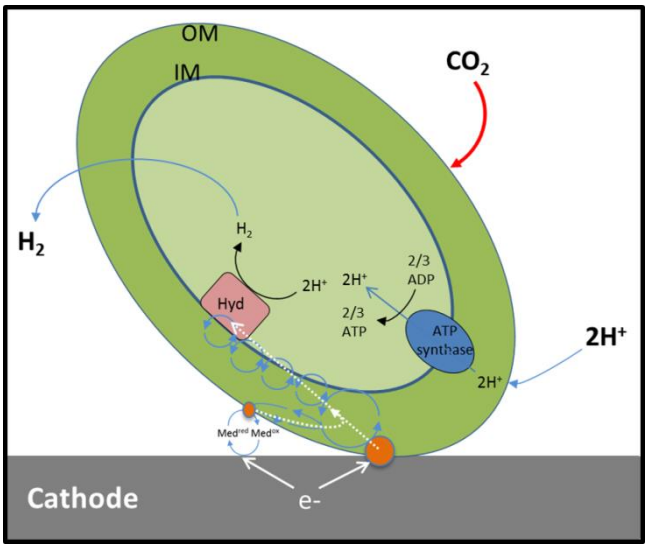

Schematic 3 Suggested mechanism for energy conservation and growth of H_2-producing bacteria using the cathode as the sole electron donor and CO_2 as carbon source. Hyd, hydrogenase, IM, inner or cytoplasmic membrane, OM, outer membrane, Med ox and red, mediator in oxidized and reduced form.

Additionally, this work demonstrates a novel method for the enrichment of H_2-producing microorganisms from starter cultures obtained from natural and engineered environments. This method does not require the establishment of syntrophic interactions with H_2-consuming populations, nor the addition of chemicals such as methanogenesis inhibitors. Even after switching the applied cathode potential from -0.5 to -0.75 V vs. SHE, which is low enough to support the growth of acetogens and methanogens [15, 190], neither organics nor methane were generated even after 100 days. This minimizes hydrogen losses compared to the reported studies working with mixed cultures [94, 177, 191-193] and provides more simplicity and flexibility than working with pure cultures. The fact that the hydrogen-producing activity can be sustained for such a long period of time (> 1 year) gives further confidence that this indeed represents a successful strategy for the selective enrichment of these hydrogen generating, electroactive biocatalysts. Additionally, it is believed that it is most likely not necessary to wait a whole year to get an enriched community of H_2-producing microorganisms, and further study should demonstrate this by performing microbial community analyses over time, starting at earlier stage.

In conclusion, autotrophic biofilm growth sustained by a cathode as the sole electron source for the reduction of proton to hydrogen alone was hence proven in this study. Indeed, a microbial biocathode was generated with living cells, able to self-regenerate and conserve energy during long-term (> 1 year) continuous hydrogen production at a cathode potential of -0.5 V vs. SHE. Moreover, a dramatic change in the microbial community composition was observed, which was devoid of methanogens (confirmed by lack of methane production), and of any other H_2-consuming microorganisms (e.g. acetogens). Future research should focus on elucidating the electron transfer mechanism and the metabolic pathway employed by these organisms.

6 A novel carbon nanotube modified scaffold as an efficient biocathode material for improved microbial electrosynthesis[2]

As discussed in sections 2.4 and 3.1, a novel biocompatible, highly conductive three-dimensional electrode manufactured by direct growth of flexible multiwalled carbon nanotubes on reticulated vitreous carbon (NanoWeb-RVC) is believed to hold many advantages for enhancement of MES from CO_2 and was investigated in this study. Results below show that NanoWeb-RVC achieves enhanced bacteria attachment and proliferation within its porous structure. The combined effect of both the macrostructure and the nanostructure of NanoWeb-RVC can effectively enhance current consumption and microbial electrosynthesis rates.

Two NanoWeb-RVC electrodes (electrode 3 and 4) were immersed in one reactor as duplicates for current consumption (see Table 4 in Chapter 4). Similarly, two unmodified RVC electrodes (electrode 1 and 2) were introduced in another reactor (Table 4). A third reactor with two graphite plate electrodes was used as control. Each bioelectrochemical reactors was filled with 0.25 L of inorganic medium that contained bicarbonate as sole carbon source. About 60 mg L^{-1} as COD of the mixed natural and engineered sludge was inoculated at time 0.

Starting right after inoculation, current consumption at a fixed cathode potential of -0.85 V vs. SHE was recorded during 140 days for the three electrode types. During this period, carbon dioxide consumption as well as volatile fatty acids production was followed for each reactor. Results for the three different types of electrodes were compared to assess efficiency. All data points in Figure 17 and 18 have been normalized to the total surface area of the electrodes. Reported values in the text have also been normalized to total surface area unless otherwise specified. Values normalized to both projected and total surface area are presented in Table 8 and Table 9. It is important to understand the difference between these two ways of normalizing the current density (see Materials and Methods section 4.1.5).

Current density enhancement

[2] This chapter has been published and modified for incorporation in this thesis: **Ludovic Jourdin**, Stefano Freguia, Bogdan C. Donose, Jun Chen, Gordon G. Wallace, Jurg Keller, and Victoria Flexer. A novel carbon nanotube modified scaffold as an efficient biocathode material for improved microbial electrosynthesis. *J. Mater. Chem. A*, 2014, 2, 13093-13102.

The cumulative electron consumption curves during chronoamperometry at constant applied potential of -0.85 V are shown in Figure 17. In all cases, the average of the two duplicate electrodes is plotted. Results of duplicates were in very good agreement and the standard deviation minimal.

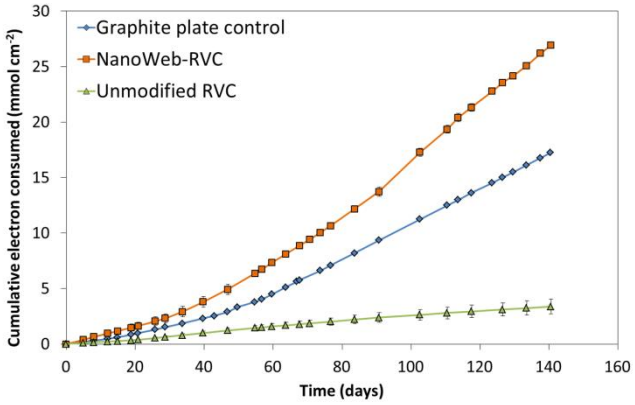

Figure 17 Cumulative electron consumption over time on graphite plate (red square), NanoWeb-RVC (blue diamond) and unmodified RVC (green triangle), normalized to the total surface area.

The electron consumption rate is defined as the slope of those curves at different time intervals. Table 8 summarizes the maximum electron consumption rate and the maximum current density values reached on each electrode. On graphite plate, the electrons were consumed at a slower rate within the first 33 days. Then, the electron consumption rate increased up to maximum rate of 0.157 mmol cm^{-2} day^{-1} over the last 85 days of the test. Three phases were observed on NanoWeb-RVC. A first lag period of 33 days, followed by a 2.3-fold rate increase with the consumption of 0.19 mmol cm^{-2} day^{-1} of electrons from day 33 to 91. Finally, from day 91 to the end of the test, 0.260 mmol cm^{-2} electrons were consumed, corresponding to a cathodic current density of 0.291 mA cm^{-2}. Conversely, a constant current throughout the 140 days of the experiment was recorded on unmodified RVC electrodes, with an electron consumption rate of 0.025 mmol cm^{-2} day^{-1}.

Table 8 Maximum electron consumption rates and corresponding current densities reached on the three types of electrodes normalized both to the projected and total surface area. Values shown were averaged from day 55 to 140 for graphite plates, from day 91 to 140 for NanoWeb-RVC and over the whole 140 days period for unmodified RVC.

	Electron consumption rate (mmol e- cm^{-2} day^{-1})		Current density (mA cm^{-2})	
	vs. projected area	vs. total area	vs. Projected area	vs. total area
Graphite plate control	0.157 ± 0.001	0.157 ± 0.001	0.176 ± 0.001	0.176 ± 0.001
Unmodified RVC	0.32 ± 0.07	0.025 ± 0.004	0.37 ± 0.08	0.028 ± 0.004
NanoWeb-RVC	3.3 ± 0.3	0.260 ± 0.004	3.7 ± 0.3	0.291 ± 0.004

Remarkably, the electron consumption rate (and hence the current density) on NanoWeb-RVC was higher than on graphite plate for the whole duration of the experiment, and reached values 65% higher over the last 50 days of the experiment. To the best of our knowledge, this is the first study reporting a higher current density normalized by total surface area for a porous three-dimensional electrode compared to a rough electrode.

Most literature reports on novel porous electrodes for bioelectrochemical systems report current values normalized to the projected surface area of the electrodes [11, 119, 122, 146, 148]. While these reports are certainly justified from an engineering perspective, they do not provide relevant information on the intrinsic efficiency of the electrode material. Indeed, for many reports on new materials, if the total current would be normalized to the total available surface area, these materials would lag behind when compared to conventional rough electrodes, such as carbon cloth or plates [11, 122, 146, 148]. With the exception of a few examples [117], the main reason for this failure is the lack of adequate porosity to guarantee efficient mass transport to and from the electrode surface.

Normalizing the NanoWeb-RVC performance by projected surface area results in a very high cathodic current density of 3.7 mA cm^{-2}. This current is 21 times higher than that measured for a rough graphite plate electrode, hence the NanoWeb-RVC is also an extremely efficient material from this perspective. Most strikingly, as far as we can ascertain, this value represents the highest current density for cathodic microbial CO_2 reduction and, in general, the highest cathodic current density ever reported. Min et al. (2013) [17], who studied MES of acetate from CO_2 in very similar experimental conditions to ours, reported about 1.8 mA cm^{-2} (vs. projected area) consumed at -0.9 V by a mixed culture on carbon felt. Rates of electron transfer from stainless steel cathodes to biofilms of Geobacter sulfurreducens consuming up to 2 mA cm^{-2} when reducing fumarate at higher applied potential (-0.4 V) were previously reported [75].

Even though a two times greater current density per projected surface area was observed on the unmodified RVC electrode compared to the rough graphite plate, this current corresponds to a 6 times lower electron consumption rate per total surface area. We will analyse the unmodified RVC case after the full experimental evidence has been presented, since in this case the current consumption seems to be associated with a different process.

For the novel NanoWeb-RVC, the combined effect of both the macrostructure and the nanostructure is believed to be the reason for such a high cathodic current density. Indeed, other CNT-based cathodes were not as efficient for microbial electrosynthesis of acetate. Zhang et al.

(2013) [11] obtained 0.022 and 0.021 mA cm^{-2} (projected surface area) with their CNT-cotton and CNT-polyester electrode versus 3.7 mA cm^{-2} obtained in this study. Evidently, even though both electrodes in that report and those described here comprise CNTs, they are inherently different in nature. Electrodes reported by Zhang et al. (2013) were prepared by dipping non-conductive substrates in a CNT ink. NanoWeb-RVC was synthetized by directly growing CNT on top of a highly conductive substrate, which will guarantee both the high conductivity of the electrodes as well as the homogeneous distribution of CNT on the electrode surface. Moreover, the experimental conditions in the previous work were different as the authors used a pure culture of *Sporomusa ovata* and a higher cathode applied potential of -0.5V.

Microbial electrosynthesis – CO_2 consumption and acetate production rate enhancement

The carbon dioxide consumption and volatile fatty acids production were followed throughout the experiments and are shown in Figure 18. The maximum rates can be seen in Table 9. The main product generated was acetate and no other volatile fatty acids or alcohols accumulated in any of the reactors, in agreement with other mixed culture microbial studies [15, 16]. We can observe that both CO_2 consumption and acetate production rates were much greater on the NanoWeb-RVC electrode than on the rough graphite electrode.

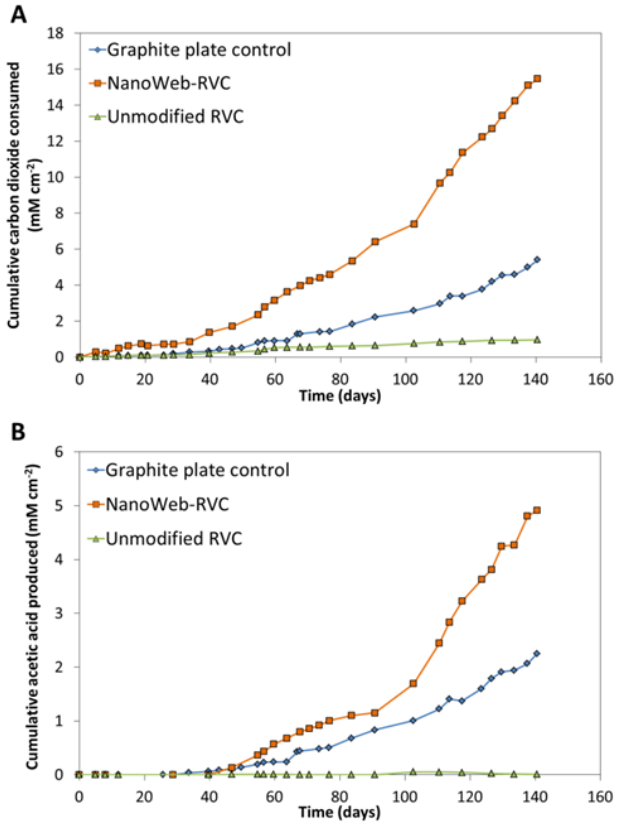

Figure 18 Carbon dioxide consumption (A) and acetate production (B) over time on graphite plate, NanoWeb-RVC, and unmodified RVC normalized by the total surface area.

Consistent with the electron consumption development shown in Figure 17, similar phases with increasing rates are observed on both graphite and NanoWeb-RVC electrodes. Lag phases of about 30 and 40 days, respectively, were observed with only a small amount of carbon dioxide consumed by the microbial cultures (0.005 and 0.028 mM cm^{-2} day^{-1}, for carbon plate and NanoWeb-RVC respectively) and no acetate generation. These lag phases can be explained by the very small amount of sludge inoculated (60 mg_{COD} L^{-1}, or 15 mg_{COD} in the cathode compartment). Quite linear trends were then observed on graphite plate electrodes, with maximum CO_2 consumption and acetate production rates of 0.078 and 0.039 mM cm^{-2} day^{-1}. On NanoWeb-RVC electrodes, a first increase was observed up to day 102 followed by a further rate enhancement until the end of the experiment. During this final period, maximum CO_2 consumption (0.210 mM cm^{-2} day^{-1}) and acetate production (0.10 mM cm^{-2} day^{-1}) rates were measured, which are 2.7 and 2.6 times greater than measured for the graphite electrode. It was calculated that, within the last phase of the experiments, 88 ± 16% and 77 ± 10% of the total inorganic carbon consumed was transformed into acetate in the graphite plate and NanoWeb-RVC reactors, respectively. It is assumed that the remaining inorganic carbon was assimilated into biomass. Similarly, 44 ± 22% and 70 ± 11% of the electrons consumed were recovered in acetate in the graphite plate and NanoWeb-RVC reactors respectively.

Table 9 Maximum CO_2 consumption and acetate production rates reached on the three types of electrode (averaged from day 102 to 140), normalized both by the projected and total surface area.

	CO_2 consumption rate (mM cm^{-2} day^{-1})		**Acetic acid production rate (mM cm^{-2} day^{-1})**	
	vs. Projected area	vs. total area	vs. Projected area	vs. total area
Graphite plate control	0.078 ± 0.007	0.078 ± 0.007	0.039 ± 0.009	0.039 ± 0.009
Unmodified RVC	0.070 ± 0.007	0.005 ± 0.001	0	0
NanoWeb-RVC	2.70 ± 0.08	0.210 ± 0.006	1.3 ± 0.2	0.10 ± 0.01

Remarkably, neither acetate nor any other organics were detected throughout the 140 days of operation in the unmodified RVC reactor. This is an indication of the significant importance of the nanostructure of the electrode material to achieve microbial electrosynthesis. Therefore, even though no apparent hydrogen was detected in the reactor, it is believed that most of the electrons consumed on the unmodified RVC were used for proton reduction to hydrogen and the (very small) amount produced may have diffused out of the reactor through the membrane and/or rubber stoppers and tubing. Similar diffusion losses have been reported previously [22, 23, 104, 186].

Comparatively, Zhang et al. (2013) [11] obtained a maximum rate of about 0.01 mM cm^{-2} day^{-1} of acetate with their CNT-cotton and CNT-polyester materials, versus 1.3 mM cm^{-2} day^{-1} on NanoWeb-RVC reported in this study. Min et al. (2013) [17] reported 0.387 mM cm^{-2} day^{-1} (vs. projected area) of acetate produced by a mixed culture at -0.9 V on carbon felt, under experimental conditions very similar to ours. Marshall et al. (2012) [15], who also used mixed microbial cultures, reported a high acetate production rate of 4 mM day^{-1} with graphite granules as cathode material. However, the available cathode surface area was not mentioned and a comparison can therefore not be made. Hence, to the best of our knowledge, we report here the highest acetate production rate obtained in a biocathode from CO_2 reduction, a production increase of more than an order of magnitude compared to previously published data [11, 17].

Concomitant to acetate production, hydrogen did not accumulate in the headspaces of the reactors, unlike what was reported by Marshall *et al.* (2012) [15]. Even though hydrogen was not detected, this does not exclude a possible mechanism of electron transfer from the cathode towards acetogens, through either abiotic or bio-catalysed hydrogen production. Indeed, it could be envisioned that hydrogen is produced and consumed by acetogens before detection could be possible. Therefore, it is possible that electrons are either being directly delivered from the cathode to the acetate-producing microorganisms, or through mediated electron transfer. Electron transfer via biotically generated hydrogen was hypothesized in a previous study for microbial electrosynthesis of methane and acetate [15], and it was recently shown that H_2-producing microorganisms could indeed sustain growth for long-term hydrogen production on biocathodes (Chapter 5). However, a detailed mechanistic study was beyond the focus of this work and further research needs to be undertaken to elucidate the extracellular electron transfer mechanisms occurring in such systems.

Biofilm development

Images of both NanoWeb-RVC before and 140 days after inoculation are shown in Figure 19. The CNT NanoWeb was successfully developed and appears as a fine roughness on the surface (Figure 19A and B), in contrast to the flat and smooth unmodified RVC (Figure 20A) [146]. The CNT NanoWeb was previously characterised and showed intertwined fine carbon nanotubes with an average diameter of about 60 nm and pore size within their web of 100 nm or smaller [146, 155]. The RVC original macrostructure was not altered in this process, which is critical for biofilm development and mass transfer considerations.

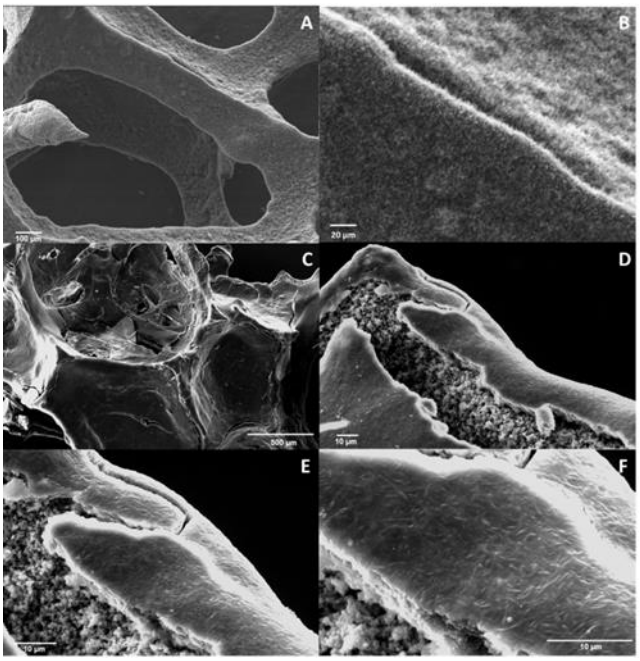

Figure 19 Scanning Electron Micrographs (SEM) images at different magnification of (A), (B) bare NanoWeb-RVC; (C) to (F) a putative electroactive biofilm grown on the NanoWeb-RVC.

At the end of the chronoamperometry experiments, the three-dimensional electrodes were taken out of the reactors, cut into pieces and prepared for SEM observation. Figure 19C-F show SEM micrographs at different magnifications depicting a uniform and fairly thick and continuous structure which is attributed to a biofilm formed on the NanoWeb-RVC electrode surface during the chronoamperometry experiment. A layer with very high density of rod shape microorganisms about 1-2 μm long entangled in an extracellular polymer-like substance can be observed.

In Figure 19D and E, the biofilm appears damaged, most probably due to the fixation and drying processes. These images allow us to estimate the biofilm thickness to be about 5 ± 2 μm in dry state. To date, very limited information on cathodic biofilm thickness has been reported in the literature. The thickness observed in this study represents a rather thin biofilm obtained after 140 days of experiment, compared to observed thicknesses of anodic biofilms of up to 100 μm [194].

Figure 20A shows an SEM image of unmodified RVC before reactor inoculation. Figure 20B and C show images of unmodified RVC that remained for 140 days in the bioelectrochemical reactor in the presence of inoculum and under the same conditions as NanoWeb-RVC and carbon plates. The surface of the unmodified-RVC appears to be largely unchanged over the 140 days of operation, with no biofilm development or any other deposits apparent on the surface.

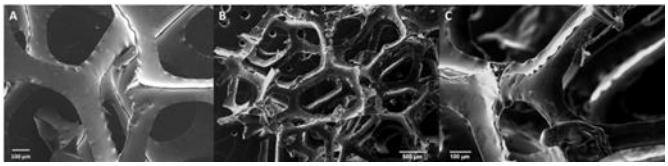

Figure 20 SEM images of unmodified-RVC before (A) and 140 days after inoculation (B-C) at different magnifications.

On the other hand, the optical density development at 660 nm of the cathodic medium of the unmodified-RVC reactor (Figure 21) suggests that microorganisms were present in suspension and their concentration slightly increased up to day 70 and stabilized thereafter. This observation is consistent with the fact that some carbon dioxide was consumed in this reactor (Figure 18) even though no acetate was produced, as previously shown. We can notice a similar trend in the NanoWeb-RVC reactor, with the optical density increasing until day 90 then flattening out for some days before decreasing.

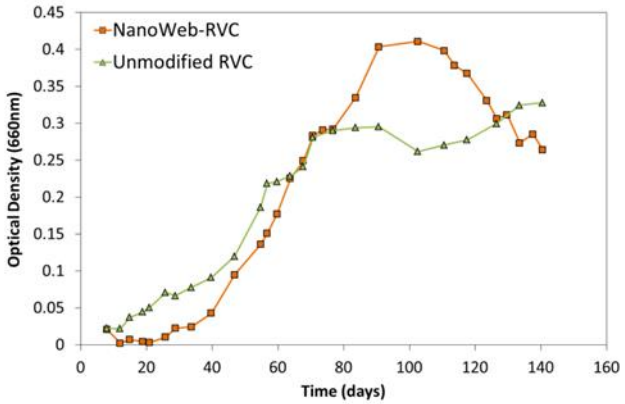

Figure 21 Optical density development over time in the cathodic media in both the NanoWeb-RVC and the unmodified RVC reactors.

The absence of biofilm and acetate production on unmodified RVC, plus the observation of similar amounts of planktonic cells in the catholyte of the NanoWeb-RVC reactor, strongly suggests that the biofilm plays a pivotal role in the high current consumption and electrosynthesis performance of the NanoWeb-RVC. Furthermore, the decrease in optical density after day 100 coincides with an actual enhancement of the carbon dioxide consumption and acetate production rates on NanoWeb-RVC. This decrease further shows that planktonic cells are unlikely to play an important role in this process and that the biofilm is primarily responsible for the CO_2 to acetate conversion. SEM observations strongly suggest that the much larger electron consumption rate reached on NanoWeb-RVC versus unmodified-RVC (10 times lower and constant current) throughout the experiment can be attributed to the development of a uniform biofilm covering the three-dimensional structure. However, further research will be needed to assess the relative

importance of both biofilm and microorganisms in suspension in microbial electrosynthesis performance.

Microbial electrosynthesis is most probably not possible on unmodified vitreous carbon as shown by our results. Nevertheless, we did want to compare the bioelectrosynthesis performance of the porous electrodes to flat electrodes, hence the choice of commercially available carbon plates as control instead of flat vitreous carbon.

All these observations indicate that the NanoWeb CNTs are highly biocompatible and support a highly enhanced bacterial attachment and biofilm development on top of the nano-porous structure. Moreover, the very high current density obtained suggests that the microorganism-electrode interaction is improved compared to the rough carbon plates, allowing for a maximisation of the electron transfer rate. The nanometre scale roughness of the NanoWeb-RVC electrodes can be seen in Figure 19A and B. It should be stressed that the maximum size of the pores created by the NanoWeb are 100 nanometre, *i.e.* are at least one order of magnitude smaller than typical bacterial sizes (about 1 µm length, see Figure 19F). Therefore, the NanoWeb does not increase the available surface area for bacteria immobilisation but primarily enhances the interaction between the electrode surface and the microbial cells [146]. We hypothesize that the somewhat flexible NanoWeb surface structure [155] offers multiple anchoring points for bacterial adhesion, as opposed to the unmodified, flat and rigid RVC surface or rough carbon plates. Additionally, the fact that the CNTs are chemically 'grown' on the RVC surface likely creates a high density of active electron transfer locations, which can then directly interact with the microbial cells growing on top. Irrespective of which electron transfer mechanism these bacteria use (direct membrane-bound proteins, bacterial nanowires or soluble extracellular redox mediators), the NanoWeb surface seems to stimulate and support effective, likely multipoint electron transfer processes between each attached bacteria and the electrode surface. The combination of this effective nano-scale surface modification with the large specific surface area and high porosity of the RVC macrostructure is believed to be largely responsible for such strong enhancement of the current density, CO_2 consumption and acetate production rates achieved in this study with the novel NanoWeb-RVC electrode material.

In conclusion, we have demonstrated in this study that the performance of microbial electrosynthesis of organics from carbon dioxide reduction can be significantly improved using a novel microbial biocathode, NanoWeb-RVC. To the best of our knowledge, results presented here correspond to the highest current density (37 A m^{-2} normalized by projected surface area) and

bioproduction rate (1.3 mM cm^{-2} day^{-1} of acetate equivalent to 192 g m^{-2} day^{-1}) reached to date on biocathodes for bio-reduction of carbon dioxide (Table 1).

The electron transfer rate between electrode-microorganisms (1.65-fold) and the acetate bioproduction rate (2.6-fold) were substantially enhanced on NanoWeb-RVC (normalised by total surface area) compared to rough graphite plate electrodes. From our understanding, this is the first study showing higher performance normalized to total surface area reached by a porous three-dimensional electrode versus a rough graphite electrode (we stress once more the difference in normalizing vs. total surface area or normalizing vs. projected surface area; as defined in section 4.1.5). The results show that the NanoWeb-RVC has a very high intrinsic performance as a biocathode material for MES. This also suggests that mass transfer through the macropores, to and from the biofilm, was very effective. Multiwalled-CNT directly grown on a highly conductive three-dimensional substrate such as RVC enables such MES performance improvements. Other studies that tested electrodes produced by dipping a non-conductive substrate in a CNT ink did not show such improvements compared either to their control or to the results presented here [11]. Moreover, we have shown that on unmodified RVC (without CNT) microbes did not attach to the surface and bio-reduction of CO_2 to acetate did not occur. Therefore the CNT nanostructure increases the electrode's biocompatibility and actually makes it possible for a continuous, electroactive biofilm to be formed, with increased microbial extracellular electron transfer. Additionally, NanoWeb-RVC electrodes offer a high available surface area for biofilm development per volume, which is important from a reactor design and engineering perspective.

7 Exceptional acetic acid production rate obtained by microbial electrosynthesis from carbon dioxide[3]

The NanoWeb-RVC showed excellent performance as biocathode material for acetate production. That electrode structure benefits from all the advantages of both the macrostructured RVC and nanostructured surface modification. The high surface area to volume ratio of the macroporous RVC maximizes the available biofilm area while ensuring effective mass transfer to and from the biocatalysts. The carbon nanostructure, in turn, putatively enhances the microbe-electrode interaction, bacterial attachment, biofilm development and microbial extracellular electron transfer. Therefore, in addition to showing very high intrinsic performance as a biocathode material for MES, NanoWeb-RVC electrodes create an extremely efficient material from an engineering perspective as well. However, for scale-up beyond certain sizes, there are some limitations with the chemical vapour deposition technique. Indeed, the requirement for specialised equipment and the complexity of the CVD process make this method unsuitable both for production of large size samples, and large scale production. Therefore, the quest for new electrode materials to be incorporated in bioelectrosynthesis reactors is still ongoing.

One of the most efficient methods to generate thin films from colloidal suspensions is electrophoretic deposition (EPD) [195-197]. EPD has been extensively used in the deposition of carbon nanotubes to form highly porous electrodes for electrochemical applications [198-201]. Depending on the settings used, the deposited CNT layer may be highly uniform with no agglomeration [202]. Compared to other methods of processing CNTs, EPD is relatively easy to carry out with simple equipment requirements [203, 204]. Moreover, it is capable of producing thin films from colloidal suspensions on irregularly shaped substrates [197]. Furthermore, scale up of this method can be easily accomplished by simply increasing the dimensions of the departing substrate to be coated. Since the synthetic protocol only uses aqueous suspensions of MWCNT, the risk of fire hazards is minimized. All these characteristics make the EPD method highly attractive for large size and industrial scale production of hierarchical porous electrodes.

---

[3] This chapter has been submitted to *Energy & Environmental Science* for publication and modified for incorporation in this thesis: **Ludovic Jourdin,** Timothy Grieger, Juliette Monetti, Victoria Flexer, Stefano Freguia, Jun Chen, Mark Romano, Gordon G. Wallace, and Jurg Keller. Exceptional acetic acid production rate obtained by microbial electrosynthesis from carbon dioxide. *Energy and Environmental Science* (under revision), 2015.

Here we report on a microbial electrosynthesis process achieving a very high acetic acid production rate of up to 685 g m^{-2} day^{-1} from CO_2. This was possible through to the combination of a well acclimatized and enriched microbial culture and a newly synthesized electrode material. We harnessed the throwing power of EPD to form MWCNT coatings onto RVC to generate a new hierarchical porous structure, hereafter called EPD-3D, which we used as biocathode electrode.

EPD-3D characterization

Typically, an EPD setup consists of two conductive substrates, i.e. electrodes, oriented such that they are parallel to each other [203] in such a configuration that a uniform electric field is generated around the substrate to be coated. These electrodes are submerged in a solvent wherein the colloidal nanoparticles are dispersed [158]. EPD occurs in two steps, initially electrophoresis followed by deposition [205]. In electrophoresis, the MWCNT (which are negatively charged due to the oxidation process) migrate towards the positive electrode due to the electric field being applied to the dispersion (Schematic 1). The MWCNT, due to particle coagulation then form a coherent deposit on the RVC surface (deposition step) [206]. The layer of MWCNT deposited on the surface of the RVC samples is depicted in Figure 22a. The porous layer of MWCNT can clearly be seen in Figure 22b. The MWCNT layer does not block the pores in RVC; i.e. the original macroporous structure is maintained (Figure 22c).

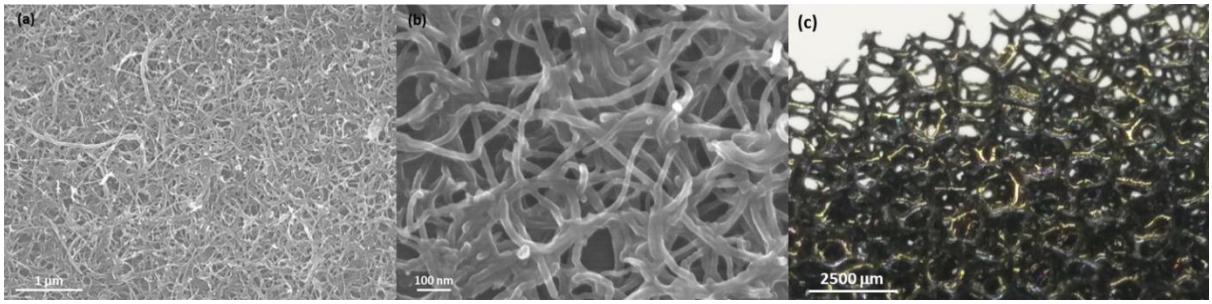

Figure 22 (a) and (b) Scanning Electron Micrographs (SEM) images at different magnifications and (c) photographic image of EPD-3D.

The simplicity of the cell needed for EPD and short deposition time make this method suitable and very attractive for industrial large scale production [158]. The other advantages of EPD include the high degree of uniformity of the deposited MWCNT layer and the ability to deposit on substrates that are irregularly shaped [200].

Current density enhancement

Two bioelectrochemical fed-batch reactors were filled with 0.25 L of inorganic medium that contained bicarbonate as sole carbon source. Each was equipped with one EPD-3D 45 ppi electrode (electrode 5 and 6; Table 4) and polarized at -0.85 V vs. SHE. About 200 mg L^{-1} as COD of

enriched mixed microbial culture that showed capable of electrosynthesis of acetate from carbon dioxide on a different electrode material (see Chapter 6) was added to both reactors at day 0. Starting right after inoculation, current consumption at a fixed cathode potential of -0.85V vs. SHE was recorded during 63 days and is plotted in Figure 23 a and b for each of the duplicate reactors. During this period, carbon dioxide consumption as well as volatile fatty acids production was followed for each reactor. The plots below (Figure 24 and 25) show their averaged performance with standard deviations represented as error bars. All data points in Figures 23, 24, 25, and 26 as well as in Table 10 have been normalized to projected surface area. Reported values in the text have also been normalized to projected surface area unless otherwise specified.

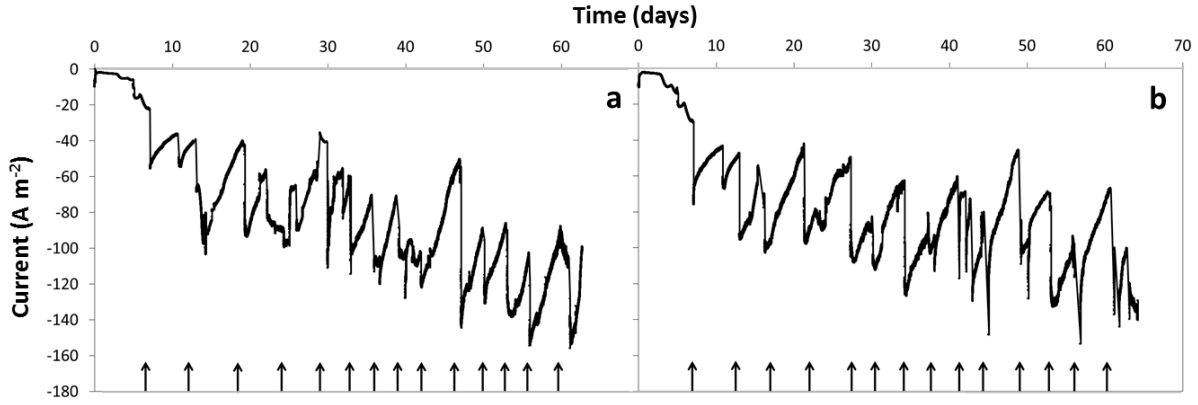

Figure 23 Current density evolution over time on EPD-3D for two duplicate reactors (a and b), at applied cathode potential of -0.85 V vs. SHE, normalized to projected surface area. The arrows show the days bicarbonate was added to the cathode chamber and pH adjusted to 6.7.

The current density right after inoculation was fairly low, as was expected, but gradually and exponentially increased after only 2 days following inoculation. After 10 days, the current density already reached about -50 A m^{-2}. The reactors were run in fed-batch mode and bicarbonate was periodically added, while at the same time the pH was adjusted to 6.7 as represented by the arrows in Figure 23. The plot indicates that the current increased right after each carbon source addition and pH adjustment and then slowly decreased following its consumption. The pH appeared to have some influence on microbial electrosynthesis rates as previously observed as well [12, 14]. Lowering the pH from near neutral to 5 was shown by LaBelle et al. (2014) [14] not to affect acetate production while concomitant H_2 production significantly increased. Further decrease of the pH below 5 was found detrimental to acetate production, while electrohydrogenesis rates further increased [14]. Keeping the pH slightly acidic (ca. 5.8) was shown to increase acetate production and the current demand in another study, as either a direct effect of the low pH or due to the indirect increase of substrate availability [12]. As observed in Figure 23, the general trend was an increase of the maximum current density reached after each addition and pH adjustment. The maximum

current density reached at the end of the test was about -150 A m^{-2} which represents, to the best of our knowledge, the highest current density ever reached for cathodic microbial carbon dioxide reduction to organics.

The cumulative electron consumption curve of EPD-3D is shown in Figure 24. The average of the two duplicate electrodes is plotted. Results of duplicates were in good agreement and the standard deviation small.

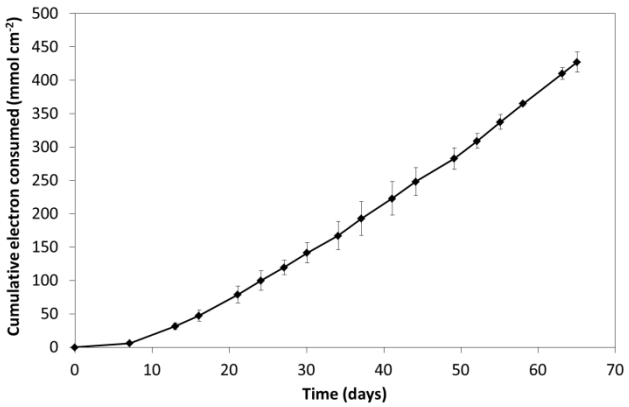

Figure 24 Cumulative electron consumption over time on EPD-3D, normalized to projected surface area.

The electron consumption rate is defined as the slope of that curve at different time intervals. Three phases in the electron consumption pattern could be observed on EPD-3D with increasingly higher rates which can be correlated to biofilm growth (Chapter 6). The start-up time was remarkably short as seen in Figure 24. This can be explained by the successful transfer of an enriched microbial culture, which is an important characteristic for practical implementation and scale-up of a biological system. Within the first seven days, a relatively slow electron consumption of 8.4 mol m^{-2} day^{-1} was recorded. A first significant increase up to 67 ± 2 mol m^{-2} day^{-1} of electrons consumed was observed between day 7 and 44. Finally, from day 44 to the end of the test, 91 ± 1 mol m^{-2} day^{-1} electrons were consumed, corresponding to a cathodic current density of -102 ± 1 A m^{-2}. This value is significantly higher than what has been reported to date (see Table 10 below). It is important to stress here again that this value is based on the average between both duplicates but also that significant fluctuations in actual current were observed following carbon dioxide consumption and pH increase (Figure 23). It is likely that a more constant current profile could be established under continuous carbon dioxide feeding and/or controlled, slightly acidic pH conditions. Under such 'steady-state' conditions an even higher current density would be expected, given that a peak current density as high as -150 A m^{-2} was reached immediately following carbon dioxide addition and pH adjustment, as seen in Figure 23. However, the optimisation of the

operational strategy was outside the scope of this study and the experimental set-up did not allow such a continuous operation and control of the process.

Microbial electrosynthesis enhancement

The carbon dioxide consumption and volatile fatty acids production on both EPD-3D reactors were followed throughout the experiments and are shown in Figure 25. The maximum rates can be seen, compared to other studies, at the bottom row of Table 10. The sole product generated was acetate and no other volatile fatty acids or alcohols accumulated in any of the reactors.

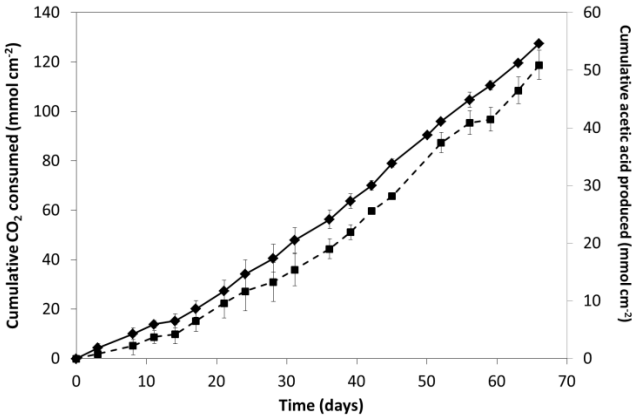

Figure 25 Carbon dioxide consumption (diamonds) and acetate production (squares) over time on EPD-3D, normalized to projected surface area.

Consistent with the electron consumption development shown in Figure 24, similar phases with increasing CO_2 consumption and acetate production rates were observed with fast start-up time following the culture transfer to the EPD-3D reactors. A maximum average CO_2 consumption rate of 24.8 ± 0.5 mol m^{-2} day^{-1} and an acetic acid production rate of 11.6 ± 0.5 mol m^{-2} day^{-1} were reached from 50 days onwards on EPD-3D. Based on a carbon balance, 94 ± 2 % of carbon dioxide was found to be converted to acetate only (with the remaining carbon likely being used for biomass production), while an electron balance revealed an even more striking result with 100 ± 4 % of the electrons consumed being recovered as acetate. The conversion efficiencies and product purity achieved in these experiments are exceptionally high, especially for mixed cultures, which makes it very interesting for potential large-scale production applications and downstream processing. Furthermore, the achieved acetate production rate of almost 685 ± 30 g m^{-2} day^{-1} is about 3.6 times higher than the highest production rate reported previously (Chapter 6; Table 10). Moreover, a fairly high acetate titer of up to 11 g L^{-1} was obtained at the end of the test, with no signs of product inhibition of the active microorganisms at that point. It is therefore quite conceivable that the titer would have reached even higher values had the test not been stopped. A high product titer is a critical characteristic for prospective large-scale implementation as it renders the downstream

processing much easier than when the product concentration is low. Indeed, product separation and recovery is one of the main costs of established chemical production plants, such as industrial fermentation [88, 89].

Bioelectrocatalytic activity

Hydrogen did not accumulate in the headspace of the reactors during the chronoamperometry test at -0.85V vs. SHE. However, this fact does not exclude H_2-mediated electron transfer (abiotically and/or bio-catalytically generated) as a possible mechanism of electron transfer from electrodes to acetate-producing microorganisms. Such an electron transfer pathway via biotically produced hydrogen was indeed hypothesized in a previous study for methane and acetate production in bioelectrochemical systems [15]. Moreover, H_2-producing microorganisms were also shown to sustain autotrophic growth and self-regenerate under purely cathodic conditions without any external electron or organic carbon sources (Chapter 5). Alternatively, electrons could also be delivered directly from the cathode or via another soluble mediator than H_2 to the acetate-producing bacteria. A detailed study of the specific extracellular electron transfer mechanism active in these experiments is currently underway, but is beyond the scope of work presented here. Nevertheless, the electrochemical performance of the biocathode EPD-3D was compared to that of an abiotic control EPD-3D electrode on the basis of linear sweep voltammetry recorded at pH 7 (Figure 26).

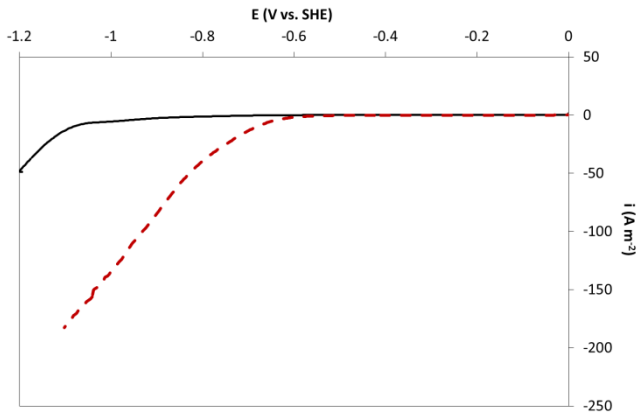

Figure 26 Linear sweep voltammetry on abiotic cathode (solid line) and biocathode (dashed line). Scan rate, 1 mV s^{-1}.

A clear shift of the reductive wave onset towards higher potentials (ca. -0.65 V vs. SHE) compared to the onset of current in the abiotic reactor (ca. -1 V vs. SHE) can be observed. As reported previously [15, 104] (Chapter 5 and 6), this may be an indication of biological catalytic activity on the surface of the electrode. In addition, a predominant biofilm development on top of the EPD-3D was clearly revealed at the end of the chronoamperometry experiment, using scanning electron microscopy (Figure 27).

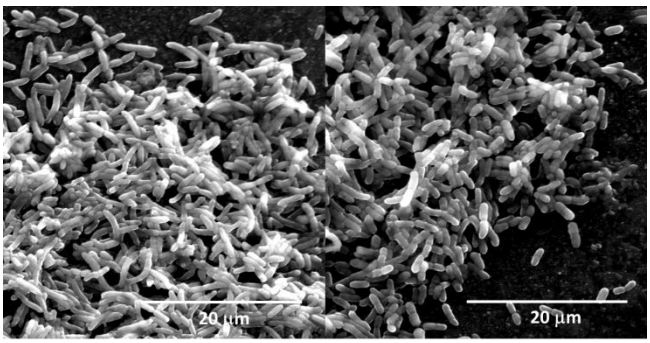

Figure 27 Scanning Electron Micrographs (SEM) images at different magnification of a biofilm developed after 63 days on EPD-3D.

Remarkably for a biocathode, the SEM images show a well-developed, almost contiguous biofilm with entangled, multi-layered microorganisms with an approximate total thickness of 5-10 μm. This strongly suggests that the exceptionally high electron consumption and microbial electrosynthesis performance reached in these experiments may be attributed to sustained bioelectrocatalytic activity through the development of a uniform biofilm covering the three-dimensional structure of the EPD-modified RVC. Indeed, previous experiments with the same inoculum on unmodified-RVC showed that the surface appeared to be largely unchanged with no biofilm development (Chapter 6, Figure 20).

Implications towards practical implementation

Microbial electrosynthesis performance can be assessed using several key parameters; these are listed in Table 10, for most MES to acetate studies reported to date.

Table 10 Key performance parameters of most microbial electrosynthesis to acetate studies reported to date.

Microbial inoculum (Reactor operation)	Cathode material	$E_{cathode}$ (V vs. SHE)	Current density (A m^{-2})	Acetate production (g m^{-2} day^{-1})	Max acetate titer (g L^{-1})	Electron recovery into acetate (%)	Reference
S. ovata (continuous)	Graphite rods	-0.4	-0.208	1.3	0.063	86 ± 21	Nevin et al. 2010 [9]
C. ljungdahlii (continuous)	Graphite rods	-0.4	-0.029	0.14	n.d.	72	Nevin et al. 2011 [8]
Brewery WW sludge (fed-batch)	Graphite granules	-0.590	n.d.	n.d. (8 mmol C L_{NCC}^{-1} d^{-1})	1.71	67	Marshall et al. 2012 [15]
Enriched brewery WW sludge (fed-batch)	Graphite granules	-0.590	n.d.	n.d. (34.5 mmol C L_{NCC}^{-1} d^{-1})	10.5	69	Marshall et al. 2013 [16]
Enriched WWTP sludge (fed-batch)	Carbon felt	-0.9	n.d.	34.5	n.d.	89.5	Su et al. 2013 [17]
S. ovata (continuous)	Carbon cloth-chitosan	-0.4	-0.475	2.7	0.118	86 ± 12	Zhang et al. 2013 [11]
S. ovata (continuous)	CNT-cotton CNT-polyester	-0.4	≈ -0.215	≈ 1.2	0.059	83 ± 10	Zhang et al. 2013 [11]
S. ovata (continuous)	Ni-nanowire-network-coated graphite	-0.4	≈ -0.625	3.3	n.d.	82 ± 14	Nie et al. 2013 [10]
Enriched brewery WW sludge (fed-batch)	Graphite rods	-0.6	-0.92 ± 0.12	8.56 ± 3.22	n.d.	40	LaBelle et al. 2014 [14]
Mesophilic WW anaerobic sludge (fed-batch)	Graphite felt	-1.1	≈ -2.8	10.1	1.4	65	Xafenias et al. 2014 [19]
Anaerobic digester / retention basin (continuous)	Graphite granules	-0.6	n.d. (12.3 A m_{NCC}^{-3})	n.d. (0.98 mmol C L_{NCC}^{-1} d^{-1})	n.d.	28.9 ± 6.1	Batlle-Vilanova et al. 2015 [12]
Mixed natural & engineered sludge (fed-batch)	NanoWeb-RVC	-0.85	-37	192	1.65	70 ± 11	Chapter 6
Enriched Mixed natural & engineered sludge (fed-batch)	EPD-3D	-0.85	-102	685	11	100 ± 4	This study

The results summarized in Table 10 were obtained with both pure and mixed microbial cultures, in either fed-batch or continuous mode, using different cathode electrode materials and cathode applied potentials, which makes the comparison between those studies somewhat difficult. Regardless, it seems clear that the performance (current density and acetate production rate) reached in this study is at least 1 order of magnitude higher than what has been reported to date (except our own study presented in Chapter 6).

Looking at the requirements for modern industrial scale bio-production processes such as industrial fermentations, production rates in the range of 2 to 4 g L^{-1} h^{-1} with a high yield of at least 99% (conversion of substrate into final product) is necessary for process viability. Usually, a high titer of above 100 g L^{-1} is also regarded as a considerable advantage for downstream processing. In the past few years, several research groups have attempted to assess the scale-up feasibility of bioelectrochemical systems [109-111], in particular of MFC and microbial electrolysis technologies [112-114]. The engineering and economic potential of electricity-driven bioproduction processes has also been recently discussed.[207] It has become common practice within the research community to assess BES efficiency for engineering application by normalizing current and other production related parameters to projected surface area. However, taking into account the 3D nature of the electrode and its total surface area per volume unit (2620 m^2 m^{-3}), the rates obtained on

EPD-3D corresponds to a volumetric production rate of 2.8 ± 0.1 g L^{-1} h^{-1} of acetate with a 100 ± 4 % product yield, which are parameters well within the desired characteristics window of industrial bio-production processes, and similar to what is being achieved in bioreactors pressurized with H_2/CO_2 gas [208]. This corresponds to about 66 kg m^{-3} day^{-1} of acetate and 98 kg_{CO2} m^{-3} day^{-1} captured. These volumetric rates are 22 times higher than that of the MES system also driven by a mixed community at -0.8 V vs. SHE developed by LaBelle et al. (2014) [14] which recorded concomitant production of hydrogen and formate and hence only 40% electron recovery into acetate.

We hypothesize that the extremely high efficiency shown by the new EPD-3D electrode originates from its MWCNT nanostructure, which enhances the microbe-electrode interaction, bacterial attachment, biofilm development and microbial extracellular electron transfer rate, as previously suggested for microbial anodes [119, 122, 138, 146, 153, 209] and cathodes (Chapter 6). In addition, the high surface area to volume ratio of the EPD-3D scaffolds maximizes the area available for biofilm development, while the large porosity (0.56 mm diameter) ensures effective mass transfer to and from the biocatalysts. This makes EPD-3D an extremely suitable material for practical implementation of the MES technology.

The best performing biocathode reported to date (NanoWeb-RVC) has an acetate production rate 3.6-times lower than that obtained in this study. Furthermore, with the NanoWeb-RVC only 70% of the electrons were assimilated into acetate (Chapter 6). Said electrode benefited from the same macroporous structure as EPD-3D, which probably explains its good performance compared to other work listed in Table 10. However, the morphology of that electrode structure is clearly different from the new EPD-3D material. Firstly, the MWCNT in EPD-3D are considerably thinner in diameter as those previously grown (9.5nm now vs 60nm average diameter in work previously reported) by CVD (Chapter 6). Moreover, the MWCNT layer on the EPD-3D consists of functionalized MWCNT, since the nanotubes underwent a strong chemical oxidation prior to the electrophoretic deposition step [134, 136, 137]. Finally, when comparing the high resolution SEM images of both structures, we observe that the MWCNT layer in EPD-3D is much denser than work previously reported (Chapter 6, Figure 19). A denser structure will most probably improve the electrical conductivity of this new material, plus it will increase the probability of the CNTs being at the right position to better electrically communicate with bacteria.

The titer reached in this study, 11 g L^{-1}, even though one of the highest reported to date on MES process (Table 10), is still not comparable to the product titer obtained by fermentation processes. However, it is believed that a higher titer is achievable. Acetate concentrations as high as

44 g L^{-1} have been reported in bioreactors pressurized with H_2/CO_2 gas using *Acetobacterium woodi* [208]. Moreover, continuous MES product extraction at relatively low titer is also currently being investigated. Therefore, increases in the product concentrations or alternative extraction methods will likely be possible in future. Overall, product titer and production rate have a direct impact on the capital and operation costs of a plant, while the product yield is directly linked to the substrate(s) cost, and purity influences the product separation costs. The results presented in this study advance most of these parameters in a highly beneficial way and therefore bring microbial electrosynthesis a significant step closer to its practical implementation.

In conclusion, we have demonstrated in this study that the production of organics by microbial electrosynthesis from carbon dioxide reduction can reach industrial production process standards (e.g. fermentation). We report a previously un-achieved biocathode current density of -102 ± 1 A m^{-2} and acetic acid production rate of 685 ± 30 g m^{-2} day^{-1} (66 kg m^{-3} day^{-1}), with a CO_2 and electron recovery of up to 100 ± 4 % into the final product (product yield) and a high acetic acid titer of up to 11 g L^{-1}. Current density as high as -150 A m^{-2} was reached periodically after carbon dioxide addition and pH adjustment. This impressive performance was possible due to the combination of a well acclimatized and enriched microbial culture coupled with the use of a newly synthesized electrode material. A very fast start-up after culture transfer was achieved, with significant MES performance increase after just a few days. An electrophoretic deposition technique was exploited to form a uniform carbon nanotube coating onto reticulated vitreous carbon to generate a hierarchical porous structure, EPD-3D, which was successfully used as biocathode in MES system. EPD requires very simple and inexpensive equipment. The method is indeed applicable to large departing substrates and the short deposition times make the deposition method suitable for industrial scale production of EPD-3D. Even though several issues regarding the actual scale-up of the BES technology in general still need to be overcome, these results bring MES a large step closer to practical applications. This bioproduction-comparable performance should favour realistic discussions within the research community on strategies to adopt for microbial electrosynthesis scale-up to economically-viable practical applications (see Chapter 10).

8 Biologically-induced hydrogen production drives high rate / high efficiency microbial electrosynthesis of acetate from carbon dioxide[4]

We have showed an exceptionally high biocathode current density of up to -102 A m^{-2} with a concurrent acetic acid production rate of 685 ± 30 g m^{-2} day^{-1} (equivalent to 66 kg m^{-3} day^{-1} and 98 kg_{CO2} m^{-3} day^{-1} captured). The CO_2 and electron recovery in this study was up to 98 ± 3 % into the final product (product yield) and a high acetic acid titer of up to 11 g L^{-1} could be reached. This was possible thanks to the combination of a well acclimatized and highly performing microbial culture (very fast start-up after culture transfer), coupled with the use of a newly synthesized electrode material (multiwalled carbon nanotubes deposited on reticulated vitreous carbon by electrophoretic deposition, called EPD-3D) (Chapter 7). That study showed that industrial production process standards, such as fermentation-type volumetric production rate and product yield, can be reached by microbial electrosynthesis of organics from CO_2, though there are still several issues to be overcome for the actual bioelectrochemical system (BES) technology scale-up and practical implementation. In this regard, a more in-depth understanding of the process and particularly on how electrons flow from the cathode to the terminal electron acceptor is still missing, even though it may be of paramount importance (e.g. for improved reactor design), in addition of providing some fundamental information about the process.

As discussed in section 2.1.2, information on the electron flow from electrodes (cathodes) towards the terminal electron acceptor, is rather limited. In the context of microbial electrosynthesis from carbon dioxide, potential mechanisms of electron transfer from the cathode have been discussed by several groups [13, 15] with the possibility of at least part of the electrons being transported to the acetate-producing bacteria via hydrogen which is either abiotically or biologically produced. However, there is a clear lack of experimental evidence towards these H_2-mediated

[4] This chapter is ready for submission (fully written and internally peer-reviewed) to *Energy & Environmental Science* for publication and modified for incorporation in this thesis: **Ludovic Jourdin,** Yang Lu, Victoria Flexer, Jurg Keller, and Stefano Freguia. Biologically-induced hydrogen production drives high rate / high efficiency microbial electrosynthesis of acetate from carbon dioxide. *Energy & Environmental Science* (to be submitted), 2015. Waiting for submission upon receiving comments on the paper already submitted to *Energy & Environmental Science* (Chapter 7).

electron transfer assumptions. Additionally, other electron transfer mechanisms such as DET or through other electron shuttles could not be ruled out from those studies.

In this study, the titration and off-gas analysis (TOGA) sensor developed by Pratt et al. [161] was modified to allow the online measurement of gaseous products (i.e. H_2, CH_4, CO_2) from bioelectrochemical systems (BESs) [210]. Different tests were carried out (e.g. chronoamperometry and linear sweep voltammetry with and without carbon dioxide) on both biotic BESs for microbial electrosynthesis of acetate from carbon dioxide and abiotic BESs lacking the microorganisms (pure electrochemical reactions) using the TOGA sensor. In addition, microorganisms involved in the process were identified and the relative importance of both biofilm and planktonic cells in terms of overall process performance was investigated. We demonstrate that the CO_2 reduction to acetate is driven by biologically-induced hydrogen production at high rate (1.15 m^3_{H2} $m^{-2}_{electrode}$ day^{-1}) with ca. 99 ± 2% of total supplied electrons recovered into acetate (at a high production rate of ca. 685 g m^{-2} day^{-1}) in turnover conditions.

A high rate microbial electrosynthesis reactor, equipped with EPD-3D 45ppi synthetized by electrophoretic deposition (electrode 6; Table 4) as biocathode material, which was run in fed-batch mode for about 70 days as previously described (Chapter 7), was used in this study. After this long-term chronoamperometry test at -0.85 V vs. SHE, the reactor was setup to be used in combination with the TOGA sensor at the same applied cathode potential, as described in the materials and methods Chapter. The current evolution over time (about 87 days) can be seen in Figure 28.

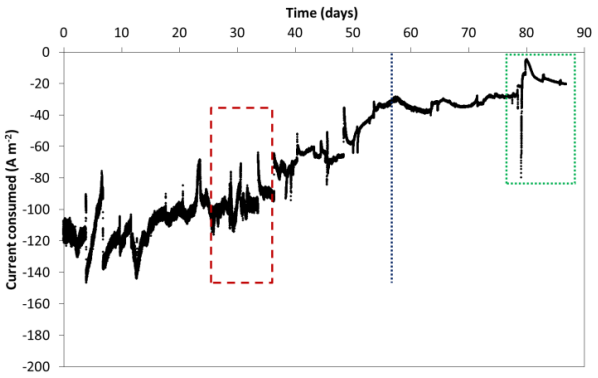

Figure 28 Current density evolution over time on EPD-3D, at applied cathode potential of -0.85 V vs. SHE and pH 6.7, normalized to projected surface area. The dashed rectangle shows the time period, chronoamperometry and LSV tests on the TOGA were performed before planktonic cells removal. The dotted line shows when planktonic cells were removed. The dotted rectangle shows the time period when the reactor was submitted to extreme conditions (low pH, sterilisation, air drying).

Throughout all the tests, no methane was detected. The H_2 flow rate could be determined, and the corresponding current consumed into H_2 as an end-product was calculated. Some of the

tests described below were also run on a duplicate reactor (as indicated in the text), equipped with a EPD-3D 60 ppi biocathode electrode using the exact same setup and experimental conditions and showing high MES rate. Results obtained on both replicate reactors are shown below and are in close agreement. All data points in the figures have been normalized to the projected surface area of the electrode. Reported values in the text have also been normalized to projected surface area unless otherwise specified.

MES of acetate driven by biologically-induced hydrogen production

After about 25 days of acclimation to the new setup and experimental conditions, the TOGA sensor was used alternatively in turnover and non-turnover conditions. The total current consumed and the current assimilated into hydrogen over time can be seen in Figure 29. The TOGA sensor also allowed confirming that no methane was produced during the course of the experiment (data not shown). Liquid samples were also taken at the beginning and end of each period, and volatile fatty acid concentrations were monitored.

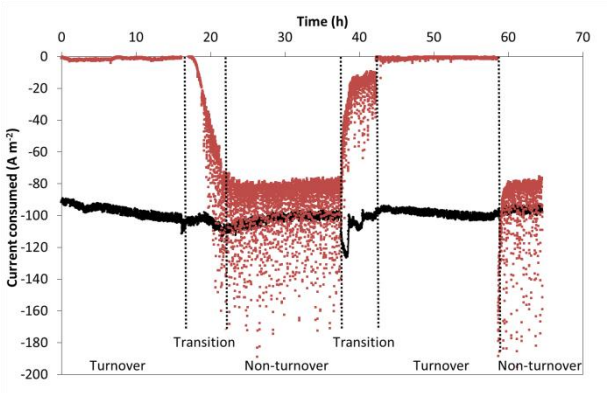

Figure 29 Chronoamperometry test with the TOGA in both turnover and non-turnover conditions, at -0.85 V vs. SHE applied cathode potential and pH 6.7. The solid black line represents the total current consumed while the red dotted line represents the current consumed into hydrogen (more negative values represent higher hydrogen production). The current values were normalized to projected surface area.

It can be observed that essentially no H_2 was detected from the reactor when CO_2 was continuously fed to the reactor. VFA analysis also showed that acetate was the sole product and that about 99 ± 1% of the total electrons consumed were assimilated into acetate (averaged on both turnover periods showed in Figure 29). This confirms observations made in previous studies on fed-batch reactors fed with bicarbonate (Chapters 6 and 7). However, the notable difference is that in this case, gases (He:CO_2) were continuously bubbled through the reactor, and any hydrogen that would be produced and not directly consumed would be stripped out due to its low solubility in water. Remarkably, it can be seen that when CO_2 was removed, i.e. pure He was sparged (referred to as non-turnover condition in Figure 29 and the following discussion), no current decrease was

observed and electron recovery into H_2 as the end-product went up to 95 ± 3%. This indicates that the electron flux from the electrode to the terminal electron acceptor, CO_2, when present, occurs mostly through hydrogen. Indeed, if direct electron transfer from the electrode to the acetate-producer microorganisms was occurring, a decrease in current consumed would be expected in non-turnover conditions.

Moreover, acetate concentration was found to stay constant in non-turnover conditions, i.e. it was not consumed despite being the sole carbon source present in the system. This confirms that the active microbial community enriched is purely autotrophic, even though fairly high concentration of acetate had been present in the reactor for more than 100 days (included the previous fed-batch experiment). This was expected, as methanogens were inhibited and no other electron acceptor was present in the system.

Around day 30 to 35, linear sweep voltammograms (LSVs) in both turnover and non-turnover conditions were obtained and can be seen in Figure 30.

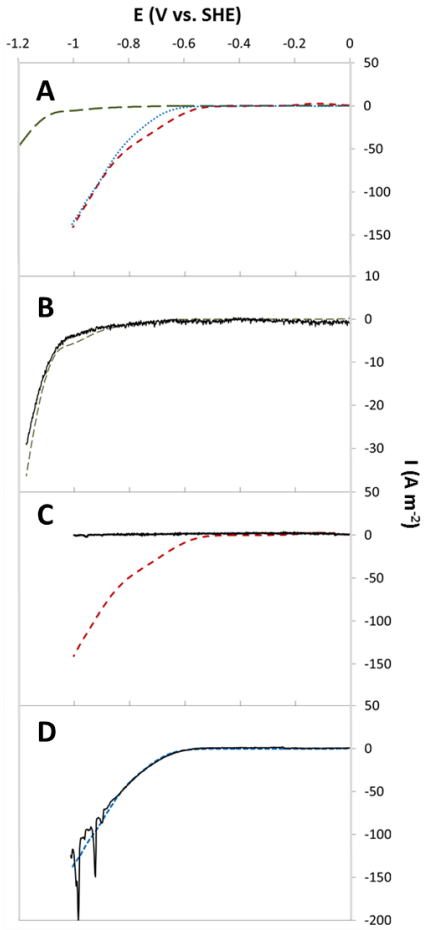

Figure 30 A) Linear sweep voltammograms recorded on abiotic reactor (green large dashed line), and biotic reactor in turnover (red dashed line) and non-turnover condition (blue dotted line). LSVs were recorded with the TOGA sensor with the black solid lines representing the current consumed into hydrogen in B) abiotic condition, C) biotic turnover condition, and D) biotic non-turnover condition. The current values were normalized to projected surface area. Scan rate: 0.1 mV s^{-1}.

They confirmed the observations made above during chronoamperometry tests, with no H_2 being detected in turnover conditions, while all electrons consumed in non-turnover conditions were assimilated into H_2. Both chronoamperometry and LSV tests using the TOGA sensor were also performed on an EPD-3D 45ppi abiotic control setup, but without the microbial inoculum, and are shown in Figure 30 and 31, respectively.

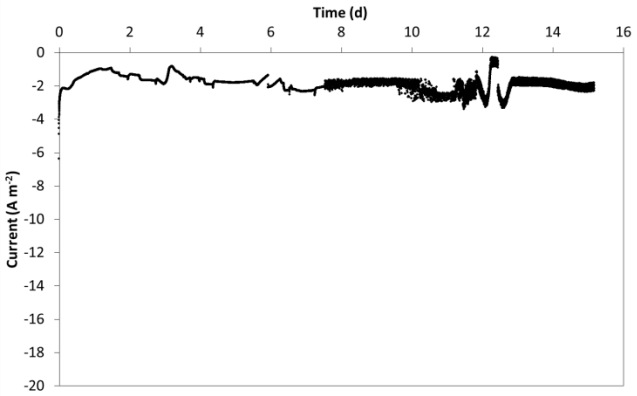

Figure 31 Current density evolution over time on abiotic EPD-3D 45 ppi, at applied cathode potential of -0.85 V vs. SHE and pH 6.7, normalized to projected surface area.

Significantly lower, and constant, current density of about -2 A m^{-2} was recorded throughout the chronoamperometry test at -0.85 V vs. SHE, compared to the current density of about -100 A m^{-2} recorded in the biocathode (using the same EPD-3D electrode material). Even at this low current the TOGA sensor was able to detect that all the electrons were directed towards H_2 production only, in the abiotic control, during both the chronoamperometry and LSV tests.

Unlike other studies that generally report H_2 diffusion losses hence are unable to close electron balances at low current [23, 186], the TOGA sensor allows us to close the electron balance to within 1% in this study. As previously reported, a significant shift of the reductive wave towards higher potentials was observed on the biocathode compared to the abiotic control. This has been attributed to biological catalytic activity in many studies [15, 104] (Chapters 5 and 7). The combination of LSVs, in both turnover and non-turnover conditions, with the TOGA sensor confirms that this increase in catalytic activity is directed towards higher H_2 production rates. Moreover, the significantly lower current density recorded in the abiotic control indicated that abiotically produced H_2 cannot account for all the H_2 and acetate produced in non-turnover and turnover conditions, respectively, in the biocathode system. Therefore, the hydrogen production must be biologically-induced.

Highly specific microbial enrichment

Pyrosequencing recovered total 227,991 high quality sequences with average 56,997 ± 3172 (standard error) per sample. Microbial communities were consistent between duplicates and distinguishable between biofilm and planltonic cells. The dominating microorganisms were either a niche including *Burkholderiales*, *Clostridiales*, *Natranaerobiales* and *Methanobacteriales* in biofilm or *Burkholderiales* alone in planktonic cells with other OTUs presented as less than 1% relative abundance (Figure 32).

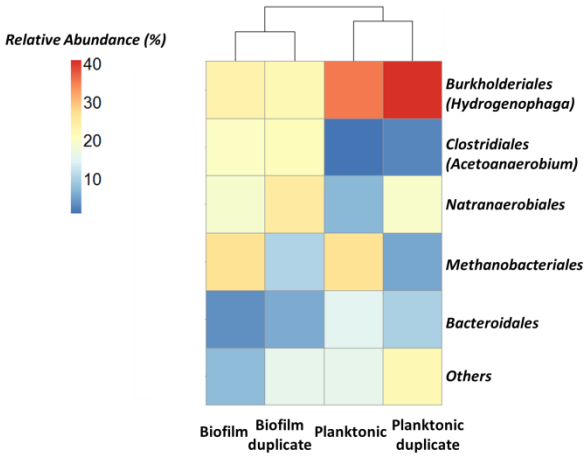

Figure 32 Heatmap of microbial community in biofilm and planktonic cells from two replicate reactors based on order level summary from pyrosequencing analysis. Genus information is also provided in bracket, if it dominates in the corresponding order. Other Orders that contains OTUs with less than 1% relative abundance are summarized and presented as "Others".

Three main bacterial orders accounted for up to 65% of the whole community in the biofilm: *Burkholderiales*, *Clostridiales* and *Natranaerobiales*. This shows that the specific experimental conditions allowed for the high enrichment of a few species only, starting from a large variety of microorganisms (Chapter 5; Figure 14). Descending from the order *Clostridiales*, the main genus was *Acetoanaerobium*. *Acetoanaerobium* is an anaerobic bacterium that has been reported in the past for its ability to produce acetate from CO_2 and H_2 [211]. Remarkably, *Acetoanaerobium* was mainly dominant in the biofilm and present in suspension at only a low abundance. The main genus of *Burkholderiales* detected was *Hydrogenophaga* with more than 37% of abundance in suspension and also fairly high abundance (ca. 22%) in the biofilm. To the best of our knowledge, *Hydrogenophaga* has only been reported as a facultative autotrophic hydrogen-oxidizing bacteria [212]. It was isolated from anodic biofilms of acetate-fed microbial fuel cells [213] and speculated to work in close syntrophy with acetate-oxidizer *Geobacter* as hydrogen-utilizing exoelectrogen, hence directly transferring electrons to the electrode [214]. *Hydrogenophaga* was also reported to be the dominant species and a key player in autotrophic biofilms active in denitrification [215, 216]. More in-depth investigation is needed to shed light on its function in these peculiar biocathode

conditions. *Natranaerobiales* are fermentative polyextremophiles and normally grow under high saline and pH conditions [217]. Due to the difficulty on further classification (low identity to cultured microorganisms), the function of this group remained unclear in this study.

MES of acetate exclusively occurs within the biofilm

The relative abundance of these key biofilm microorganisms, except hydrogenophaga, considerably dropped in the community in suspension, highlighting the likely major importance of the biofilm in the process performance. To confirm this hypothesis, the planktonic cells were removed by replacing the whole catholyte suspension with fresh cell-free catholyte solution.Chronoamperometry tests using the TOGA sensor were performed before and after the planktonic cells removal and can be seen in Figure 33.

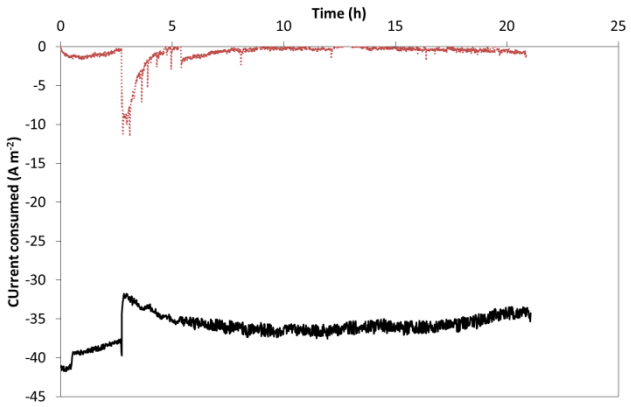

Figure 33 Chronoamperometry test with the TOGA in turnover condition, at -0.85 V vs. SHE applied cathode potential and pH 6.7 before and after planktonic cells removal (represented by the vertical dotted line). The solid black line represents the total current consumed while the red dotted line represents the current consumed into hydrogen. The current values were normalized to projected surface area.

Similar current densities were recorded before and after the planktonic cells were removed and still about 100% of the electrons consumed were assimilated into acetate after the medium was replaced. This confirms the paramount importance of the biofilm in the MES performance.

It can be noticed that the current densities in Figure 33 are lower than those in Figure 29. This reflects a progressive decrease over time of the reactor current density as shown in Figure 28. We speculate that the repeated recording of many LSVs may have affected the performance of this biocathode, as corroborated by further experiments as described below (see Figure 39). Therefore, we repeated this planktonic cells removal experiment on the fully active 60 ppi MWCNR-RVC duplicate biocathode, on which no LSV was performed, and can be seen in Figure 34.

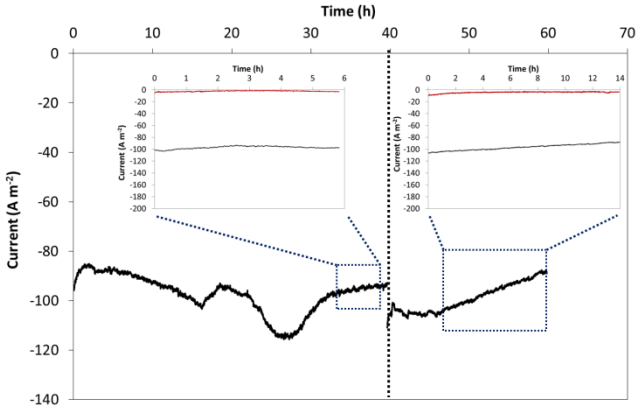

Figure 34 Chronoamperometry test with the TOGA in turnover condition, at -0.85 V vs. SHE applied cathode potential and pH 6.7 before and after planktonic cells removal (represented by the vertical dotted line), on the duplicate reactor. The solid black line represents the total current consumed while the red dotted line represents the current consumed into hydrogen. The current values were normalized to projected surface area.

Similarly, it can be seen that the current remained constant after the planktonic cells were removed, even at the very high current density of around -100 A m^{-2}, and that H_2 was not detected either, hence all the electrons were assimilated into acetate, as confirmed by VFA analysis.

As described above, the main electron transfer to the acetogens occurs through biologically-induced hydrogen. This shows the quite extraordinary capability of the acetogens to consume such a high H_2 flow rate (1.15 m^3_{H2} m^{-2} day^{-1}) within the biofilm, without the H_2 able to escape from it (and hence be detected by the TOGA sensor). This finding is of high importance for the potential large-scale implementation of this technology and reactor design. Not only would high acetate production rates be desirable, but also the handling of extra hydrogen could be problematic and a technical challenge. The direct H_2 consumption within the biofilm is an opportunity and presents several advantages over other technologies that would rely on the mass transfer of H_2 molecules to microorganisms suspended in aqueous solution, such as the artificial photosynthetic system proposed by Jian Yu [218]. This system comprises of a photovoltaic assembly which generates electricity to drive a water electrolyser for the formation of H_2 which is introduced in a dark-fermenter in which H_2-oxidizing bacterial cells assimilate CO_2 to form bio-based products [218]. High gas feed rates and superficial gas velocities while avoiding H_2 wastage are needed for efficient mass transfer and consumption and for economic viability and operational safety. However, the very low solubility of H_2 (1.26 mmol L^{-1} atm^{-1}) poses a technical challenge to maintaining a high mass transfer in large bioreactors, without substantial loss of H_2 [218]. Comparatively, the system described here allows combining both H_2 production and CO_2 assimilation to a bio-based product, acetate, within a unique microbial electrosynthesis reactor, without H_2 waste and extra-handling. Moreover, it was showed that if supplied with sufficient H_2

and CO_2, autotrophic H_2-oxidizing bacterial growth can be very fast, comparable to heterotrophic growth [218-220]. It was concluded that the microbial metabolism of the gases was not the limiting factor, but that maintaining an appropriate mass transfer rate of the gases to the microorganisms was actually the technical bottleneck of autotrophic technologies such as the dark fermenters described above [218]. This could also partly explain the observation made in our previous study, showing very fast start-up of MES biocathode inoculated with an enriched culture (Chapter 7).

High H_2 production capability unaffected by biofilm removal

We further investigated the high biologically-induced H_2 production capability of these biocathode systems by subjecting the biofilm to extreme conditions in order to remove it, as described in the Materials and Methods Chapter. After each treatment, the electrode was reconnected and current recorded at the same applied potential of -0.85 V vs. SHE and is plotted in Figure 35.

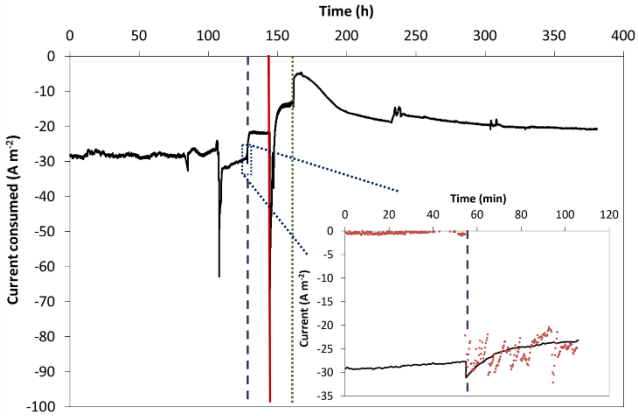

Figure 35 Chronoamperometry test with the TOGA sensor connected, in turnover condition, at -0.85 V vs. SHE applied cathode potential. The vertical dashed, solid and dotted lines represent the time periods when pH was adjusted to 2 for 2-3 hours, the reactor and the recirculation bottle were autoclaved (and the rest of the setup sterilized with ethanol), and the electrode taken out of the reactor and left to dry in air for 1 week, respectively. During those three periods, current evolution over time was not recorded and all experimental results are collapsed as a continous result in this figure. The inset graph shows the current consumed into hydrogen (red dotted line) measured with the TOGA sensor during two distinct periods of the chronoamperometry test, before and after the low pH period (marked by the dashed line).

The current density before those treatments was about -29 A m^{-2}. Remarkably, after the low pH treatment the current was still high, about -22 A m^{-2}. The TOGA sensor was used before and after the low pH step (Figure 35) and we can observe that the acetogens were successfully inhibited, or killed, by the low pH as H_2 was the sole product generated afterwards. Further sterilisation and air treatment also did not significantly affect the H_2 production capability of the cathode, as the current density increased back up to about -20 A m^{-2} few days after the air-drying treatment. The low pH and autoclave treatments were repeated on the biocathode duplicate at high current density (ca. -100 A m^{-2} before treatments) and can be seen in Figure 36.

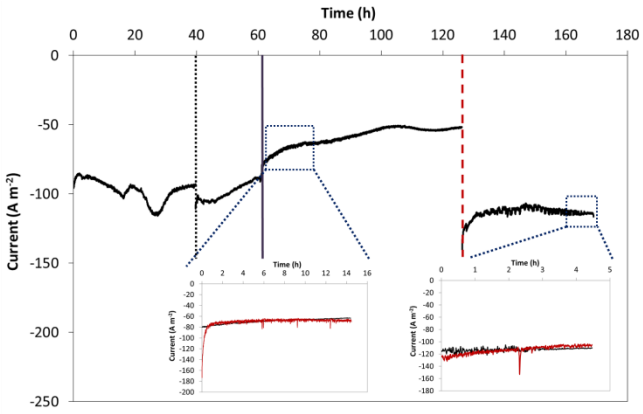

Figure 36 Chronoamperometry test with the TOGA in turnover condition, at -0.85 V vs. SHE applied cathode potential and pH 6.7 on the duplicate reactor. The vertical dotted line, solid line and dashed line represent the time periods when planktonic cells were removed, the pH was adjusted to 2 for 2-3 hours, and the reactor and the recirculation bottle were autoclaved (and the rest of the setup sterilized with ethanol), respectively. During those three periods, current evolution over time was not recorded for practical reasons. The two inset graphs show the current consumed into hydrogen (red solid line) measured on the TOGA during two distinct periods of the chronoamperometry test, after the pH was lowered and adjusted back to 6.7 and after sterilisation.

We first confirmed that acetogens' activity after low pH was inhibited. But remarkably, the current after autoclaving was similar, even slightly higher, ca. -110 A m^{-2} than before exposing the biocathode to those extreme conditions. The slightly lower current recorded after the low pH exposure was due to the reference electrode being faulty leading to an applied cathode potential of about -0.77 V vs. SHE instead. It has to be stressed here once again that the current recorded in the same conditions on an abiotic control was far lower (-2 A m^{-2}) and cannot account for this high H_2 production rate. We also confirmed that autoclaving a RVC-CNT electrode does not affect its surface properties (e.g. its CNT layer), by recording the same current on an abiotic control before and after autoclave treatment (data not shown).

To further confirm these extreme treatments effectively removed the biofilm off the electrodes, SEM images were taken on both a fully active biocathode biofilm and the electrodes that went through those treatments and can be seen in Figure 37. Abiotic EPD-3D SEM images are also shown. FISH images of the active biocathode biofilm dispersed in solution have also been taken and are shown in Figure 38.

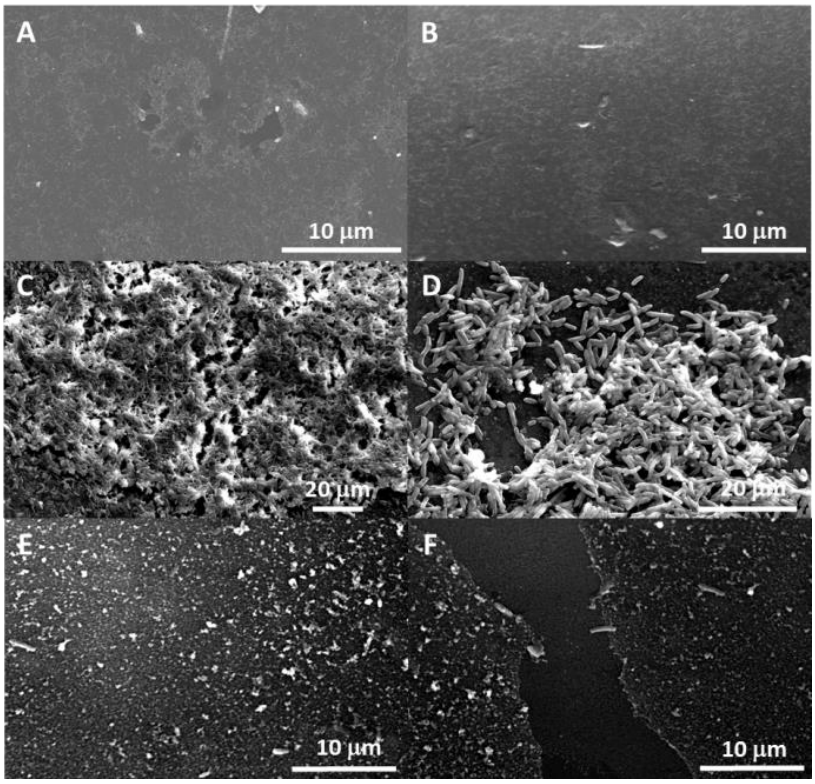

Figure 37 Scanning Electron Micrographs (SEM) images at different magnification of (A) and (B) bare EPD-3D abiotic control; (C) and (D) fully active EPD-3D biocathode biofilm; (E) and (F) EPD-3D biocathode after extreme conditions treatments (low pH, autoclave, air drying).

First of all, a predominant biofilm could be observed on the live biocathode electrode surface. Remarkably for a biocathode biofilm, it shows a biofilm of a few layers of microorganisms and of an approximate total thickness of only 5-10 µm. This is relatively thin compared to bioanode biofilm that have been reported up to 100 µm [194]. However, to the best of our knowledge, previous biocathode studies generally reports microorganisms dispersed on electrode surfaces [11, 16] but rarely a well-established biofilm with entangled multi-layered microorganisms. This could be correlated to the high acetate production rates showed above and previously reported (Chapters 6 and 7), and the ability of the acetate-producers to consume this high rate of H_2 before it could escape from the biofilm. As previously reported, the special electrode surface characteristics with the nanoscale structure formed by the CNTs may favour microorganisms' attachment and biofilm development over its surface (Chapters 6 and 7). Comparatively, no biofilm could be observed on the electrodes that were subjected to extreme conditions, with only a few dispersed cells observed. Those were confirmed to be dead cells by FISH, by no or very few microorganism hybridizing with the general bacteria probes (*EUBmix*), as opposed to the active biocathode as visualised in Figure 38.

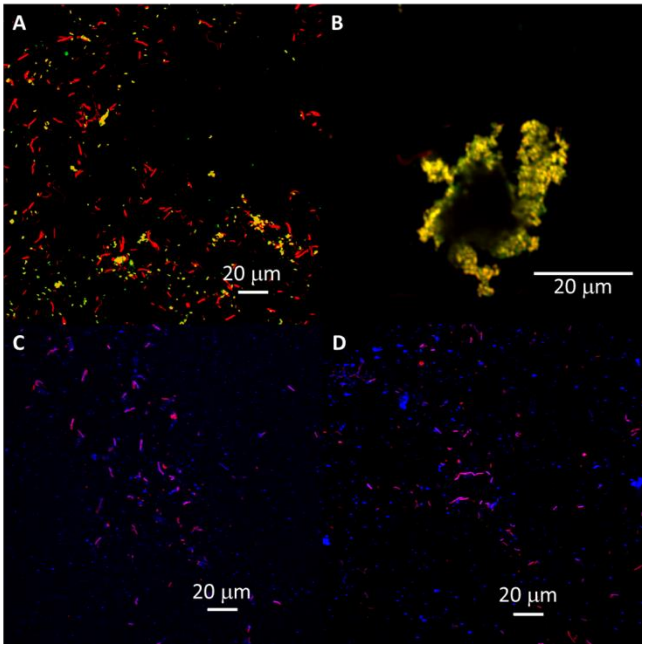

Figure 38 FISH images on suspended biofilm taken from the electrode. *Betaproteobacteria* (*BET42A*) are shown in yellow (A and B) (Colour was modified from original fluorochrome to avoid confusion). *Firmicutes* (*SRB365*) are shown in purple (C and D). Other bacteria (*EUBmix*) are shown in red (A-D). Auto-fluorescent can be observed in blue (C and D) with no overlay to other channels. Scale bars are shown as 20µm.

Firmicutes, believed to be the acetate-producers as discussed above, were observed as long straight or curved rods up to 5 µm in size, whereas the *Betaproteobacteria*, mainly *Hydrogenophaga*, were shown to be small rods or cocci about 1µm in size. Those two different cell types appeared entangled together within the biofilm (Figure 37 C and D). In addition, we can observe on both the sterilized and active electrodes, some inorganic material deposited on the surface of the electrode, which is not observed on the abiotic control surface (Figure 37). This electrode surface 'modification' is hence showing to be permanent and not affected by the extreme sterilizations they were subjected to.

Bacterial surface modification directly involved in the significant H_2 production enhancement

To further investigate the cause of such high H_2 production performance, even after the biofilm was removed, cyclic voltammetry experiments were performed on both the bioactive and sterilized cathodes at pH 7 and are shown in Figure 39.

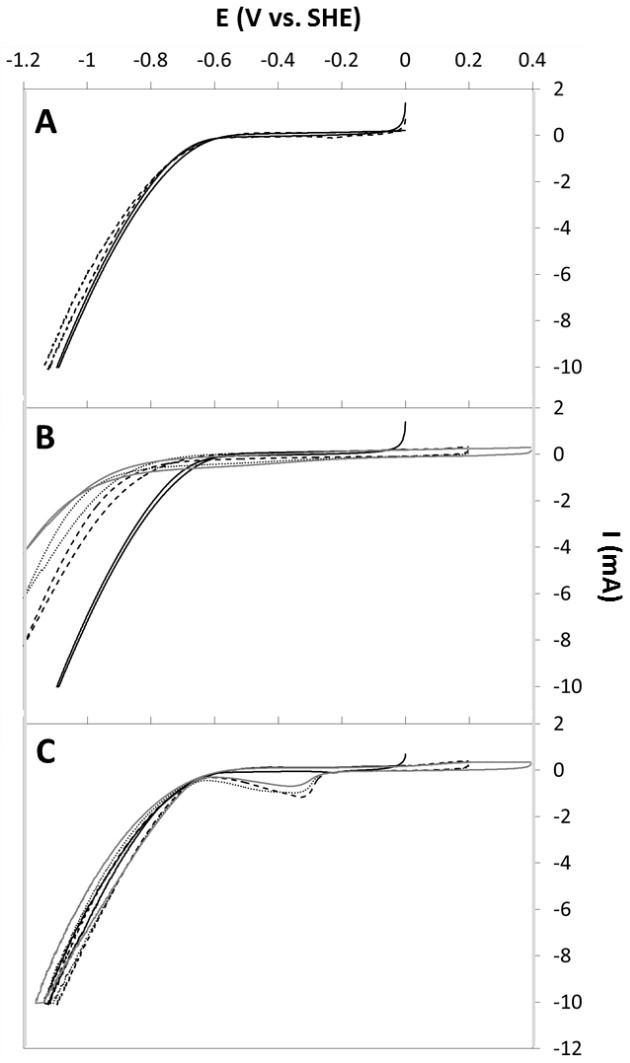

Figure 39 A) Cyclic voltammetry on both bioactive (solid line) and sterilized (dashed line) cathodes right after chronoamperometry at -0.85 V vs. SHE (also represented by solid black lines in B and C). B) CVs recorded on sterilized cathode and C) on bioactive cathode. Both cathodes were then electrochemically oxidized at +0.2 V vs. SHE for 30 min after which a CV was recorded (dashed black line). Following, CVs were recorded after further electrochemical oxidation at +0.2 V vs. SHE for 60 min (dotted grey line) and finally at +0.4 V vs. SHE for 30 min (solid grey line). CVs were recorded at pH 7 and 1 mV s^{-1} scan rate.

We can observe that the H_2 reductive wave onsets are very similar on both bioactive and sterilized cathodes after chronoamperometry at -0.85 V vs. SHE (Figure 39A). This confirms the observations made above and the similar current consumption towards H_2 production before and after extreme condition treatments. We can observe in Figure 39B however, that oxidative current from +0.2 V vs. SHE and above applied for a short period of time (30 to 60 min) irreversibly affected the cathode performance and H_2 production, with a progressive shift of the reductive wave towards lower potentials. This shows that the compound(s)/element(s) playing a key role in the H_2 production mechanism are irreversibly oxidized at higher potentials and performance is not recovered. Interestingly, the biofilm was shown to be able to reduce this compound back to its active form, from ca. -0.25 V vs. SHE, without affecting the H_2 reductive wave onset and H_2

production rate along the potentials range (Figure 39C). This further demonstrates the key role of the microorganisms in the high MES performance and significantly higher H_2 production capability reached after inoculation, compared to abiotic controls. Microorganisms seem to be modifying the cathode surface with catalytically active redox species, which are resistant to high temperature and extreme pH, but are irreversibly lost or damaged through oxidation at positive potentials in the absence of bacteria.

In order to elucidate what redox active species is responsible for such an enhancement of the catalysis of H_2 evolution, the surface chemistry of the bioactive and both sterilized cathodes (duplicates) were analysed by energy-dispersive X-ray spectroscopy (EDS). Several areas of each electrode were analysed for reproducibility. All scans can be seen in Figure 40. As expected only carbon and oxygen elements are present on the surface of the abiotic control. In addition of C and O, Na, P, S, Cl and K were also detected on both the bioactive and sterilized cathode. Those elements are common and are believed not to play a role in H_2 catalysis. More surprisingly, a metal, copper (Cu), was detected in each sample, as showed in Figure 40A'-D' which are zooms of the EDS scans around the area of interest. It was also confirmed that Cu was not detected on the abiotic control (Figure 40 D').

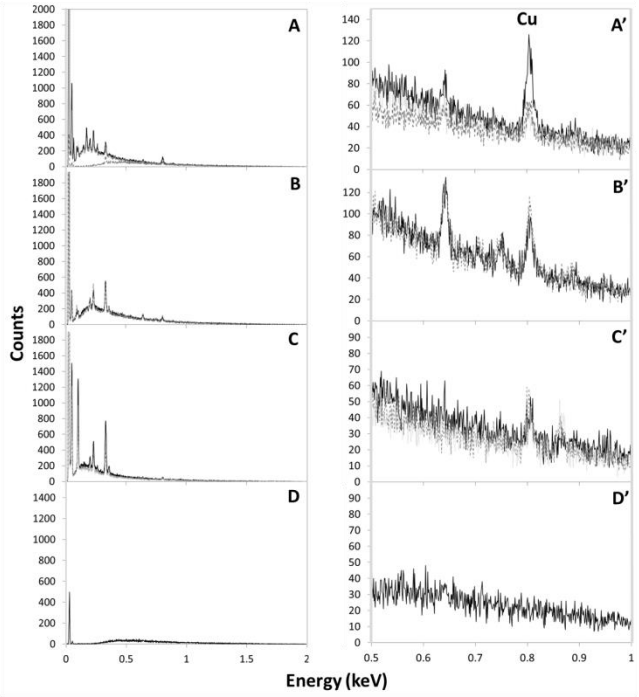

Figure 40 Energy-dispersive X-ray spectroscopy (EDS) spectra, from 0 to 2 keV, of (A) and (B) sterilized EPD-3D biocathode duplicates, (C) fully active EPD-3D biocathode and (D) EPD-3D abiotic control. (A'), (B'), (C') and (D') are the respective zoom of each spectra from 0.5 to 1 keV.

Using reported Pourbaix diagram (potential/pH diagram) of the copper system at similar dissolved concentration (1 μM) than used in this study [221], we confirmed that metal Cu gets oxidized at potentials higher than 0.05 V vs. SHE at pH 7 to another crystalline form, Cu_2O which is further oxidized to CuO above 0.25 V vs. SHE. This correlates with the observations made by CVs showing irreversible and reversible oxidation of the element responsible for H_2 production catalysis at potentials higher than 0.2 V vs. SHE in the sterilized and bioactive cathode, respectively. These observations strongly suggest that metallic copper is directly involved in the H_2 catalysis and its significant enhancement, and that its presence on the surface of the electrode is biologically-induced. In the last few years, copper nanoparticles have been reported as efficient electrocatalyst for water electrolysis and the enhancement of the hydrogen evolution reaction [222-225]. Metal copper nanoparticles have attracted much attention for a wide range of applications, including biomedicine, electronics, catalysis and optics and many chemical and physical synthesis methods have been developed and were recently reviewed [226]. Interestingly, microorganisms with the ability to synthetise metal nanoparticles, and in particular metal copper nanoparticles from Cu^{2+}, have also been found [226-231]. The synthetised metal copper nanoparticles were showed to either be secreted extracellularly [227] or stay within the cell wall [230]. The results shown in the present study suggest the bacterial synthesis of metal copper particles modifies the electrode surface and directly contributes to the significant enhancement of hydrogen production. Further research needs to be carried out to confirm these observations and determine whether the copper particles are excreted onto the surface of the cathode electrode and/or are active from within the cells, and only deposited on the surface after the cells' membrane are broken under extreme conditions. Intracellular copper particles could explain the fast start-up observed after the transfer of an enriched culture in our previous study (Chapters 7). Copper-containing dehydrogenases could also be considered, but such enzymes would also be denatured by low pH and autoclave treatment. More in-depth investigation of the functions of each enriched microorganisms and of the surface chemistry in different experimental conditions will also need to be assessed.

The findings presented in this study are remarkable as they could allow switching from one technology (organics production) to the other (hydrogen production) by simply feeding carbon dioxide or not, without performance loss. This could bring biocathode microbial H_2 production at the forefront of BESs potential practical implementation. Indeed, the performance of these biocathodes reached H_2 production rates of about 1.15 $m^3_{H2}\ m^{-2}_{electrode}\ day^{-1}$ normalised to projected surface area, with a coulombic efficiency of 95 ± 3%. Due to the 3D nature of the electrodes (2620 $m^2\ m^{-3}$), this rate translates to 115 $m^3_{H2}\ m^{-3}_{electrode}\ day^{-1}$. This represents a 27 times increase of the so

far highest reported hydrogen production rate (to our knowledge) in microbial electrolysis cells, which used a Ni- based gas diffusion cathode [93, 232].

In conclusion, we have demonstrated in this study that the main electron transfer mechanism from the electrode to the terminal electron acceptor, CO_2, occurs through H_2 and leads to high microbial electrosynthesis rate of acetate. This high H_2 production rate was found to be biologically-induced, most likely through the biological modification of the electrode surface via synthesis of metal copper (nano)-particles. The biofilm was found to be of far greater importance compared to the planktonic cells with the significant enrichment of *Acetoanaerobium*, *Hydrogenophaga* and *Natranaerobiales*. Indeed, the hydrogen consumers (putatively *Acetoanaerobium*) were shown to be able to utilise a high H_2 flow rate (1.15 m^3_{H2} m^{-2} day^{-1}) within the biofilm, without H_2 able to escape from it. This finding is of critical importance for the potential large-scale implementation of this technology, which allows combining both H_2 production and CO_2 assimilation to an organic final product, within a unique microbial electrosynthesis reactor, without H_2 waste and extra-handling. Finally, we also highlighted the remarkable possibility to switch from organics production technology to pure hydrogen production technology, if desired, by simply stopping the CO_2 feed, without performance loss. Further in-depth investigations into the microbial processes and the surface chemistry will be needed to fully understand this remarkable electron transfer mechanism (see section 10.3).

9 Bringing high-rate, CO_2-based microbial electrosynthesis closer to practical implementation through improved design and operating conditions[5]

We have demonstrated a significant increase in productivity and product specificity of MES to acetate with a specifically enriched microbial culture and using a highly biocompatible, conductive three-dimensional cathode material with surface modifications based on electrophoretic deposition methods that are easily reproducible and scalable (EPD-3D). We also demonstrated that the main electron transfer mechanism from the electrode to the terminal electron acceptor, CO_2, occurs via H_2, while achieving high microbial electrosynthesis rates and conversion efficiencies for acetate production. The H_2 production was found to be biologically-induced, likely through the biological synthesis of metal copper particles.

Further investigation is though needed towards reactor sizing, operating conditions optimization and the need for cheap and easily usable carbon dioxide source. Therefore, we investigated in this study the effect of three different EPD-3D electrode pore sizes (2.54, 0.56 and 0.42 mm average pore diameter) on MES performance from CO_2 to acetate, from both intrinsic and engineering performance. The significant effects of pH and applied potentials on MES performance were also assessed. MES to acetate was also showed successful as a potential biogas cleaning technology when biogas was used as sole, cheap and readily available carbon dioxide source.

Mass transfer limitation vs. total surface area per volume unit - Effect of 3D electrodes' porosity

Four microbial electrosynthesis reactors, two of them equipped with one 45 ppi electrode each, one with a 60 ppi electrode and the fourth reactor with two 10 ppi electrodes (as duplicates for current consumption), were each filled with 250 mL of inorganic medium containing bicarbonate as sole carbon source, and polarized at -0.85 V vs. SHE for 63-70 days. Electrodes 5 to 9 (Table 4)

[5] This chapter is ready for submission (fully written and internally peer-reviewed) to *Environmental Science & Technology* for publication and modified for incorporation in this thesis: **Ludovic Jourdin,** Stefano Freguia, Victoria Flexer, and Jurg Keller. Bringing high-rate, CO_2-based microbial electrosynthesis closer to practical implementation through improved design and operating conditions. *Environmental Science & Technology* (to be submitted), 2015. Waiting for submission upon receiving comments on the paper already submitted to *Energy and Environmental Science* (Chapter 7).

were used in this study. For the tests on the 45 ppi electrode, the average of the two duplicate reactors is plotted in Figure 41 and 42 and referred to in the text, for each parameter studied. Similarly, the electron consumption average of the two 10 ppi electrodes is plotted and referred to in the text. Results of duplicates were in good agreement and the standard deviation minimal, as seen in Figure 41.

On day 0, each reactor was inoculated with about 50 mg (as COD) of enriched mixed microbial culture from a reactor that previously showed electrosynthesis capacity for carbon dioxide to acetate conversion in identical experimental conditions (Chapter 6). Starting right after inoculation, current consumption, carbon dioxide consumption and volatile fatty acids production were followed for each reactor, during 63 to 70 days. Results for the three different electrode porosities were compared to assess the respective performance in terms of intrinsic performance as biocathode material and of the engineering upscaling potential. To do so, results were normalized either by total surface area or projected surface area of the electrodes, respectively.

The cumulative electron consumption and acetate production over time, at constant applied potential of -0.85 V vs. SHE, are shown in Figure 41, respectively, normalized to both projected (left; A and C) and total (right, B and D) surface area. No other volatile fatty acids or alcohols accumulated in any of the reactors. The transfer of an enriched microbial culture achieved a rapid colonisation and activity in all reactors, which is an important demonstration for a successful start-up strategy for larger scale reactors. The first significant observation is the difference in the start-up time required for each electrode type. On 45 ppi electrodes, current and acetate production started increasing after few days (ca. 3-4 days), while it took about 10 days on the 10 ppi electrodes and even longer (ca. 20 days) on the 60 ppi electrode. It is speculated that the 45 ppi electrode may have an optimal combination of high total surface area and accessibility which provides a good initial distribution and adhesion of the microorganisms throughout the electrode.

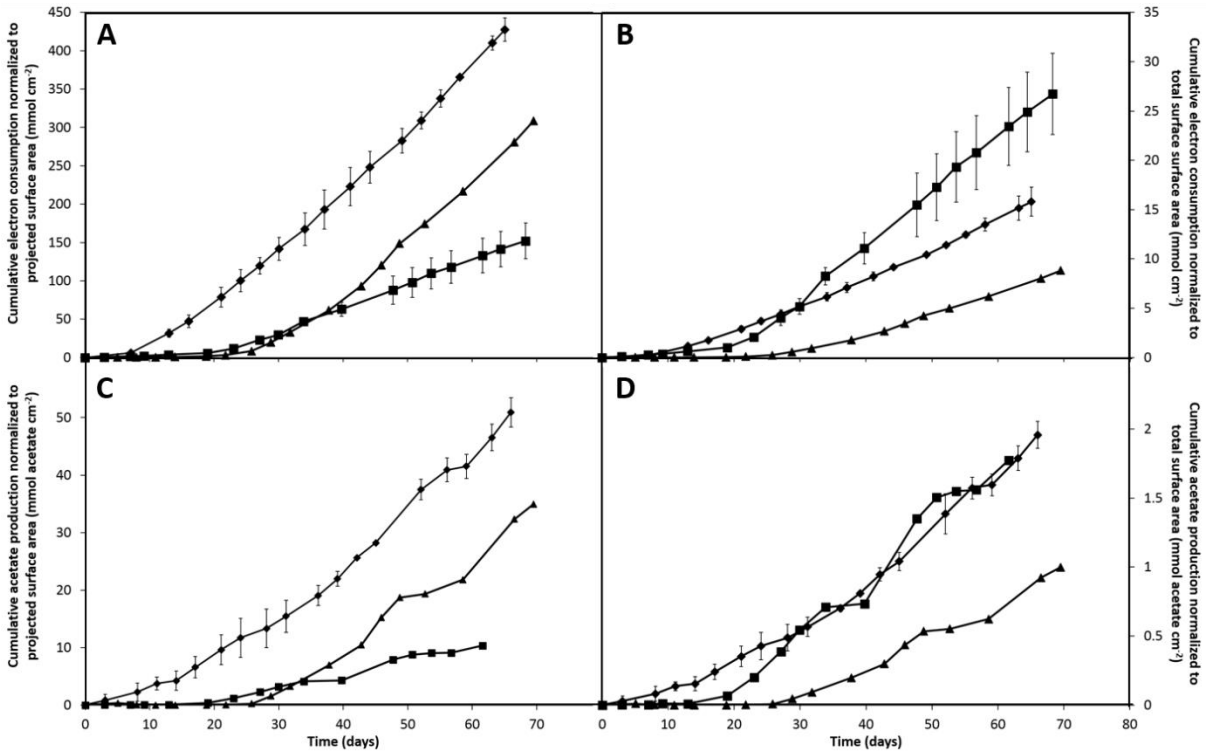

Figure 41 Cumulative electron consumption normalized to projected (A) and total surface are (B) and cumulative acetate production normalized to projected (C) and total surface are (C) over time on 10 ppi (square), 45 ppi (diamond) and 60 ppi (triangle) EPD-3D electrodes.

As previously reported (Chapters 6 and 7), after a first phase of slow electron consumption (start-up phase), electron consumption gradually increased up to a maximum from about 50 days onwards, for each electrode type (Figure 41A-B). A similar trend can be observed for the acetate production in each reactor (Figure 41C-D). Maximal current density (as A m^{-2}) and acetate production rate (as g m^{-2} day^{-1}) were deducted from Figure 41 for each electrode type and are shown in Figure 42. Carbon dioxide consumption was also followed over time (not shown) and maximal rates are plotted in Figure 42 as well. Remarkably, particularly for a mixed culture system, both carbon dioxide and electron conversion efficiencies into acetate were very high and consistent for all three electrode types, with an average of 98 ± 4% and 100 ± 1%, respectively. As discussed in the introduction, high product specificity is of critical importance for large-scale implementation of a production technology. Product separation and recovery is one of the main costs of established chemical production plants, such as industrial fermentation [88, 89]. Therefore, obtaining one 'pure' product instead of a mixture of different products could be a significant benefit for practical applicability of microbial electrosynthesis technology, from both a technical and economic point of view.

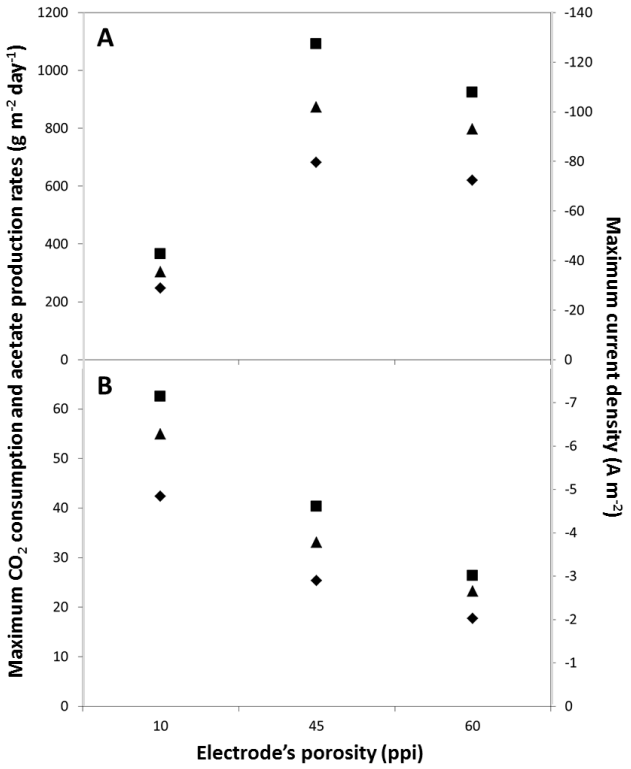

Figure 42 Maximum carbon dioxide consumption rate (square), acetate production rate (diamond) and cathodic current density (triangle) obtained on 10, 45 and 60 ppi EPD-3D, both normalized to projected surface area (A) and total surface area (B).

Figure 42B shows the efficiency of the process in relation to each electrode's porosity, by normalizing the maximum CO_2 consumption and acetate production rates and current density to total surface area. It is clearly evident that the intrinsic performance decreases as the pore diameter decreases, from ca. 42 g m^{-2} day^{-1} of acetate (ca. -6.28 A m^{-2}) for pores with ca. 2.54 mm diameter, to about 2.3 times lower rates when the pores are 6 times smaller (ca. 0.42 mm), i.e. ca. 18 g m^{-2} day^{-1} of acetate (ca. -2.7 A m^{-2}). This shows that mass transfer of substrate / nutrients and/or of product to and from the surface of the electrode becomes limiting as the pores within the 3D structured electrode material become smaller. It has to be pointed out that the mixing rate in each reactor was identical (i.e. same size and rotation rate of magnetic stirrer bars) to allow a valid comparison. It is assumed that the mass transfer through the 3D macrostructure itself (i.e. in the liquid phase) is the limiting factor rather than the mass transfer within the biofilm itself. This is because mass transfer limitations within the biofilm will be independent from the macroporous structure. Moreover we previously observed that the cathodic biofilms in this system remained fairly thin (ca. 7.5 ± 2.5 μm in dry state) (Chapters 6, 7, and 8). At this small thickness, the diffusive mass transfer in the biofilm is very rapid, unlike some of the anodic biofilms that can become fairly thick, up to 100 μm [194], and hence are potentially limited by mass transfer within the biofilm.

In comparison, different trends were observed in Figure 42A, which is more relevant when considering the reactor engineering application potential of each electrode material, as the performance is normalized to the projected surface area. To achieve the maximal electrode performance, both the mass transfer rate and the total surface area per unit volume are critical parameters from an overall productivity perspective. Therefore, the large porosity ('void space') and hence lower surface area for biofilm development within the 10 ppi (2.54 mm average pore diameter) structure produced the lowest overall performance with a current density of ca. -35 A m^{-2} and an acetate production rate of ca. 247 g m^{-2} day^{-1}. When the average pore diameter was decreased by a factor 4.5 (i.e. 0.56 mm; 45ppi), the projected surface area performance was increased by a factor 2.9, achieving the highest MES rates with a current density of -102 A m^{-2} and an acetate production rate of 685 g m^{-2} day^{-1}. Considering the 3D nature of the electrode, this corresponds to an acetate production rate of 66.5 kg m^{-3} day^{-1}. It can also be observed from Figure 42A that this strategy of increasing the total surface area per volume has its limit and that the associated reduction in mass transfer rate can limit the overall productivity. A further decrease in pore size to 0.42mm (60ppi) did achieve a slightly lower performance than for the 45 ppi electrodes, with -92 A m^{-2} current density and 620 g m^{-2} day^{-1} of acetate production. Therefore, for this reactor configurations and under the given forced mass transfer conditions, an EPD-3D electrode pore diameter in the order of 0.6 mm is optimal.

Interestingly, this optimal pore size range in this set-up is different to that found for anode biofilms [117] in similar reactor configurations. Although on a different electrode material and under stagnant conditions, in that work, it was found that the optimal pore diameter was 2.2 mm, i.e. much larger than our finding. This difference could be due to the higher catalytic activity and the larger thickness of anodic biofilms. However, further investigations need to be carried out to determine the influence of different (forced) mass transfer through the 3D electrode matrix. Indeed, this porosity influence is highly dependent on the actual flow rate through the electrode material. A better compromise between mass transfer and total surface area per volume unit available for biofilm development could then be found in a forced flow-through system, in which case the pore size could possibly be smaller to achieve the maximal performance.

Effect of cathode applied potential

The effect of the applied cathode potential on the microbial electrosynthesis performance was investigated by linear sweep voltammetry (LSV), on the 45 ppi electrode reactors, in turnover condition (i.e. with continuous gaseous CO_2 feed). In parallel, online flow monitoring of key target gases (H_2, CH_4, and CO_2) using the titration and off-gas analysis (TOGA) sensor was employed, as

described in a previous study (Chapter 8). The TOGA measurements confirmed that no methane was produced during the course of the experiment (data not shown). The TOGA also allows to continuously monitor any H_2 that would be stripped off the reactor by the continuous gas flow (He-CO_2) bubbling through the reactor. The H_2 flow rate could then be determined, and the corresponding current transformed into H_2 as end-product was calculated (see materials and methods). H_2 that might have been produced but consumed within the biofilm, and hence not detected by TOGA, is not taken into account by the parameter "current transformed into H_2" (see Chapter 8). Unlike long-term chronoamperometry tests, LSV experiments were too short to obtain an easily measurable change in acetate concentration during the potential scan. However, based on the 100% electron conversion efficiency into acetate in continuous operating conditions at -0.85 V vs. SHE applied cathode potential (see above), and building on previously reported results with the TOGA sensor on similar systems (Chapter 8), it is reasonable to assume that any current not recovered as H_2 flow during the LSV was converted into acetate. The total current consumed, the current converted into H_2 as well as the deducted acetate production along the potential range covered in the LSV are plotted in Figure 43A. The potentials were scanned from 0 to -1.1 V vs. SHE at a scan rate of 0.1 mV s^{-1} (unidirectional). The pH was controlled at 6.7 throughout the test. This experiment was run in duplicate, with the result being very similar as shown in Figure 43B. A comparison of biotic versus abiotic LSV can also be seen in Figure 44.

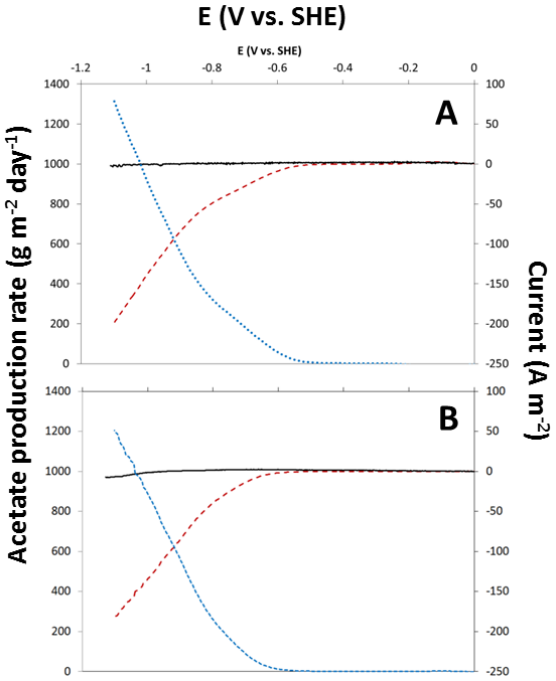

Figure 43 Linear sweep voltammetry (current shown by dashed red line) of biotic reactor in turnover conditions recorded using the TOGA sensor, in duplicate (A and B). The solid (black) line represents the current converted into hydrogen while the dotted blue line represents the calculated acetate production rate. The plotted values were normalized to projected surface area. Scan rate: 0.1 mV s^{-1}.

As previously reported, a clear shift of the reductive wave towards higher potential was observed compared to the abiotic control, which has been regarded as evidence of biological catalytic activity [15, 104] (Chapters 5, 7, and 8).

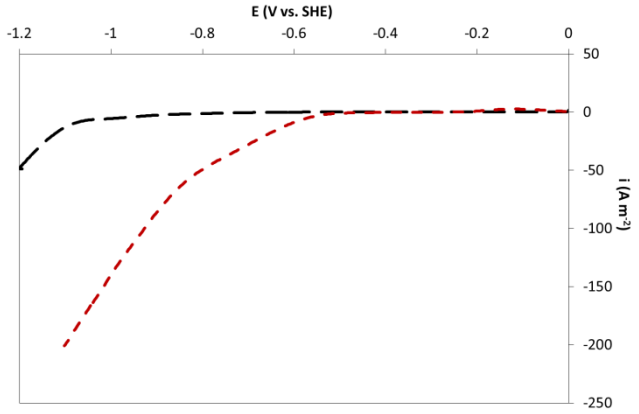

Figure 44 Linear sweep voltammetry of both abiotic control (black) and biotic (red) reactor in turnover condition. The plotted values were normalized to projected surface area. Scan rate: 0.1 mV s^{-1}.

Acetate production started occurring at fairly high potential, ca. -0.5 V vs. SHE. According to observations made during the chronoamperometry experiments described above, 100% of the electrons derived from the electrode were assimilated into acetate at -0.85 V vs. SHE. However, more strikingly, still 99% of the electrons were converted into acetate at -1.1 V vs. SHE, achieving a potential acetate production rate of 1330 g m^{-2} day^{-1} at this cathode potential. This corresponds to an impressive 133 kg m^{-3} day^{-1} of acetate, which means the above reported production rate could be doubled by applying 250 mV lower cathode potential, while still conserving very high product specificity. This observation could have an important impact for the practical application of this technology. It is very likely that the higher production rate would bring larger benefits in terms of capital cost savings (halving the cathodic reactor volume) compared to the additional operating costs due to the higher power requirements to achieve the lower cathodic potential. Remarkably, a very high cathodic current density of about -200 A m^{-2} was reached at -1.1 V vs. SHE. As previously reported, biologically-induced hydrogen is the main electron shuttle from the electrode to the acetate-producing biomass, which forms a thin biofilm on the surface of the electrode (Chapter 8). This current density corresponds to a high hydrogen production rate (ca. 2.3 m^3_{H2} m^{-2} day^{-1}) and it highlights the very high hydrogen consumption capability of the acetogens located in the biofilm. It could be expected that such a high H_2 production rate would remove a biofilm from the electrode surface due to the large gas volume generated, but this experiment showed that the hydrogen-utilising acetogens are able to cope very effectively with this hydrogen production. Furthermore Figure 43 seems to indicate that -1.1 V vs. SHE is most likely not the maximally

applicable potential and lower potentials could be applied to further increase the acetate production rate as long as the acetogenic biofilm can still fully convert the increased H_2 production. Such optimisations would need to be incorporated in an overall economic assessment to evaluate the impact of the higher power costs in relation to the maximum acetate production rate that can be achieved.

Effect of pH

Using the TOGA sensor, the effect of the operating pH on the MES performance of the 60 ppi EPD-3D was also assessed. Figure 45A shows the evolution of the total current consumed at an applied cathode potential of -0.85 V vs. SHE (same as chronoamperometry tests above) as well as the current assimilated into H_2 as end-product, while the pH was decreased step-wise from 6.7 to 3. Figure 45B shows the electron recovery into H_2 and acetate production rate relative to the pH. No methane was detected by the TOGA sensor throughout this pH variation experiment.

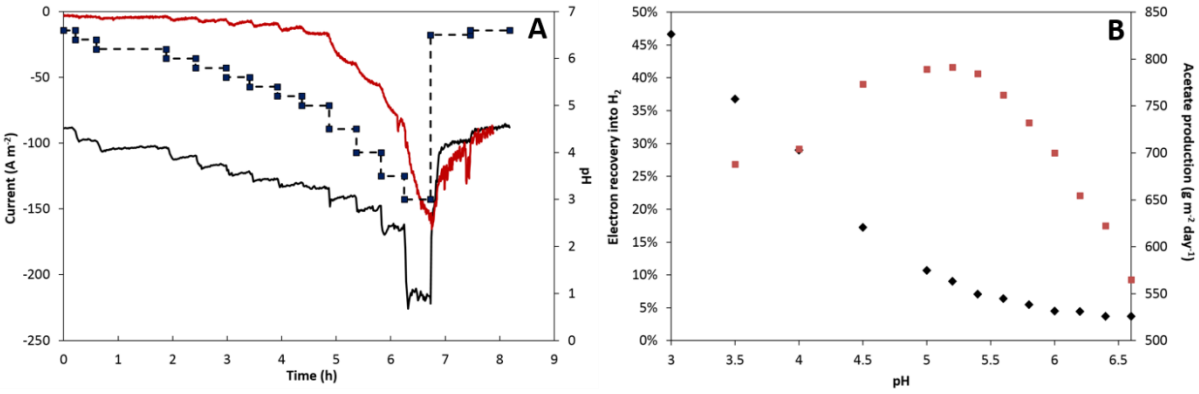

Figure 45 A) pH variation experiment on EPD-3D 60ppi using the TOGA sensor. Both total current consumed (solid black line) and current converted into H_2 (solid red line) were followed at -0.85 V vs. SHE applied cathode potential while the pH was decreased step-wise from 7.5 to 3 (blue square, dashed line). The current values were normalized to projected surface area. B) represents the electron recovery into H_2 (black diamond) and acetate production rate (red square) at each pH.

Microbial electrosynthesis from CO_2 to acetate was found to be very dependent of the pH. Slight changes on the pH led to significant change on the total amount of current consumed. Unlike the above chronoamperometry and LSV tests above, 'only' about 97% of the electrons consumed were assimilated into acetate at pH 6.7. The most remarkable observation from this test is that an optimum pH of 5.2 was required to achieve the maximal acetate production rate of about 790 g m^{-2} day^{-1} (77 kg m^{-3} day^{-1}). It has to be pointed out here that the 60 ppi electrode material was typically not achieving the best acetate production performance due to mass transfer limitations in this configuration. This low operating pH is not only interesting to achieve a 40 % higher acetate production rate, but could also likely inhibit any methanogenic activity. For large-scale application, avoiding the addition of an external chemical inhibitor (bromoethanesulfonate) would have a large

positive impact both technically and economically. This result confirms the findings of a recent study where a continuous operation at a controlled pH of 5.8 achieved a higher acetate production rate than at higher pH [12]. It was not clear whether this was due to the direct effect of the low pH on the metabolism of the microorganisms or to the indirect increase of substrate availability. Since the main electron transfer mechanism for acetate production has shown to be via biologically-induced hydrogen (Chapter 8), the improved acetate production performance would likely be due to the direct effect of significantly higher proton availability at lower pH. This would further support the hypothesis that mass transfer limitations into the 3D electrode matrix, likely in the form of limited proton availability, is the main reason for the reduced acetate production in the 60 ppi RVC foam compared to the more porous materials. Indeed, from all the reactants needed for acetate biolectrosynthesis, H+ is by far the more diluted one in our reaction media, and therefore an increase of more than an order of magnitude in its concentration is very likely going to increase the production rate, provided the microorganisms are still active at the new pH. The ongoing increase in current even below pH 5.2 demonstrates that even higher current densities can be achieved (at a given potential) by increasing the proton availability further. However, at these more acidic conditions, the acetogenic activity seems to be limited and hence more current is converted to H_2 directly.

The effective inhibition of methane production would also have to be investigated in these conditions without bromoethanesulfonate addition, for a prolonged period of time. Moreover, we can observe in Figure 45 that about 9% of the electrons consumed were 'lost' in H_2, hence not assimilated into acetate, making the process slightly less specific. However, this could also be due to the fact that the culture was acclimated at pH 6.7, and that the duration of the pH variation steps was relatively short. It is believed that culture enrichment at a lower pH would remedy this.

Finally, it can be observed that pH lower than 4.5 is detrimental to the acetate-producing microorganisms. Significantly higher proportion of H_2 was detected. Remarkably, but in the line of the previous electron transfer mechanism findings (Chapter 8), a significant absolute cathodic current increase was observed when the pH was decreased towards even lower pH, with the highest current density of about -220 A m^{-2} recorded at pH 3. We previously showed that hydrogen production was most likely due to the biological synthesis of copper particles and catalysis effect was maintained even after the biofilm was removed (Chapter 8). When the current was increased back to 6.7, all the electrons were derived to H_2 production only, confirming that too low pH removed or strongly inhibited the acetogens. This finding has potential implication for pure H_2 large-scale implementation. Once the H_2 maximum performance are obtained due to biological

activity, one can either decide to stop feeding CO_2, or sterilise the reactor to obtain H_2 as sole product, and could decrease the pH to low values to increase the production rate further. Taking into account the 3D nature of the electrode (2600 m^2 m^{-3}), a current of -220 A m^{-2} (22000 A m^{-3}) would correspond to ca. 250 m^3_{H2} m^{-3} day^{-1}, which is one of the highest H_2 production rate reported to date on MEC, to the best of our knowledge.

Use of biogas as a readily available carbon dioxide source

Another key consideration for potential practical applications is the source of carbon dioxide. Several options are available, but not all of them are economically attractive for MES applications to produce relatively low-value end-products such as acetate. Therefore, a cheap and readily available carbon dioxide source would be favoured, which would likely be in a mixed gas situation. Biogas could be regarded as an interesting option in this context as it is primarily composed of methane (CH_4) and carbon dioxide. Biogas is produced during anaerobic digestion and can be used on-site for power generation but could also be more economically used as a transport fuel for buses/cars etc. For the latter application the CO_2 fraction needs to be removed to improve gas compression/storage and combustion efficiency. Therefore, an MES process to convert the CO_2 fraction to acetate could be perfectly suitable for such a biogas 'cleaning' operation. This option could then be both environmentally and economically attractive for both applications, organics production and biogas utilisation as fuel. Consequently, a synthetic biogas mixture, CH_4-CO_2 (70%:30% v/v), was fed to an MES reactor with 45 ppi electrode for a period of about 2 weeks. The cathode potential was controlled at -0.85 V vs. SHE and the pH at 6.7, while the current consumption and VFA production were followed over time. The current consumption evolution can be seen in Figure 46. Two chronoamperometry experiments in the same conditions were performed with the TOGA sensor, and the current converted into H_2 in comparison to the total current consumed in test are shown in the inserts in Figure 46.

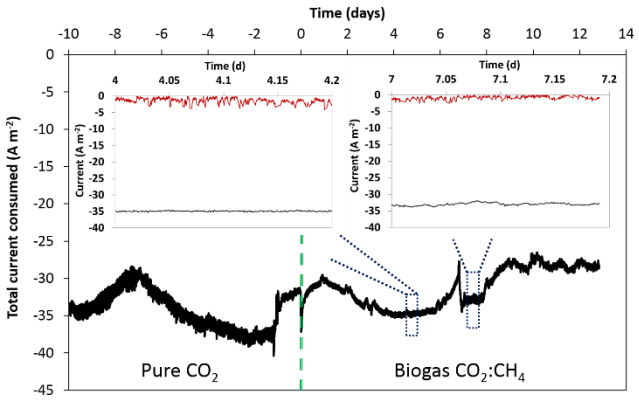

Figure 46 Current density evolution over time (solid black line) on EPD-3D 45 ppi while being fed with pure CO_2 from day -10 to 0 and with a synthetic biogas mixture (CH_4-CO_2 70%:30% v/v) from day 0 onwards, at -0.85 V vs. SHE applied cathode potential. The two inserted graphs show the current converted into hydrogen (red solid line) measured on the TOGA during two distinct periods of the chronoamperometry test.

We can observe that feeding the biogas mixture instead of pure CO_2 did not influence the total current consumed; the current had already decreased to about -30-35 A m^{-2} before this test, as observed in Figure 46. The chronoamperometry experiments run with the TOGA sensor also showed that no H_2 was detected from the reactor, and the VFA analyses over the 13 days of the experiment confirmed that 98 ± 2% of the electrons consumed were assimilated into acetate, with no other VFAs produced. Using biogas as carbon dioxide source showed therefore very similar MES performance as compared to using pure CO_2, making biogas a potentially useful and efficient CO_2 source for large-scale MES implementation. Obviously, the authors realise that this test is mainly a successful proof of concept, and further investigations would need to be carried out using real biogas, which may also contain small traces of hydrogen sulphide that could affect MES performance.

In conclusion, we have demonstrated in this study that higher proton availability significantly affects MES performance, with a drastic acetate production rate increase to 790 g m^{-2} day^{-1}, at the optimal pH of 5.2 and -0.85 V vs. SHE. As an additional advantage, this high acidity would likely inhibit methanogenesis completely without the addition of a chemical inhibitor, which would have a significant technical and economic impact. Applied cathode potential as low as -1.1 V vs. SHE was shown to still achieved 99% of electron recovery into acetate at a current density of around -200 A m^{-2}. This performance led to an impressive acetate production rate of up to 1330 g m^{-2} day^{-1} (133 kg m^{-3} day^{-1}) at pH 6.7. We have also investigated the optimization of the 3D macroporous electrode structure. The total surface area available to biofilm development per volume unit and mass transfer were identified as the two main components governing this optimization. The major source of mass transfer limitation was found to be the transport of

substrate(s) / product(s), likely in the form of limited proton availability, throughout the electrode's macrostructure as opposed to their transport within the biofilm itself. An EPD-3D pore diameter of about 0.6 mm was found to be optimal in this respect, with maximal acetate production rate of about 685 g m^{-2} day^{-1} (66.5 kg m^{-3} day^{-1}) at pH 6.7 and -0.85 V vs. SHE. Furthermore, we successfully demonstrated the use of a synthetic biogas gas mixture as carbon dioxide source yielding similar high MES performance. This would allow MES to be used effectively for both biogas quality improvement and conversion of the available CO_2 to acetate. We also highlighted in this study the high potential of pure H_2 as an end-product using the same MES set-up. We report here that lowering the pH down to 3 increased H_2 productions up to 250 m^3_{H2} $m^{-3}_{cathode\ chamber}$ day^{-1} at -0.85 V vs. SHE. These findings have an important impact on the practical implementation potential of microbial electrosynthesis and electrolysis processes, both technically and economically.

10 Conclusions, perspectives and recommendations for future work

10.1. Main conclusions

The main objective of this thesis was to develop new approaches to significantly enhance performance of microbial electrosynthesis from CO_2 while elucidating the process mechanisms.

A very effective mixed microbial consortium was successfully enriched and demonstrated drastic performance enhancement of microbial electrosynthesis of acetate from CO_2 reaching comparable productivity levels as in industrial fermentation processes (volumetric production rate and product yield). An unprecedented biocathode current density of -102 ± 1 A m^{-2} and acetic acid production rate of 685 ± 30 g m^{-2} day^{-1} (equivalent to 66 kg m^{-3} day^{-1} and 98 kg_{CO2} m^{-3} day^{-1} captured) was achieved in this Thesis. This corresponds to more than an order of magnitude increase of the highest acetate production rate reported to date (Table 10). Very high recoveries of 94 ± 2% of the CO_2 supplied as sole carbon source and 100 ± 4 % of electrons into the final product (acetic acid) were achieved, reaching an impressive product titer of up to 11 g L^{-1}. This high product specificity is remarkable for mixed microbial cultures, which would make the product downstream processing easier and the technology more attractive. This performance enhancement was enabled through the combination of a well acclimatized and enriched microbial culture (very fast start-up after culture transfer), coupled with the use of newly synthesized electrode materials. Novel biocompatible, three-dimensional hierarchical cathodes manufactured by deposition of flexible multiwalled carbon nanotubes on reticulated vitreous carbon were firstly developed by chemical vapour deposition and further enhanced by electrophoretic deposition, which was found to lead to significantly different electrode characteristics. Very importantly, electrophoretic deposition is a suitable technique for industrial scale production of this new material as it requires simple, inexpensive equipment and short deposition times.

This is the first study showing better intrinsic efficiency as biocathode material of a three-dimensional electrode versus a rough electrode: this comparison was made considering the total surface area of the porous electrode, and not just the projected surface area. The nanostructure was shown to enhance the bacteria-electrode interaction and biofilm development. The high surface area to volume ratio of the macroporous RVC maximizes the available biofilm area while ensuring

effective mass transfer between the bulk liquid and the electrode/biofilm surface. Using pore sizes of about 0.6 mm diameter was found to be optimal in this respect.

High-rate acetate production was demonstrated to occur exclusively within the biofilm via biologically-induced hydrogen, before H_2 could escape from the biofilm. This is a major advantage for large-scale implementation of this process over technologies that rely on mass transfer of H_2 to microorganisms suspended in aqueous solution. First evidence suggests that bacterial synthesis of copper particles modifies the electrode surface and is directly involved in the significant enhancement of the hydrogen production.

Additionally, further enhancement of microbial electrosynthesis rates were demonstrated by optimizing key operating conditions. A 40 % increase in production rate were observed with higher proton availability, with pH 5.2 found to be optimal. Furthermore, this low pH would likely suppress methanogenic activity without the addition of a chemical inhibitor which would positively impact the applicability of the technology. Moreover, twice higher acetate production rates were achieved at pH 6.7, up to an exceptional 1330 g m^{-2} day^{-1} (133 kg m^{-3} day^{-1}), by applying an extra 250 mV (cathode applied potential of -1.1 V vs. SHE) while maintaining high product specificity with still 99 % electron recovery in the form of acetate.

In conclusion, this work takes microbial electrosynthesis a considerable step forward, with high performance levels and elucidation of mechanism, which could potentially support large-scale practical implementations of such cathodic processes. In addition, this PhD thesis reports some valuable novel findings that could assist many other researchers to advance their related studies.

10.2. Perspectives

Even though several issues regarding actual scaling-up of BES technology still need to be overcome, as discussed below (section 10.3), the performance reached in this PhD work should favour realistic discussions within the research community on strategies to adopt for microbial electrosynthesis scale-up to practical applications.

Here, we discuss potential practical implementation of MES to acetate in terms of carbon dioxide source, acetate utilisation and possible use of the enriched microbial consortium in other biological systems, as represented in Figure 47. An in-depth discussion and economic feasibility study for several scenarios are presented below.

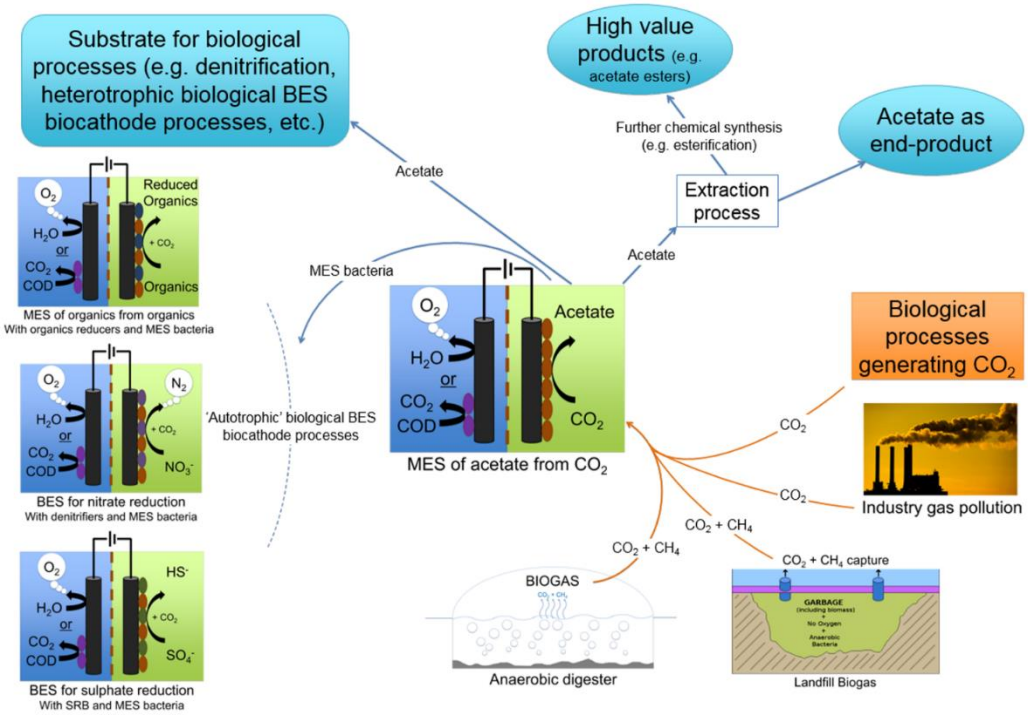

Figure 47 Microbial electrosynthesis technology versatility scheme displaying the many possible choices regarding the nature of the carbon dioxide source, the utilisation of acetate and other uses of the enriched MES microbial consortium

Assumptions for economic feasibility studies

Table 11 presents the main assumptions used for the economic feasibility studies discussed below. All costs are given in Australian dollars.

In the past few years, several research groups have attempted to assess the scaling-up feasibility of bioelectrochemical systems [109-111, 233], in particular of MFC and microbial electrolysis cells technologies [112-114]. It has become common practice within the academic community to assess BES for engineering application by normalizing current and other production related parameters to projected surface area of 1 square meter. It would also be primordial to limit the distance between anodes and cathodes (electrode spacing) to limit (ohmic) resistance and proton diffusion time issues. Therefore, for scale up and cost analysis purposes the dimensions of the cathode and anode chambers were assumed at 1 m^2 and 1 cm wide (Flat-plate design). As previously discussed in Chapters 7 and 9, in addition of offering higher MES performance normalized to total surface area versus flat and rough electrodes, the EPD-3D electrode developed in this PhD work offers a very high surface area to volume ratio which significantly maximise the available biofilm area and consequently the CO_2 consumption and acetate production rates per volume unit, compare to using a flat electrode. Therefore, the number of cells needed to treat a certain amount of CO_2, hence the capital costs for the cells, is drastically reduced by using effective three-dimensional scaffold electrode such as EPD-3D. For the purpose of cost analyses, we

assumed a successful scale-up reaching similar rates than demonstrated in this thesis at laboratory scale. We assumed the highest current density observed of -200 A m^{-2} (Chapter 9) and the corresponding acetate volumetric production rate (Table 11). Although the cathode chamber volume would also be determined by other parameters, EPD-3D was assumed to occupy the whole volume at this stage. However, such performance remains to be observed on a longer-term and scale-up to be tested. Regardless of the assumptions necessarily made at this early research and development stage, it is believed these feasibility studies will give valuable insight and research and development objectives to be aimed at in the near future, as developed further in section 10.3.

Table 11 Estimated BES practical dimensions, BESs capital and operational costs, MES performance at large scale, and other important considerations. The capital costs of BESs were either estimated based on materials currently used in laboratory systems [(a)] or on predicted future capital costs [(b)].

BES practical dimensions				
Dimension of cathode and anode chamber (m x m x m)	1 x 1 x 0.01			
Cathode chamber volume (m^3)	0.01			
BES cell volume (m^3 $reactor^{-1}$)	0.04			
Estimated capital costs of BES (CAPEX) (single cell design)				
Electrodes (x2) ($ m^{-2})	2000[(a)]	1100[(b)]	500[(b)]	200[(b)]
Membrane (x1) ($ m^{-2})	100[(a)]			
Current collectors (x2) ($ m^{-2})	50[(a)]			
Replace the 3 above every (year) [234]	5			
Reactor frame ($ $cell^{-1}$)	100[(a)]			
Replace reactor frame every (year) [234]	25			
BES cost at time 0 ($ $reactor^{-1}$)	2250	1350	750	450
BES cost at time 0 ($ m^{-3})	56250	33750	18750	11250
Estimated operational costs of BES (OPEX)				
Electricity cost ($ kWh^{-1})	0.07			
Hydrochloric acid cost ($ kg^{-1}) [235]	0.26			
MES process performance				
Current density (A m^{-2})	-200			
Current density (A m^{-3})	-19522			
Acetate production rate (kg m^{-3} day^{-1})	129			
CO_2 consumption rate (kg m^{-3} day^{-1})	192			
Anodic oxygen production rate (kg m^{-3} day^{-1})	140			
Others				
Current acetate market value ($ ton^{-1}) [235]	900			
Current oxygen market value ($ ton^{-1}) [235]	760			
Oxygen compression (kWh kg^{-1})	0.87			

The cost assumptions of the laboratory materials are based on the author and his colleagues' experience and the cost assumptions of the future materials (electrodes) used in the developed model were also chosen to give objectives towards which research should eventually tend to. EPD-3D manufacturing cost was calculated to be about 1000 $ per 1x1x0.01 m electrode, using RVC and CNT costs obtained for small laboratory-scale systems used in this study. It is very likely that the

cost per electrode will be significantly lower for large-scale production of EPD-3D. The additional costs of 2 electrodes per reactor (anode and cathode) are shown in Table 11, as well as for the collectors. The electricity and oxygen compression costs were provided by industry partners based in Australia. It should be noted that electricity prices may fluctuate between countries and off-peak power may be obtained cheaper than the bulk industrial rate. Maintenance, labour, civil works (etc.) were not included in the operational costs at this stage.

H_2O oxidation abiotic anode vs. bioanode for COD removal

Up till now, investigations on MES from CO_2 has logically focused on the process understanding and development of the biocathode side, while the anode side was overlooked. However, cathode and anode reactions have to be synchronised in terms of electron flow and ion flow, i.e. the total current flow in both chambers has to be identical [207]. In this PhD work, noble platinum metal was used as counter electrode to prevent the anodic reaction to be limiting. However, future research will need to investigate the combination of cheap and effective anode together with highly efficient cathode as developed in this study. Two main anodic reactions could be envisioned, abiotic O_2 evolution by water electrolysis and biological COD oxidation as schematised in Figure 48, and referred to below as MES A and MES B, respectively.

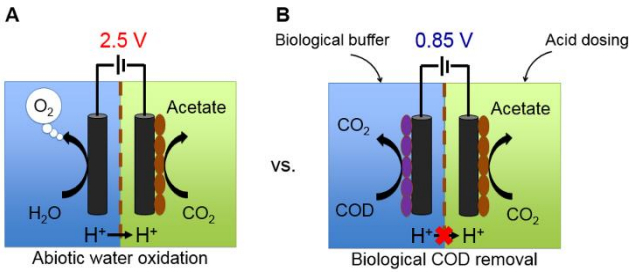

Figure 48 Representation of the two main options for anodic reaction (A) abiotic anode for water oxidation and (B) bioanode for COD removal.

The chemical equation of the cathodic reaction can be seen below (Equation 1). The reverse reaction schematise the oxidation reaction occurring at the bioanode, using acetate as model compound. Equation 2 represents the oxygen evolution reaction.

Equation 1 Carbon dioxide reduction to Acetate $$2\,CO_2 + 8\,H^+ + 8\,e^- \rightarrow CH_3COOH + 2\,H_2O$$

Equation 2 Water oxidation to oxygen $$4\,H_2O \rightarrow 2\,O_2 + 8\,H^+ + 8\,e^-$$

On one hand, a higher cell voltage will need to be applied to run MES A than MES B. We assume a cell voltage of around 2.5 V for MES A, while a cell voltage as low as 0.85 V could theoretically be envisioned for MES B. Those cell voltages were calculated based on the cathode potential applied in this study and the theoretical redox potential of both anode oxidation reactions

under consideration rounded-up with assumed overpotentials. Therefore, electricity consumption could be 3 times higher in the case of an abiotic anode. However, a biological buffer will need to be added in the anode of MES B for pH control and anolyte conductivity, unlike in MES A where the pH will go down as desired for effective proton crossover to the cathode side as well as high anolyte conductivity without addition of an external buffer. Therefore, the proton concentration on the anode side of MES B will remain very low (ca. neutral pH) and crossover of other cations (e.g. NH_4^+, K^+, Ca^{2+}, Na^+) will occur for charge balance. Consequently, protons necessary for the cathode reaction will need to be provided in MES B whereas the necessary amount of protons crosses from the anode side in MES A (Equation 1Equation 2). MES A would then allow 100% of the CO_2 to be converted to the final product, as reported in this PhD thesis.

Two practical scenarios can then be envisioned for MES B. Feeding CO_2 continuously to MES B reactor (referred to as MES B1) will lead to one mole of CO_2 out of five converted to acetate while the remaining 4 moles will be used to buffer the cathode solution (Equation 2). Therefore, depending on the implementation and the desired outcome (production vs. carbon capture), converting only one fifth of the CO_2 would affect the economic feasibility of the process. Five times less valuable end-product will be generated (at same production rate) but on the other hand 5 times less reactors will be necessary, significantly decreasing the capital cost of the BES installation. Another option (referred to as MES B2) would be to occasionally feed CO_2 in a fed-batch manner and convert it all into acetate in between each CO_2 addition. In the latter case, acid dosing will be necessary (4 mole of HCl per mole of CO_2 consumed) to prevent the pH to increase and negatively affect bacterial activity and MES performance. Additional costs would then need to be considered. Moreover, practical implementation of this process is likely to occur on-site of a CO_2-generating industry which CO_2 stream is continuously produced, thus requires continuous conversion (to prevent loss and/or storage). Therefore, in the latter case (fed-batch mode), a higher number of reactors will be required to be able to continuously convert all the CO_2 to acetate compared to MES A and MES B1. However, this number of reactors is hardly identifiable at this stage.

Omitting the capital costs, MES A, B1 and B2 were assessed in term of operational costs per kilogram of acetate produced, i.e. taking into account electricity and acid dosing (for MES B2) costs (buffer and nutrient costs were not included at this stage) and is shown in Figure 49A according to the cost of electricity per kWh and versus the current market value of acetate.

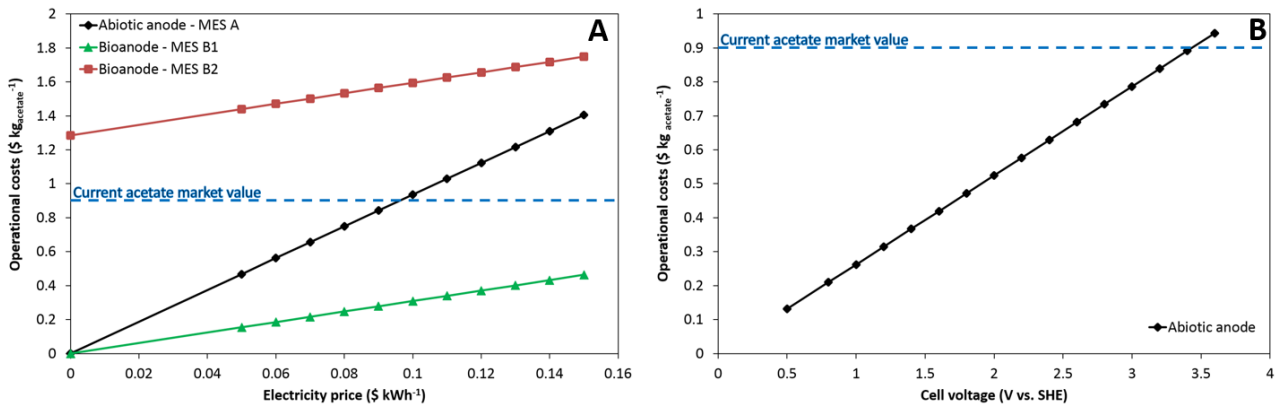

Figure 49 A) Operational costs according to electricity price for both abiotic anode and bioanode anodes, and B) operational costs according to the cell voltage at 0.07 $.kWh^{-1} using the abiotic anode.

It can be observed that under 10 cents per kWh, MES A remains profitable relative to the current market value of acetate, unlike MES B2 which operational costs are always above the selling price of acetate. Therefore, even though three times less electricity is required, the acid dosing is detrimental to MES B2 applicability. MES B1 was found profitable along the whole range of electricity cost. However, the use of a bioanode would most likely be limited to niche industries where an organic waste stream with the right characteristics would be available on-site. Additionally, the highest current densities per projected surface area reached to date by microbial anodes are roughly 100 A m^{-2} (using synthetic influent) [117, 146, 156], twice lower than necessary to synchronise the electron flow at the cathode. Synchronizing / controlling two biological reactions would also be more difficult than only controlling the cathode. Therefore, for the following case studies, an abiotic anode for oxygen evolution was considered, for 100% CO_2 conversion to acetate, unless otherwise specified.

An operational cost of about 0.65 $ $kg_{acetate}^{-1}$, corresponding to a small profit margin of 0.25 $ $kg_{acetate}^{-1}$, was calculated for MES A at 0.07 $ kWh^{-1}; electricity cost for Australian industries. Even though a cell voltage of 2.5 V was deemed reasonable to run such system, the effect of cell voltage on the OPEX of MES A was also modelled, at 0.07 $ kWh^{-1}, and can be seen in Figure 49B. Higher overpotentials than expected, leading to cell voltages superior than 3.4 V would be detrimental to the process economic applicability. For the following case studies, a cell voltage of 2.5 V and electricity cost of 0.07 $ kWh^{-1} have been used, unless otherwise specified.

Carbon dioxide source

Increasing availability of CO_2 as a feedstock has spurred research into processes that can convert it into valuable end-products. However, a key consideration for potential practical application of such MES technology is the source of carbon dioxide. Several options are available,

but not all of them are attractive for MES applications to produce relatively low-value end-products such as acetate.

Human activities produce an annual excess of approximately 3.9% CO_2 with respect to the natural "carbon cycle", which is not balanced by CO_2 fixation mainly due to deforestation [236]. Most of these anthropogenic carbon dioxide emission comes from power generation, public electricity and heat production from fossil fuel combustion [4]. However, the carbon intensity of those fossil fuels, i.e. the amount of CO_2 emitted for each unit of energy produced, is such that the CO_2 generated by their combustion is not plausible for use as feedstock for MES. For example, the carbon intensities of coal and natural gas were reported to be about 1029 kg_{CO2} MWh^{-1} and 515 kg_{CO2} MWh^{-1}, respectively [237]. Following the assumptions made above (Table 11), the MES system requires about 6.1 kWh per kg of CO_2 reduced, which corresponds to 4 and 2 times more electricity (MWh) required to run the BES than originally generated by combustion of coal and natural gas, respectively. Therefore, MES is not suitable as a carbon capture technology for fossil fuel combustion plants.

However, many other carbon dioxide sources could be appropriate. As represented in Figure 47, we propose biogas from anaerobic digesters or from landfill sites or CO_2 from other biological processes such as some industrial fermentation processes, as cheap and readily available carbon dioxide sources and plausible options for use in MES. As presented in Chapter 9, we successfully demonstrated the use of a synthetic biogas gas mixture as carbon dioxide source, yielding similarly high MES performance, which would allow this process to be used effectively for both biogas quality improvement and conversion of the available CO_2 to acetate (this solution is further discussed below).

Several scenarios for practical implementations of MES were envisioned and economically assessed more in details below, with both the OPEX (electricity cost) and CAPEX (reactor cost) considered in the cost analyses with operational parameters discussed previously (Table 11).

Case study n°1: CO_2 conversion to acetate as end-product

The first case study considers the carbon dioxide conversion (100%) to acetate as the end-product (Figure 50). Currently, most of the acetate produced worldwide originates from petrochemistry, mainly through methanol carbonylation [238].

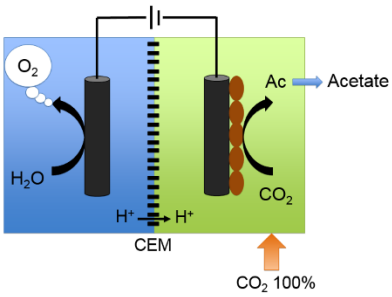

Figure 50 MES scheme for CO_2 conversion to acetate as the end-product.

Costs of acetate production, in dollars per ton of acetate, are compared to the current market value of acetate to determine whether a profit can be made by using BES. The main variable in the assumptions presented above regards the CAPEX of the BES system, with the cost of the electrodes found to be the main parameter that greatly influence the economic feasibility of the system. Figure 51 shows the comparative costs over a period of 25 years, using the 4 different proposed costs of electrodes versus the market value.

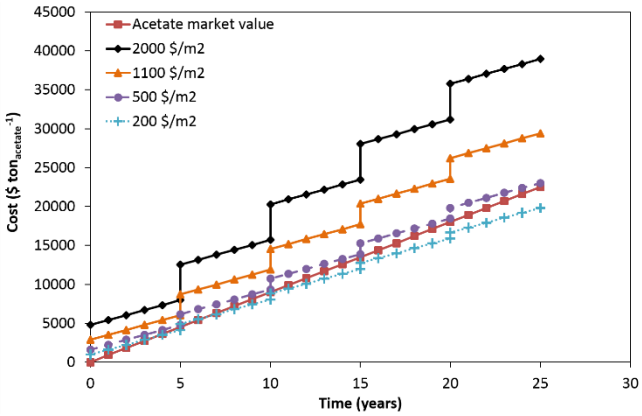

Figure 51 Comparative costs over a period of 25 years, using 4 different electrodes costs, with membranes, electrodes and current collectors' replacement every five years, compared with the market value of acetate (red square).

The cost steps observed every five years correspond to the replacement of the reactors' components (membrane, electrode and current collectors). The non-applicability of the system as such with acetate as sole valuable product is clearly observable at the current state of the art. The initial capital cost of the system is clearly limiting. A high CAPEX of up to 5000 \$ $ton_{acetate}^{-1}$ at current electrode cost of 2000 \$ m^{-2} was calculated. The CAPEX obviously increases proportionally to the amount of acetate desired. Even at very low electrode cost of 200 \$ m^{-2}, a pay-back time of more than 10 years would be necessary to compete with the current market. In addition of significantly decreasing the capital cost of BES, the CO_2 reduction rate would have to be enhanced further (several fold) to make MES feasible at industrial scale.

In this MES configuration (Figure 50), another valuable product generated has generally been overlooked. Indeed, for each ton of acetate produced on the cathode side, about 1.08 ton of oxygen is generated on the anode side as well. Oxygen has a fairly high market value of about 760 \$ ton^{-1} [235], which corresponds to 830 \$ $ton_{acetate}^{-1}$. Therefore, using the exact same setup with the same capital and operational costs as above, an almost twice higher revenue could be made by adding the value of both acetate and oxygen as valuable end-product. However, if oxygen was to be sold, it will likely have to be compressed on-site, adding compression station capital cost as well as operational cost (electricity). Figure 52 shows the comparative costs over a period of 25 years, using the 4 different proposed costs of electrodes versus the combined current market values of both acetate and oxygen. The electricity cost for oxygen compression was accounted for in the general operational cost of the MES at a rate of 0.87 kWh kg^{-1} (Table 11). The capital cost of the compression station was not accounted for at this stage.

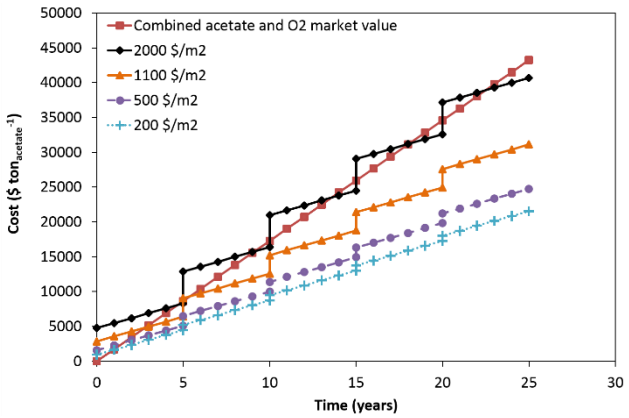

Figure 52 Comparative costs over a period of 25 years, using 4 different electrodes costs, with membranes, electrodes and current collectors' replacement every five years, compared with the combined market values of both acetate and oxygen (red square).

It can now be observed that at current costs (2000 \$ m^{-2}), MES cost follows a similar trend than the market values. At similar performance, reducing the CAPEX by developing cheaper electrodes would have a significant impact on the process applicability. It can be seen that at realistically achievable electrodes cost of 1100 \$ m^{-2}, an acceptable pay-back time of about 5 years, comparable to existing technologies, will be achievable. However, the needed peripherals (e.g. pumps) need consideration as well and were not accounted for in this cost analyses. At this early stage of development and economic assessment, the peripherals needed are hardly identifiable. Nevertheless, this analysis highlights that oxygen may have to be considered as a valuable end-product as well in order for MES of acetate to become economically viable.

Case study nº2: CO_2 conversion to acetate + further conversion to higher value chemicals

An additional strategy to improve the economic potential of MES to acetate could be to further convert it to higher value chemicals. Agler et al. (2011) reviewed a range of processes for the production of higher value compounds (e.g. alcohols and long chain fatty acids) from short-chain carboxylates, such as acetate, described as "the carboxylate platform" [88]. Acetate can be further processed by separate post-processing steps (e.g. bio/chemical, electrochemical and/or thermochemical steps). Carbonyls, esters, alcohols and alkanes are examples of high-value end-products generated through such reactions, producing directly usable fuels and/or industrial solvents. Liu et al. (2015) very recently described a new direct solar-powered process for the production of acetate from CO_2 coupled with the biosynthesis of complex organic molecules, such as n-butanol, PHB biopolymer and isoprenoid compounds using genetically engineered *E. coli*, in a separate vessel [92]. The used *E. coli* strain can activate acetate into the common biochemical intermediate acetyl-CoA which is then used for the biosynthesis of these higher value complex molecules [92].

Membrane Electrolysis (ME) was also showed successful for the extraction of carboxylates from cathode to anode compartment, combined with Biphasic Esterification (BE) for the production of fine chemicals [91]. A similar concept could be coupled to microbial electrosynthesis of acetate with the recirculation of the acetate in a separate reactor where the esterification reaction takes place, as represented in Figure 53.

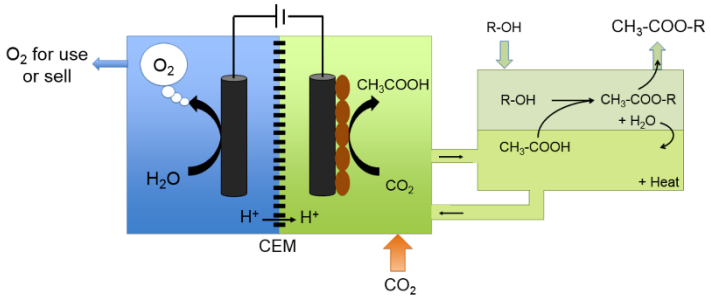

Figure 53 MES scheme for CO_2 conversion to acetate coupled with a biphasic esterification process.

This strategy (Figure 53) may prove particularly relevant in some situations. As a specific example, an Australian company, that produces bioethanol by fermentation of starch, generates a large CO_2 stream of 400 tons a day, 300 of which are released into the atmosphere. They are currently looking at making a profitable use of this 'free' CO_2 stream while diversifying their product spectrum. This proposed combination of MES and biphasic esterification, using both their CO_2 and EtOH on-site streams, and possible solar energy to power MES, is of particular interest, as

the market value of EtOH is about 2 times lower than the ethyl-acetate generated, 930 $ ton^{-1} versus 1900 $ ton^{-1}, respectively. The market value of ethyl-acetate is more than twice higher than acetate, which enhance the economic potential of this strategy. However, a more in-depth technical and economic assessment of the combination of both technology will need to be performed.

Case study nº3: Biogas as cheap and readily available carbon dioxide source

As previously mentioned and successfully demonstrated as a proof of concept in Chapter 9, biogas gas mixture, primarily composed of methane and carbon dioxide, can be used as carbon dioxide source leading to very similar high MES to acetate performance as compared to using pure CO_2. Biogas quality improvement, by removing the CO_2 fraction, is of particular interest for gas compression/storage and combustion efficiency. Currently, technologies for removal of carbon dioxide from biogas are scrubbing with water or other physical solvent, chemical scrubbing, membranes and Pressure Swing Adsorption (PSA) [239]. Economic assessment of each of those technologies was out of the scope of this PhD thesis. However, the monetary value of upgrading biogas will need to be added to the other benefits of MES and could potentially make MES in its whole, economically viable. It will then have to be assessed in comparison to the established technologies.

A few MES from biogas configurations could be envisioned, four of them are briefly discussed here and represented in Figure 54.

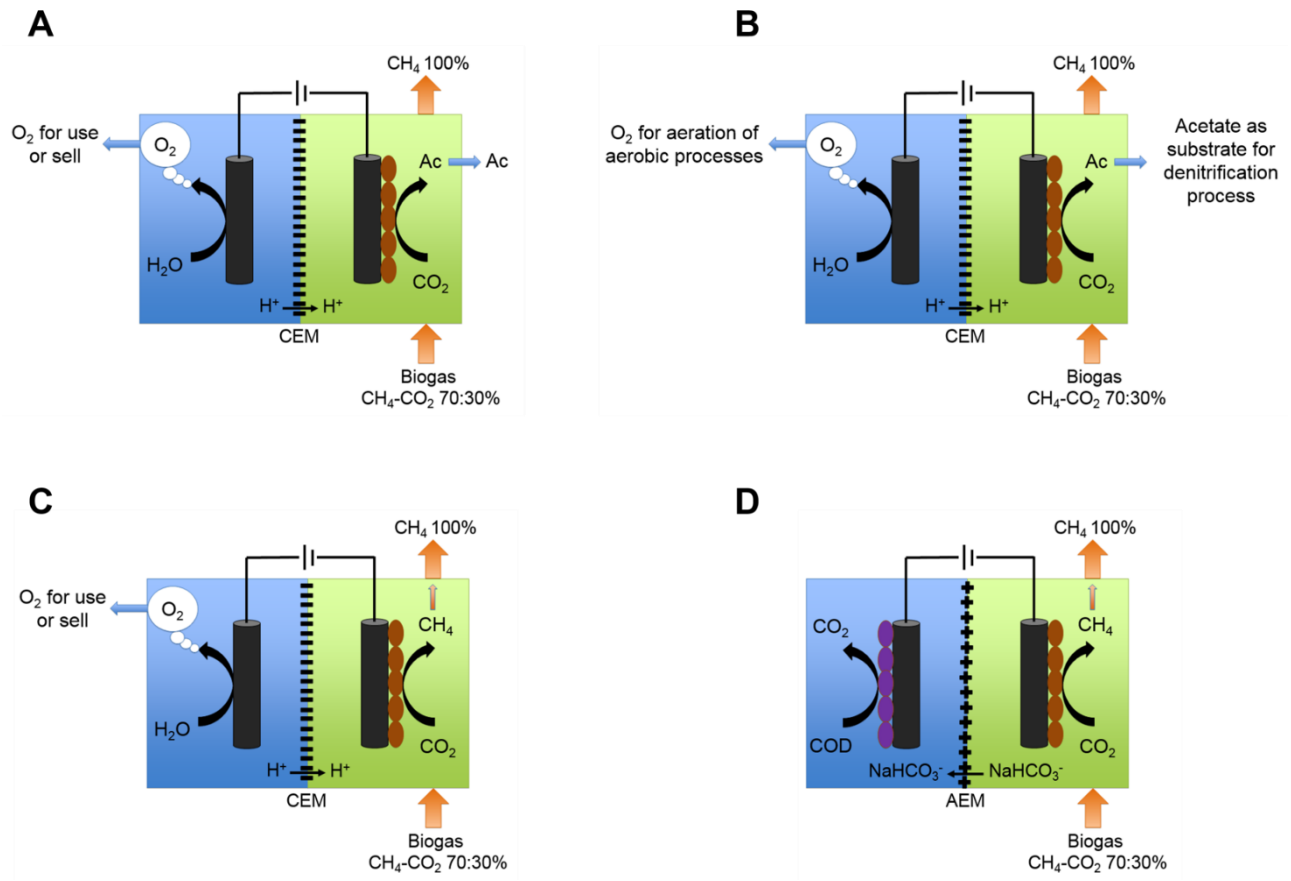

Figure 54 Different potential practical implementations of MES coupled to biogas upgrading. A) CO_2 fraction conversion to acetate as end-product, and B) MES implementation within a wastewater treatment plant for biogas quality upgrade, with CO_2 fraction converted to acetate for use as substrate for on-site denitrification process and O_2 used for on-site aerobic processes, C) CO_2 fraction conversion to methane to upgrade and enrich CH_4 content of the biogas, D) MES primarily used as carbon capture technology and biogas quality upgrade, with a fifth of the CO_2 fraction converted to methane and 4 fifths used as pH buffer for both biocathode and bioanode using an anion exchange membrane.

- Carbon dioxide to acetate scenarios

The first configuration is identical to case study 1 discussed above for acetate production as end-product or further converted to higher value chemicals, using biogas as compared to using pure CO_2 (Figure 54 A). Economic assessment discussed above showed the need for electrode material costs to be decreased (while keeping high performance or increased further) and the oxygen to be sold for MES to potentially become economically attractive. In the present case, the economic value of biogas upgrading may enhance further MES perspective for large-scale implementation.

Figure 54 B illustrates a specific scenario of MES to acetate implementation in a wastewater treatment plant wherein biogas is upgraded with the carbon dioxide fraction converted to acetate which is then used as COD substrate for on-site biological processes (e.g. denitrification). The pure oxygen generated could in turn be used for aeration of on-site aerobic processes (e.g. nitrification). In this configuration, MES could then fulfil up to three main functions. Currently, methanol and ethanol are the main COD sources utilized. They are both cheaper on the market and have a higher

COD content, 1.5 g_{COD} g_{MeOH}^{-1} and 2.09 g_{COD} g_{EtOH}^{-1}, than acetate (0.95 g_{COD} $g_{acetate}^{-1}$). However, they are both more hazardous than acetate, therefore more costly to transport and to store on site. In addition, producing acetate on-site could allow for no storage and related costs. Generally, aeration is performed through air compression. Air is only composed of about 21% of oxygen. Using pure O_2 from MES, possibly without compression (effective design required), would allow for higher efficiency of the aerobic process and cost savings on air compression (electricity), which requires a flow rate of air 5 times greater to reach the same amount of O_2. The example of the Luggage Point Wastewater Treatment Plant (WWTP; Queensland, Australia) is used for preliminary cost calculations. Table 12 lists the WWTP characteristics of interest for this comparative study.

Table 12 Luggage Point WWTP denitrification, anaerobic digestion and air compression characteristics.

Population (persons)	750000
Denitrification process	
NO_3-N concentration (mg_N L^{-1})	50
Ethanol: buy, transportation & storage (\$ kg^{-1})	1.39
Ethanol used (ton $year^{-1}$)	505
Anaerobic digestion process	
Biogas production (m^3 day^{-1})	15000
Biogas composition (%)	CH_4 57.90 - CO_2 39.10
CO_2 production (ton $year^{-1}$)	3850
Air compression	
Power requirement (kWh kg^{-1})	1.05
Electricity cost (\$ kWh^{-1})	0.07

In the assumption of using acetate instead of ethanol, the denitrification process would require around 1100 $ton_{acetate}$ $year^{-1}$. At MES performance presented above (Table 11), the CO_2 fraction of the biogas would be converted to 2581 ton $year^{-1}$ of acetate, about 2.3 times the amount required for the denitrification process. This shows the practical feasibility of this concept in a real plant configuration. Regarding the economic feasibility as opposed to using ethanol, we assume the production of 1100 ton of acetate per year by MES. This corresponds to a production of oxygen of about 108 m^3 h^{-1}, several orders of magnitudes lower than necessary for aerobic processes. Consequently, air compression would still need to be carried out in parallel. However, using this pure oxygen stream could in theory allow for slightly less air to be compressed, thus saving electricity cost. Figure 55 shows the comparative operational costs of MES (electricity) versus the combined operational cost related to ethanol (Table 12) and air compression (electricity) to obtain the same flow rate of oxygen generated by MES (corresponding in turn to the electricity savings that the MES implementation would generate).

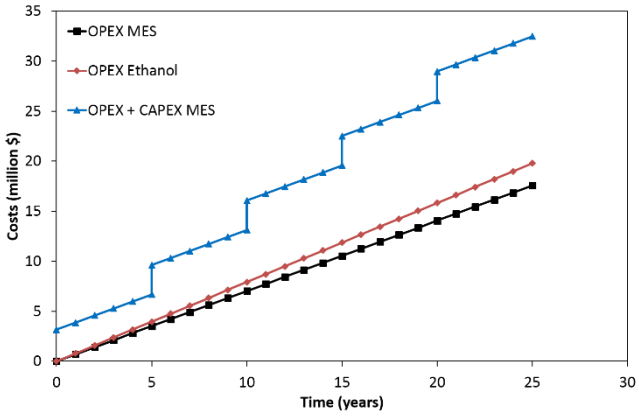

Figure 55 Comparative cost analysis of MES OPEX (black square) and CAPEX (Blue triangle) versus buying, transporting and storing ethanol and compressing air (red diamond).

The operational cost of microbial electrosynthesis is shown to be slightly lower than buying, transporting and storing ethanol. Without considering any savings on electricity cost for air compression, i.e. assuming not using the O_2 generated by MES, the operational costs of both options would be very similar. As previously shown, the electricity cost for MES is about 0.65 $ $kg_{acetate}^{-1}$ which corresponds to 0.68 $ kg_{COD}^{-1}, while the cost of ethanol corresponds to 0.67 $ kg_{COD}^{-1}. Further economic benefit from selling the O_2 as compared to using it on-site could be actually made. Figure 55 also shows the capital costs of the MES option, assuming 1100 $ m^{-2} electrodes cost, which is obviously higher than the OPEX of the ethanol option. However, the capital costs related to ethanol storage and air compression will also need to be considered for viable comparison. Moreover, the monetary value of upgrading the biogas quality was not considered here as well. Even at similar capital costs for both options, microbial electrosynthesis could be more interesting due to its larger panel of application.

- Carbon dioxide to methane scenarios

Bioelectrochemical CO_2 conversion to methane has also been investigated in the last few years [65-67, 240]. Methane has been reported to be the dominant end-product when methanogenesis activity was not suppressed in CO_2-fed cathode compartment [15, 19, 73]. The MESs described in this PhD thesis could be envision to convert CO_2 to methane as efficiently as they reduce it to acetate. A first configuration could be as represented in Figure 54 C, with an abiotic anode and cation exchange membrane for the conversion of all the CO_2 to methane to upgrade the biogas and increase the net flow of methane. A second configuration could be mainly centred on CO_2 capture, neglecting partly the CO_2 conversion to more methane, by using an anion exchange membrane and a bioanode for COD removal (e.g. from a waste stream), using CO_2 mainly as a biological pH buffer for both compartments (Figure 54).

However, according to the chemical equation of the cathodic reaction (Equation 3), twice more moles of electron are required to reduce the same amount of CO_2 than when reducing it to acetate (Equation 1).

Equation 3 Carbon dioxide reduction to methane $\boldsymbol{CO_2 + 8\,H^+ + 8\,e^- \rightarrow CH_4 + 2\,H_2O}$

Therefore, twice more reactors would be required, hence increasing the capital cost by a factor 2. Moreover, the market value of methane is a lot lower (0.49 \$ m^{-3} [235]) than the market value of acetate. Consequently, even considering the economic value of biogas upgrading, this option will likely never meet the economic requirement for practical implementation.

Use of enriched MES microbial consortium in other biological cathodic processes

Part of the electrons flux mechanisms occurring from the electrode to the last electron acceptor, CO_2, has been revealed in this PhD thesis (Chapter 8). The observations strongly suggest that metallic copper is biologically synthesized on the surface of the electrode and is directly involved in the H_2 catalysis and its significant enhancement. The copper-modified electrode was shown to be particularly biocompatible, with the acetate-producing microorganisms converting all the H_2 and CO_2 within the biofilm.

In a similar fashion, the particular characteristics of the enriched microbial consortium could significantly enhance other biological cathodic processes, as represented in Figure 47. Adding a denitrifying microbial consortium or a sulphate-reducing community to the enriched cathodic community developed in this work is currently showing significant performance improvement of the respective reductive processes in our lab (data not shown). The enriched mixed microbial culture could also potentially be used for cathodic microbial electrosynthesis from organics to more reduced and valuable organic compounds.

Conclusive remarks

As seen above, microbial electrosynthesis of acetate from CO_2 could have many attractive practical implementations potentially fulfilling several key functions, which however requires further improvement/development. In addition of what has been discussed previously, some other parameters have not been considered and could have an impact on the economic feasibility of MES. For example, regarding the cost of electricity, surplus electricity (off-peak overcapacity) could be obtained cheaper than the bulk industrial rate. Nowadays, industrial companies admit that sustainability also has a monetary value, mainly through their public image. Finally, politics could also have a contribution on MES perspectives. A number of countries have implemented environmentally-related taxes such as carbon or energy taxes as means of reducing greenhouse gas

emissions. This should induce carbon dioxide not to be considered as a waste stream anymore but as a valuable platform. For example, the European Union (EU) launched in 2005 an Emissions Trading System (EU ETS) which puts a price on carbon and thereby gives a financial value to each ton of emissions saved [241].

10.3. Recommendations for future research and development

From the investigations carried out in this thesis and the case studies presented above, several questions were raised and the need for further research and development was identified:

- **Microbial investigations:** The results from this thesis shed light on the electron flux occurring at the biocathode (Chapter 8). However, further in-depth investigation at microbial level is needed to fully understand what the functions of each of the species are (e.g. proteomic studies in different operational conditions). First of all, microbial identification at species level still need to be carried out. Our results strongly suggests the biological synthesis of copper particles contributes to the significant enhancement of hydrogen production. Further research needs to be carried out to confirm these observations and determine whether the copper particles are excreted onto the surface of the cathode electrode, and/or are active from within the cells, and only deposited on the surface after the cells' membrane are broken under extreme conditions. The ability of microorganisms to synthesize copper nanoparticles from Cu^{2+} has been observed in other environment but never in these peculiar conditions. Identifying and performing functional analysis of the species responsible for this reaction, and understanding how they gain energy for growth and maintenance, is of particular interest. Moreover, the surface chemistry of the modified electrode surface should be studied further. Observing and characterising the copper particles (size, shape, etc.) would be of interest. In addition, the very effective syntrophic relationship that seems to occur in MES developed here, and the impressive capability of the acetate-producing bacteria to assimilate such high rate of hydrogen within the biofilm, needs to be investigated further as well at microbial level.
- **Copper-based material development:** From the suggested biologically copper-modified electrode that proved extremely biocompatible, a new perspective for electrode material development rises. In order to bypass the need for the particular microbial culture enriched in this study, it could be particularly interesting to design a biocompatible copper-based electrode and to investigate whether similar or higher MES performance could be reached.

Understanding the surface chemistry and visualising the biologically-induced copper particles could give primordial information towards this objective.

- **Operating conditions optimization / methanogenesis inhibition:** The effect of pH and cathode applied potential have clearly been observed (Chapter 9), but their effect on the long-term needs to be investigated. The lowest applied potential at which electron recovery into acetate, in the order of 95-100%, is concomitantly maintained remains to be assessed. In addition of investigating whether controlled slightly acidic pH (e.g. pH 5.2, pH found optimal in Chapter 9) enhance performance over long period of time, it is critical to investigate whether methanogenic activity can be effectively suppressed in these conditions without the addition of chemical inhibitor. Other strategies could also be studied to inhibit methanogenesis. Moreover, the effect of the concentration of Cu^{2+} in the cathode solution could impact on the start-up time and/or on the maximal MES performance obtainable and should be looked into further. For example, an assumption is that higher availability of soluble Cu^{2+} could enhance the metabolism of metal copper-producing microorganism and increase the kinetics of formation of metal copper particles.
- **Use of biogas or other biologically generated CO_2:** Further investigation needs to be carried out on the use of biogas as carbon dioxide source for MES. First of all, real biogas will have to be tested with and without pre-treatment of its impurities and observe the impact on MES performance. An assumption is that the H_2S fraction of the biogas may damage the MES microbial community; the effect of different H_2S concentration could be investigated. Long-term experiment using biogas should be performed. Similarly, CO_2 produced from other biological processes (e.g. fermentation) would likely have impurities as well and will need to be investigated.
- **Aiming at higher value compounds from CO_2:** The above economic assessment showed that the relatively low market value of acetate may prevent its large-scale applicability without further development. As discussed above, a strategy would be to convert the cathodically generated acetate into more valuable compounds. Another perspective could be to develop a biocathode that would directly convert carbon dioxide to higher-value compounds without requiring further chemical synthesis. This would circumvent the need for extra capital and would drastically improve MES large-scale perspective. A recent study has showed the simultaneous conversion of CO_2 into a mixture of products composed of acetate, butyrate, ethanol, and butanol [13]. High product specificity and production rates are regarded as key parameters for large-scale applicability of such a technology. CO_2

fixation in the sole form of butanol at similar rate and specificity than obtained in our study for acetate production could be attractive. Butanol has a two to three time higher market value than acetate, however requires 3 times more electron per mol of product generated (Equation 4) with a molecular weight only 1.26 times higher than acetate. Therefore, about 2.4 lower rate of kg of glycerol per mol of electron would be achieved as compared to kg of acetate per mol of electron. Consequently, it would seem that similar 'profit' would be made from producing butanol or acetate at same electron consumption rate (i.e. cathode current density). However, a market study should be done to assess the demand for each product. Currently, butanol has a higher demand and a larger panel of applications (e.g. biofuel for internal combustion engine). Ethanol has a similar market value and requires more electrons per mass unit of product than acetate hence its production by MES would not make sense at current state of the art.

Equation 4 Carbon dioxide reduction to butanol $4CO_2 + 24\,H^+ + 24\,e^- \rightarrow C_4H_{10}O + 7\,H_2O$

- **Cathode development**: EPD-3D developed in this PhD holds many promises, with MES performance at least an order of magnitude higher than reported to date (Chapter 7). Moreover, a cost of production of 1000 \$ electrode^{-1} (1 x 1 x 0.01 m) was calculated based on lab-scale material costs, which are expected to significantly decrease for large-scale production, possibly in the range of 600-700 \$ electrode^{-1}. This would already improve significantly the economic perspective of MES as seen above. However, future research should investigate the development of even cheaper electrode and possibly replicate similar macro- and nanostructure than EPD-3D from a cheaper macroporous substrate than RVC (e.g. carbonized sponge-like materials). Using the effective enriched culture developed in this study with basic and cheap carbon felt or carbon cloth electrode (ca. 100 \$ m^{-2}) could also be envisioned; however a stack of several of them would likely be necessary in one cathode chamber which will lead to similar electrode cost per chamber as per using EPD-3D. Further investigation of this configuration should still be performed. Larger-scale MES using graphite granules should also be investigated. Graphite granules cost less than 100 \$ per 10 L (i.e. per cathode chamber volume) but many engineering issues could occur from using granules (e.g. mass transfer limitation, resistance, etc.). Moreover, an electrode lifetime of 5 years was assumed in this study, it could however be longer which would make MES considerably more viable. The lifetimes of the reactor's components are difficult to assess.

- **Anode development**: Cheap anode material for effective oxygen evolution reaction (OER) is needed to synchronise with the electron flow at the cathode. Platinum cannot be considered for large scale due to its very high cost, while cheap carbon-based electrode would get oxidized at those anode potentials (ca. 1.5 V). So far, Iridium oxide (IrOx) and Ruthenium oxide (RuOx) are the benchmark for efficient OER catalysts in electrolytic water splitting cells [242]. Often, a mixed Ta/IrOx or Ru/IrOx coated on titanium are used to balance between stability and oxygen production. Nevertheless, these precious metals are costly and their supply is not sustainable [243]. Additionally they can also generate chlorine and their lifetimes are pretty poor. A tremendous amount of research have been devoted to the development of low-cost OER catalysts, such as cobalt-based and nickel-based composites [243-246]. However, developing an electrode able to deliver high current densities at low overpotentials and mechanically robust for long-term stability has been challenging. Very recently, a hierarchically structured 3D electrode prepared via a facile, one-step electrodeposition of amorphous, mesoporous nickel-iron hydroxide (NiFe) nanosheets onto nickel foam substrate was synthesized and showed outstanding OER performance [243]. This electrode macrostructure comprised of a nanostructure layer much resembles to EPD-3D hierarchical structure. It would be interesting to investigate this anode material in a larger scale of our MES system in combination with EPD-3D.

- **Scale-up**: Our above cost calculations are based on successful scale up yielding similar high MES performance than obtained in our laboratory scale experiments, which still remains to be investigated. To successfully implement MES from CO_2 technology at large scale, several process and engineering considerations, which were not trivial in the laboratory scale reactors, have to be taken into account. The most critical issues which demand further study were identified and succinctly listed below without going into much details as design of such MES system has not generally been discussed to date:

o *General design?* The reactor design configuration must be considered for efficient and homogeneous flow distribution and minimized electrode spacing. Some investigations have been performed for MFC and MEC systems, with tubular shaped and flat plate the most investigated designs [110, 233]. The surface area of electrode per volume of chamber ratio in large-scale forced-flow through configuration must be optimized. In the cost calculations above, EPD-3D was assumed to fully occupy the cathode chamber. However, enough liquid volume is a requirement for concentrations not to change too quickly, for sufficient substrate and buffer capacity, etc. Other

important parameters such as hydraulic retention time (flow regime) of the catholyte and dead space reduction are not identifiable so far without further tests.

- *In parallel vs. in series configuration?* A configuration in parallel would require the division of the CO_2 inflow and a complex gas recirculation loops system to prevent any loss of CO_2. A configuration in series with both liquid and gas flows circulating from one cell to another is another strategy. In the latter, CO_2 concentration gradient (lower concentration in the last cells) could potentially limit the maximal conversion rates, yielding performance gradient from one reactor to another. The way of effectively feeding CO_2 gas (where and how) while preventing any loss and pressure issues in the system, and maintaining high performance in each reactor, needs to be investigated. A combination of both parallel and series configuration may be considered. Obviously, decisions will also have to be made individually for each scenario, mainly depending on the CO_2 flow capacity.
- *pH issues / biological buffer?* As in any electrochemical systems, pH issues and gradient from one reactor to another can be expected. However, as seen above from Equation 1Equation 2, the low pH and the absence of other cations in the anode chamber and assuming effective proton crossover, the pH of the cathode broth should be balanced while consuming all the CO_2 to acetate. Biological buffer may still be required to ensure sufficient ionic conductivity of the catholyte. Biological buffer, if used in high concentration, can get costly. Further investigation should look into cheap buffer and optimal concentration. An advantage of using an abiotic OER anode is that high ionic conductivity is maintained due to high proton production rate (low pH) without buffer addition. Reducing electrolyte resistance can also be achieved by reducing electrode spacing. Costs of nutrients will also have to be accounted for, but should remain marginal.
- *Amount of water needed?* Depending on the plant capacity and the amount of CO_2 to be reduced, relatively high amount of water will be needed on the anode side, with 1.22 kg of water converted to oxygen at the anode per kg of acetate produced at the cathode. This amount of water can be limiting in region where water is sparse and needs to be taken into account. Water quality needed at the anode will be another parameter to consider.
- *Electrical conductivity?* Another likely limitation of BES scale-up is that carbon electrodes are not as conductive as metals, leading to significant resistance issues across the electrode, on a larger scale in the order of 1 m^2. Maintaining a satisfying electrical conductivity and homogeneous potential throughout the whole surface of the electrode can be challenging. Efficient current collectors are thus necessary. We briefly propose here a potential current collector design strategy

for 3D electrodes that could be applied for large scale reactor. The current collector prototype can be seen in Figure 56. The current collector consists of a 3D printed titanium (Ti) plate with Ti spikes coming out of it for successful anchoring of the 3D electrode and great electrical conductivity between the electrode and the collector.

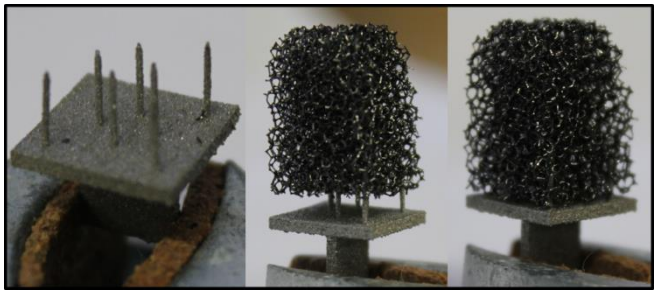

Figure 56 Potential current collector design for BES scale-up using three-dimensional electrodes.

- *Peripherals?* At this early stage of research and development, identifying the peripherals that would be needed for large scale MES system is difficult. For established electrochemical technologies (e.g. water electrolysis, chlorine generation, etc.) an approximate rule is to consider a capital cost for peripherals around three times the capital cost of the BES system alone. This would dramatically affect the cost calculations discussed above. However, the capital cost of competing technologies will also need to be considered for proper comparisons, which was not achievable at this stage.

    - **Membrane (separator) development:** Another research field of particular interest for BES improvement is the development of cheaper and selective ion exchange membrane alternative. The separator is used to keep anode and cathode solutions separated, prevent crossover processes and be conductive to ions [109]. Nafion® is generally seen as a reference material but its high price is detrimental to large-scale application. Recent trends seem to lean towards the development of ultrafiltration membranes and fluorinated ceramic as low cost separators [247].

    - **Product extraction**: Separation / extraction of the valuable end-product from the cathode broth, preferably using low-cost technologies, is also being investigated [88, 91]. On-line liquid/liquid extraction using membranes was reported as one possibility to remove acetate from engineered systems (e.g. fermenters) [90]. Membrane Electrolysis (ME) was also showed successful for the extraction of carboxylates from cathode to anode compartment, combined with Biphasic Esterification (BE) for the production of fine chemicals [91]; similar concept could be coupled to microbial electrosynthesis of acetate from CO_2 as proposed previously. Continuous MES product extraction at relatively low titer needs to be investigated.

References

1. Lovley, D.R. and K.P. Nevin, *A shift in the current: New applications and concepts for microbe-electrode electron exchange.* Current Opinion in Biotechnology, 2011. **22**(3): p. 441-448.
2. Rabaey, K. and R.A. Rozendal, *Microbial electrosynthesis — revisiting the electrical route for microbial production.* Nat Rev Micro, 2010. **8**(10): p. 706-716.
3. Desloover, J., et al., *Operational and technical considerations for microbial electrosynthesis.* Biochemical Society Transactions, 2012. **40**(6): p. 1233-1238.
4. Mikkelsen, M., M. Jørgensen, and F.C. Krebs, *The teraton challenge. A review of fixation and transformation of carbon dioxide.* Energy and Environmental Science, 2010. **3**(1): p. 43-81.
5. Lovley, D.R. and K.P. Nevin, *Electrobiocommodities: powering microbial production of fuels and commodity chemicals from carbon dioxide with electricity.* Current Opinion in Biotechnology, 2013. **24**(3): p. 385-390.
6. Rabaey, K., P. Girguis, and L.K. Nielsen, *Metabolic and practical considerations on microbial electrosynthesis.* Current Opinion in Biotechnology, 2011. **22**(3): p. 371-377.
7. Lewis, N.S. and D.G. Nocera, *Powering the Planet: Chemical Challenges in Solar Energy Utilization.* Proceedings of the National Academy of Sciences of the United States of America, 2006. **103**(43): p. 15729-15735.
8. Nevin, K.P., et al., *Electrosynthesis of organic compounds from carbon dioxide is catalyzed by a diversity of acetogenic microorganisms.* Applied and Environmental Microbiology, 2011. **77**(9): p. 2882-2886.
9. Nevin, K.P., et al., *Microbial electrosynthesis: Feeding microbes electricity to convert carbon dioxide and water to multicarbon extracellular organic compounds.* mBio, 2010. **1**(2): p. 1-4.
10. Nie, H., et al., *Improved cathode for high efficient microbial-catalyzed reduction in microbial electrosynthesis cells.* Physical Chemistry Chemical Physics, 2013. **15**(34): p. 14290-14294.
11. Zhang, T., et al., *Improved cathode materials for microbial electrosynthesis.* Energy & Environmental Science, 2013. **6**(1): p. 217-224.
12. Batlle-Vilanova, P., et al., *Continuous acetate production through microbial electrosynthesis from CO2 with microbial mixed culture.* Journal of Chemical Technology & Biotechnology, 2015: p. n/a-n/a.
13. Ganigue, R., et al., *Microbial electrosynthesis of butyrate from carbon dioxide.* Chemical Communications, 2015.
14. LaBelle, E.V., et al., *Influence of acidic pH on hydrogen and acetate production by an electrosynthetic microbiome.* PLoS ONE, 2014. **9**(10): p. e109935.
15. Marshall, C.W., et al., *Electrosynthesis of Commodity Chemicals by an Autotrophic Microbial Community.* Applied and Environmental Microbiology, 2012. **78**(23): p. 8412-8420.
16. Marshall, C.W., et al., *Long-term operation of microbial electrosynthesis systems improves acetate production by autotrophic microbiomes.* Environmental Science and Technology, 2013. **47**(11): p. 6023-6029.
17. Min, S., Y. Jiang, and D. Li, *Production of acetate from carbon dioxide in bioelectrochemical systems based on autotrophic mixed culture.* Journal of Microbiology and Biotechnology, 2013. **23**(8): p. 1140-1146.
18. Tremblay, P.-L. and T. Zhang, *Electrifying microbes for the production of chemicals.* Frontiers in microbiology, 2015. **6**.
19. Xafenias, N. and V. Mapelli, *Performance and bacterial enrichment of bioelectrochemical systems during methane and acetate production.* International Journal of Hydrogen Energy, 2014(0).
20. Chae, K.-J., et al., *Effect of different substrates on the performance, bacterial diversity, and bacterial viability in microbial fuel cells.* Bioresource Technology, 2009. **100**(14): p. 3518-3525.
21. Liu, H., S. Grot, and B.E. Logan, *Electrochemically Assisted Microbial Production of Hydrogen from Acetate.* Environmental Science & Technology, 2005. **39**(11): p. 4317-4320.
22. Logan, B.E., et al., *Microbial Electrolysis Cells for High Yield Hydrogen Gas Production from Organic Matter.* Environmental Science & Technology, 2008. **42**(23): p. 8630-8640.
23. Rozendal, R.A., et al., *Principle and perspectives of hydrogen production through biocatalyzed electrolysis.* International Journal of Hydrogen Energy, 2006. **31**(12): p. 1632-1640.
24. Guo, K., et al., *Engineering electrodes for microbial electrocatalysis.* Current Opinion in Biotechnology, 2015. **33**(0): p. 149-156.
25. Freguia, S., et al., *Bioelectrochemical systems: Microbial versus enzymatic catalysis.* Electrochimica Acta, (0).
26. Clauwaert, P., et al., *Biological denitrification in microbial fuel cells.* Environmental Science and Technology, 2007. **41**(9): p. 3354-3360.

27. Virdis, B., et al., *Microbial fuel cells for simultaneous carbon and nitrogen removal.* Water Research, 2008. **42**(12): p. 3013-3024.
28. Aulenta, F., et al., *Characterization of an electro-active biocathode capable of dechlorinating trichloroethene and cis-dichloroethene to ethene.* Biosensors and Bioelectronics, 2010. **25**(7): p. 1796-1802.
29. Butler, C.S., et al., *Bioelectrochemical perchlorate reduction in a microbial fuel cell.* Environmental Science and Technology, 2010. **44**(12): p. 4685-4691.
30. Cao, X., et al., *A completely anoxic microbial fuel cell using a photo-biocathode for cathodic carbon dioxide reduction.* Energy & Environmental Science, 2009. **2**(5): p. 498-501.
31. Tront, J., et al., *Microbial fuel cell technology for measurement of microbial respiration of lactate as an example of bioremediation amendment.* Biotechnology Letters, 2008. **30**(8): p. 1385-1390.
32. Tront, J.M., et al., *Microbial fuel cell biosensor for in situ assessment of microbial activity.* Biosensors and Bioelectronics, 2008. **24**(4): p. 586-590.
33. Zhang, Y. and I. Angelidaki, *Submersible microbial fuel cell sensor for monitoring microbial activity and BOD in groundwater: Focusing on impact of anodic biofilm on sensor applicability.* Biotechnology and Bioengineering, 2011. **108**(10): p. 2339-2347.
34. Jacobson, K.S., D.M. Drew, and Z. He, *Use of a Liter-Scale Microbial Desalination Cell As a Platform to Study Bioelectrochemical Desalination with Salt Solution or Artificial Seawater.* Environmental Science & Technology, 2011. **45**(10): p. 4652-4657.
35. Luo, H., P.E. Jenkins, and Z. Ren, *Concurrent Desalination and Hydrogen Generation Using Microbial Electrolysis and Desalination Cells.* Environmental Science & Technology, 2010. **45**(1): p. 340-344.
36. Harnisch, F. and U. Schroder, *From MFC to MXC: chemical and biological cathodes and their potential for microbial bioelectrochemical systems.* Chemical Society Reviews, 2010. **39**(11): p. 4433-4448.
37. Lowy, D.A., et al., *Harvesting energy from the marine sediment–water interface II: Kinetic activity of anode materials.* Biosensors and Bioelectronics, 2006. **21**(11): p. 2058-2063.
38. Rabaey, K., et al., *Cathodic oxygen reduction catalyzed by bacteria in microbial fuel cells.* ISME J., 2008. **2**(5): p. 519-527.
39. Potter, M.C., *Electrical Effects Accompanying the Decomposition of Organic Compounds.* Proceedings of the Royal Society of London. Series B, Containing Papers of a Biological Character, 1911. **84**(571): p. 260-276.
40. Bond, D.R., et al., *Electrode-Reducing Microorganisms That Harvest Energy from Marine Sediments.* Science, 2002. **295**(5554): p. 483-485.
41. Bond, D.R. and D.R. Lovley, *Electricity Production by Geobacter sulfurreducens Attached to Electrodes.* Applied and Environmental Microbiology, 2003. **69**(3): p. 1548-1555.
42. Schroder, U., *Anodic electron transfer mechanisms in microbial fuel cells and their energy efficiency.* Physical Chemistry Chemical Physics, 2007. **9**(21): p. 2619-2629.
43. Lovley, D.R., *Powering microbes with electricity: direct electron transfer from electrodes to microbes.* Environmental Microbiology Reports, 2011. **3**(1): p. 27-35.
44. Borole, A.P., et al., *Electroactive biofilms: Current status and future research needs.* Energy & Environmental Science, 2011. **4**(12): p. 4813-4834.
45. Gregory, K.B., D.R. Bond, and D.R. Lovley, *Graphite electrodes as electron donors for anaerobic respiration.* Environmental Microbiology, 2004. **6**(6): p. 596-604.
46. Huang, L., J.M. Regan, and X. Quan, *Electron transfer mechanisms, new applications, and performance of biocathode microbial fuel cells.* Bioresource Technology, 2011. **102**(1): p. 316-323.
47. Rosenbaum, M., et al., *Cathodes as electron donors for microbial metabolism: Which extracellular electron transfer mechanisms are involved?* Bioresource Technology, 2011. **102**(1): p. 324-333.
48. Thrash, J.C. and J.D. Coates, *Review: Direct and indirect electrical stimulation of microbial metabolism.* Environmental Science and Technology, 2008. **42**(11): p. 3921-3931.
49. Aulenta, F., et al., *Linking bacterial metabolism to graphite cathodes: Electrochemical insights into the H2-producing capability of desulfovibrio sp.* ChemSusChem, 2012. **5**(6): p. 1080-1085.
50. Shantaram, A., et al., *Wireless sensors powered by microbial fuel cells.* Environmental Science & Technology, 2005. **39**(13): p. 5037-5042.
51. Tender, L.M., et al., *The first demonstration of a microbial fuel cell as a viable power supply: powering a meteorological buoy.* Journal of Power Sources, 2008. **179**(2): p. 571-575.
52. Ieropoulos, I.A., et al., *Waste to real energy: The first MFC powered mobile phone.* Physical Chemistry Chemical Physics, 2013. **15**(37): p. 15312-15316.
53. Freguia, S., S. Tsujimura, and K. Kano, *Electron transfer pathways in microbial oxygen biocathodes.* Electrochimica Acta, 2010. **55**(3): p. 813-818.

54. Liu, X.W., et al., *Photoautotrophic cathodic oxygen reduction catalyzed by a green alga, Chlamydomonas reinhardtii.* Biotechnology and Bioengineering, 2013. **110**(1): p. 173-179.
55. Ledezma, P., et al., *Source-separated urine opens golden opportunities for microbial electrochemical technologies.* Trends in Biotechnology.
56. Kuntke, P., et al., *Hydrogen production and ammonium recovery from urine by a Microbial Electrolysis Cell.* International Journal of Hydrogen Energy, 2014. **39**(10): p. 4771-4778.
57. Gregory, K.B. and D.R. Lovley, *Remediation and Recovery of Uranium from Contaminated Subsurface Environments with Electrodes.* Environmental Science & Technology, 2005. **39**(22): p. 8943-8947.
58. Dutta, P.K., et al., *Role of sulfur during acetate oxidation in biological anodes.* Environmental Science & Technology, 2009. **43**(10): p. 3839-3845.
59. Virdis, B., et al., *Electron fluxes in a microbial fuel cell performing carbon and nitrogen removal.* Environmental Science and Technology, 2009. **43**(13): p. 5144-5149.
60. Thrash, J.C., et al., *Electrochemical Stimulation of Microbial Perchlorate Reduction.* Environmental Science & Technology, 2007. **41**(5): p. 1740-1746.
61. Aulenta, F., et al., *Electron Transfer from a Solid-State Electrode Assisted by Methyl Viologen Sustains Efficient Microbial Reductive Dechlorination of TCE.* Environmental Science & Technology, 2007. **41**(7): p. 2554-2559.
62. Strycharz, S.M., et al., *Graphite Electrode as a Sole Electron Donor for Reductive Dechlorination of Tetrachlorethene by Geobacter lovleyi.* Applied and Environmental Microbiology, 2008. **74**(19): p. 5943-5947.
63. Mu, Y., et al., *Nitrobenzene removal in bioelectrochemical systems.* Environmental Science & Technology, 2009b. **43**(22): p. 8690-8695.
64. Mu, Y., et al., *Decolorization of azo dyes in bioelectrochemical systems.* Environmental Science & Technology, 2009a. **43**(13): p. 5137-5143.
65. Van Eerten-Jansen, M.C.A.A., et al., *Microbial electrolysis cells for production of methane from CO2: Long-term performance and perspectives.* International Journal of Energy Research, 2011.
66. Villano, M., et al., *Bioelectrochemical reduction of CO2 to CH4 via direct and indirect extracellular electron transfer by a hydrogenophilic methanogenic culture.* Bioresource Technology, 2010. **101**(9): p. 3085-3090.
67. Cheng, S., et al., *Direct biological conversion of electrical current into methane by electromethanogenesis.* Environmental Science and Technology, 2009. **43**(10): p. 3953-3958.
68. Rozendal, R.A., et al., *Efficient hydrogen peroxide generation from organic matter in a bioelectrochemical system.* Electrochemistry Communications, 2009. **11**(9): p. 1752-1755.
69. Rabaey, K., et al., *High Current Generation Coupled to Caustic Production Using a Lamellar Bioelectrochemical System.* Environmental Science & Technology, 2010. **44**(11): p. 4315-4321.
70. Steinbusch, K.J.J., et al., *Bioelectrochemical ethanol production through mediated acetate reduction by mixed cultures.* Environmental Science and Technology, 2010. **44**(1): p. 513-517.
71. Zhou, M., et al., *Carbon and Electron Fluxes during the Electricity Driven 1,3-Propanediol Biosynthesis from Glycerol.* Environmental Science & Technology, 2013. **47**(19): p. 11199-11205.
72. Centi, G. and S. Perathoner, *Opportunities and prospects in the chemical recycling of carbon dioxide to fuels.* Catalysis Today, 2009. **148**(3-4): p. 191-205.
73. Jiang, Y., et al., *Bioelectrochemical systems for simultaneously production of methane and acetate from carbon dioxide at relatively high rate.* International Journal of Hydrogen Energy, 2012(0).
74. Cord-Ruwisch, R., H.-J. Seitz, and R. Conrad, *The capacity of hydrogenotrophic anaerobic bacteria to compete for traces of hydrogen depends on the redox potential of the terminal electron acceptor.* Archives of Microbiology, 1988. **149**(4): p. 350-357.
75. Dumas, C., R. Basseguy, and A. Bergel, *Microbial electrocatalysis with Geobacter sulfurreducens biofilm on stainless steel cathodes.* Electrochimica Acta, 2008. **53**(5): p. 2494-2500.
76. Strycharz, S.M., et al., *Reductive dechlorination of 2-chlorophenol by Anaeromyxobacter dehalogenans with an electrode serving as the electron donor.* Environmental Microbiology Reports, 2010. **2**(2): p. 289-294.
77. Kuramochi, Y., et al., *Electromethanogenic CO2 Conversion by Subsurface-reservoir Microorganisms.* Energy Procedia, 2013. **37**(0): p. 7014-7020.
78. Clauwaert, P. and W. Verstraete, *Methanogenesis in membraneless microbial electrolysis cells.* Applied Microbiology and Biotechnology, 2009. **82**(5): p. 829-829-836.
79. Park, D.H., et al., *Microbial Utilization of Electrically Reduced Neutral Red as the Sole Electron Donor for Growth and Metabolite Production.* Applied and Environmental Microbiology, 1999. **65**(7): p. 2912-2917.
80. Hickey, R.F., J. Vanderwielen, and M.S. Switzenbaum, *The effects of organic toxicants on methane production and hydrogen gas levels during the anaerobic digestion of waste activated sludge.* Water Research, 1987. **21**(11): p. 1417-1427.

81. Nollet, L., D. Demeyer, and W. Verstraete, *Effect of 2-bromoethanesulfonic acid and Peptostreptococcus productus ATCC 35244 addition on stimulation of reductive acetogenesis in the ruminal ecosystem by selective inhibition of methanogenesis.* Applied and Environmental Microbiology, 1997. **63**(1): p. 194-200.
82. Oremland, R.S. and S. Polcin, *Methanogenesis and Sulfate Reduction: Competitive and Noncompetitive Substrates in Estuarine Sediments.* Applied and Environmental Microbiology, 1982. **44**(6): p. 1270-1276.
83. Scholten, J.C.M., R. Conrad, and A.J.M. Stams, *Effect of 2-bromo-ethane sulfonate, molybdate and chloroform on acetate consumption by methanogenic and sulfate-reducing populations in freshwater sediment.* FEMS Microbiology Ecology, 2000. **32**(1): p. 35-42.
84. Sparling, R. and L. Daniels, *The specificity of growth inhibition of methanogenic bacteria by bromoethanesulfonate.* Canadian Journal of Microbiology, 1987. **33**(12): p. 1132-1136.
85. Chidthaisong, A. and R. Conrad, *Specificity of chloroform, 2-bromoethanesulfonate and fluoroacetate to inhibit methanogenesis and other anaerobic processes in anoxic rice field soil.* Soil Biology and Biochemistry, 2000. **32**(7): p. 977-988.
86. Alperin, M.J. and W.S. Reeburgh, *Inhibition experiments on anaerobic methane oxidation.* Applied and Environmental Microbiology, 1985. **50**(4): p. 940-945.
87. Zinder, S.H., T. Anguish, and S.C. Cardwell, *Selective inhibition by 2-bromoethanesulfonate of methanogenesis from acetate in a thermophilic anaerobic digestor.* Applied and Environmental Microbiology, 1984. **47**(6): p. 1343-1345.
88. Agler, M.T., et al., *Waste to bioproduct conversion with undefined mixed cultures: the carboxylate platform.* Trends in Biotechnology, 2011. **29**(2): p. 70-78.
89. Bechthold, I., et al., *Succinic acid: a new platform chemical for biobased polymers from renewable resources.* Chemical engineering & technology, 2008. **31**(5): p. 647-654.
90. Ozadali, F., B. Glatz, and C. Glatz, *Fed-batch fermentation with and without on-line extraction for propionic and acetic acid production byPropionibacterium acidipropionici.* Applied Microbiology and Biotechnology, 1996. **44**(6): p. 710-716.
91. Andersen, S.J., et al., *Electrolytic Membrane Extraction Enables Production of Fine Chemicals from Biorefinery Sidestreams.* Environmental Science & Technology, 2014. **48**(12): p. 7135-7142.
92. Liu, C., et al., *Nanowire–Bacteria Hybrids for Unassisted Solar Carbon Dioxide Fixation to Value-Added Chemicals.* Nano Letters, 2015.
93. Kundu, A., et al., *An overview of cathode material and catalysts suitable for generating hydrogen in microbial electrolysis cell.* International Journal of Hydrogen Energy, 2013. **38**(4): p. 1745-1757.
94. Call, D.F., M.D. Merrill, and B.E. Logan, *High Surface Area Stainless Steel Brushes as Cathodes in Microbial Electrolysis Cells.* Environmental Science & Technology, 2009. **43**(6): p. 2179-2183.
95. Selembo, P.A., M.D. Merrill, and B.E. Logan, *The use of stainless steel and nickel alloys as low-cost cathodes in microbial electrolysis cells.* Journal of Power Sources, 2009. **190**(2): p. 271-278.
96. Lojou, E., *Hydrogenases as catalysts for fuel cells: Strategies for efficient immobilization at electrode interfaces.* Electrochimica Acta, 2011. **56**(28): p. 10385-10397.
97. Lojou, É. and P. Bianco, *Electrocatalytic Reactions at Hydrogenase-Modified Electrodes and Their Applications to Biosensors: From the Isolated Enzymes to the Whole Cells.* Electroanalysis, 2004. **16**(13-14): p. 1093-1100.
98. Vignais, P.M., B. Billoud, and J. Meyer, *Classification and phylogeny of hydrogenases.* FEMS Microbiology Reviews, 2001. **25**(4): p. 455-501.
99. Vincent, K.A., A. Parkin, and F.A. Armstrong, *Investigating and Exploiting the Electrocatalytic Properties of Hydrogenases.* Chemical Reviews, 2007. **107**(10): p. 4366-4413.
100. Morozov, S.V., et al., *Bioelectrocatalytic hydrogen production by hydrogenase electrodes.* International Journal of Hydrogen Energy, 2002. **27**(11–12): p. 1501-1505.
101. Pershad, H.R., et al., *Catalytic Electron Transport in Chromatium vinosum [NiFe]-Hydrogenase: Application of Voltammetry in Detecting Redox-Active Centers and Establishing That Hydrogen Oxidation Is Very Fast Even at Potentials Close to the Reversible H+/H2 Value†.* Biochemistry, 1999. **38**(28): p. 8992-8999.
102. Lojou, E., et al., *Hydrogenase Activity Control at Desulfovibrio vulgaris Cell-Coated Carbon Electrodes: Biochemical and Chemical Factors Influencing the Mediated Bioelectrocatalysis.* Electroanalysis, 2002. **14**(13): p. 913-922.
103. Tatsumi, H., et al., *Electrochemical Study of Reversible Hydrogenase Reaction of Desulfovibrio vulgaris Cells with Methyl Viologen as an Electron Carrier.* Analytical Chemistry, 1999. **71**(9): p. 1753-1759.
104. Rozendal, R.A., et al., *Hydrogen production with a microbial biocathode.* Environmental Science and Technology, 2008. **42**(2): p. 629-634.
105. Call, D. and B.E. Logan, *Hydrogen Production in a Single Chamber Microbial Electrolysis Cell Lacking a Membrane.* Environmental Science & Technology, 2008. **42**(9): p. 3401-3406.

106. Chae, K.-J., et al., *Biohydrogen production via biocatalyzed electrolysis in acetate-fed bioelectrochemical cells and microbial community analysis.* International Journal of Hydrogen Energy, 2008. **33**(19): p. 5184-5192.
107. Jeremiasse, A.W., et al., *Acetate enhances startup of a H2-producing microbial biocathode.* Biotechnology and Bioengineering, 2012. **109**(3): p. 657-664.
108. Geelhoed, J.S. and A.J.M. Stams, *Electricity-Assisted Biological Hydrogen Production from Acetate by Geobacter sulfurreducens.* Environmental Science & Technology, 2010. **45**(2): p. 815-820.
109. Krieg, T., et al., *Reactor concepts for bioelectrochemical syntheses and energy conversion.* Trends in Biotechnology, 2014. **32**(12): p. 645-655.
110. Brown, R.K., et al., *Evaluating the effects of scaling up on the performance of bioelectrochemical systems using a technical scale microbial electrolysis cell.* Bioresource Technology, 2014. **163**(0): p. 206-213.
111. Escapa, A., et al., *Estimating microbial electrolysis cell (MEC) investment costs in wastewater treatment plants: Case study.* International Journal of Hydrogen Energy, 2012. **37**(24): p. 18641-18653.
112. Escapa, A., et al., *Scaling-up of membraneless microbial electrolysis cells (MECs) for domestic wastewater treatment: Bottlenecks and limitations.* Bioresource Technology, 2015. **180**(0): p. 72-78.
113. Lovley, D.R., *The microbe electric: conversion of organic matter to electricity.* Current Opinion in Biotechnology, 2008. **19**(6): p. 564-571.
114. Dewan, A., H. Beyenal, and Z. Lewandowski, *Scaling up Microbial Fuel Cells.* Environmental Science & Technology, 2008. **42**(20): p. 7643-7648.
115. Wei, J., P. Liang, and X. Huang, *Recent progress in electrodes for microbial fuel cells.* Bioresource Technology, 2011. **102**(20): p. 9335-9344.
116. Zhou, M., et al., *An overview of electrode materials in microbial fuel cells.* Journal of Power Sources, 2011. **196**(10): p. 4427-4435.
117. Chen, S., et al., *Layered corrugated electrode macrostructures boost microbial bioelectrocatalysis.* Energy & Environmental Science, 2012. **5**(12): p. 9769-9772.
118. Chen, S., et al., *Electrospun and solution blown three-dimensional carbon fiber nonwovens for application as electrodes in microbial fuel cells.* Energy & Environmental Science, 2011. **4**(4): p. 1417-1421.
119. Xie, X., et al., *Carbon nanotube-coated macroporous sponge for microbial fuel cell electrodes.* Energy & Environmental Science, 2012. **5**(1): p. 5265-5270.
120. Chen, S., et al., *Reticulated carbon foam derived from a sponge-like natural product as a high-performance anode in microbial fuel cells.* Journal of Materials Chemistry, 2012. **22**(35): p. 18609-18613.
121. He, Z., et al., *Architecture Engineering of Hierarchically Porous Chitosan/Vacuum-Stripped Graphene Scaffold as Bioanode for High Performance Microbial Fuel Cell.* Nano Letters, 2012. **12**(9): p. 4738-4741.
122. Katuri, K., et al., *Three-dimensional microchanelled electrodes in flow-through configuration for bioanode formation and current generation.* Energy & Environmental Science, 2011. **4**(10): p. 4201-4210.
123. Xie, X., et al., *Three-Dimensional Carbon Nanotube−Textile Anode for High-Performance Microbial Fuel Cells.* Nano Letters, 2010. **11**(1): p. 291-296.
124. Flexer, V., et al., *Plasma treatment of electrodes significantly enhances the development of anodic electrochemically active biofilms.* Electrochimica Acta, 2013. **108**(0): p. 566-574.
125. Guo, K., *The effects of electrode surface modifications on biofilm formation and electron transfer in bioelectrochemical systems.* 2014.
126. Ploux, L., A. Ponche, and K. Anselme, *Bacteria/Material Interfaces: Role of the Material and Cell Wall Properties.* Journal of Adhesion Science and Technology, 2010. **24**(13-14): p. 2165-2201.
127. Guo, K., et al., *Effects of Surface Charge and Hydrophobicity on Anodic Biofilm Formation, Community Composition, and Current Generation in Bioelectrochemical Systems.* Environmental Science & Technology, 2013. **47**(13): p. 7563-7570.
128. Cerca, N., et al., *Quantitative analysis of adhesion and biofilm formation on hydrophilic and hydrophobic surfaces of clinical isolates of Staphylococcus epidermidis.* Research in microbiology, 2005. **156**(4): p. 506-514.
129. Guo, K., et al., *Spontaneous modification of carbon surface with neutral red from its diazonium salts for bioelectrochemical systems.* Biosensors and Bioelectronics, 2013. **47**: p. 184-189.
130. Park, D.H. and J.G. Zeikus, *Improved fuel cell and electrode designs for producing electricity from microbial degradation.* Biotechnology and Bioengineering, 2003. **81**(3): p. 348-355.
131. Popov, A.L., et al., *The effect of physico-chemically immobilized methylene blue and neutral red on the anode of microbial fuel cell.* Biotechnology and Bioprocess Engineering, 2012. **17**(2): p. 361-370.
132. Wang, K., Y. Liu, and S. Chen, *Improved microbial electrocatalysis with neutral red immobilized electrode.* Journal of Power Sources, 2011. **196**(1): p. 164-168.
133. Cheng, S. and B.E. Logan, *Ammonia treatment of carbon cloth anodes to enhance power generation of microbial fuel cells.* Electrochemistry Communications, 2007. **9**(3): p. 492-496.

134. Zhu, N., et al., *Improved performance of membrane free single-chamber air-cathode microbial fuel cells with nitric acid and ethylenediamine surface modified activated carbon fiber felt anodes.* Bioresource Technology, 2011. **102**(1): p. 422-426.
135. Scott, K., et al., *Application of Modified Carbon Anodes in Microbial Fuel Cells.* Process Safety and Environmental Protection, 2007. **85**(5): p. 481-488.
136. Jin, T., et al., *Coupling of anodic and cathodic modification for increased power generation in microbial fuel cells.* Journal of Power Sources, 2012. **219**(0): p. 358-363.
137. Zhou, M., et al., *Anode modification by electrochemical oxidation: A new practical method to improve the performance of microbial fuel cells.* Biochemical Engineering Journal, 2012. **60**(0): p. 151-155.
138. Higgins, S.R., et al., *Fabrication of macroporous chitosan scaffolds doped with carbon nanotubes and their characterization in microbial fuel cell operation.* Enzyme and Microbial Technology, 2011. **48**(6–7): p. 458-465.
139. Liu, X.-W., et al., *Carbon nanotube/chitosan nanocomposite as a biocompatible biocathode material to enhance the electricity generation of a microbial fuel cell.* Energy & Environmental Science, 2011. **4**(4): p. 1422-1427.
140. Qiao, Y., et al., *Carbon nanotube/polyaniline composite as anode material for microbial fuel cells.* Journal of Power Sources, 2007. **170**(1): p. 79-84.
141. Fan, Y., et al., *Nanoparticle decorated anodes for enhanced current generation in microbial electrochemical cells.* Biosensors and Bioelectronics, 2011. **26**(5): p. 1908-1912.
142. Jena, B.K., et al., *Bioanalytical applications of Au nanoparticles.* Recent Patents on Nanotechnology, 2010. **4**(1): p. 41-52.
143. Welch, C.M. and R.G. Compton, *The use of nanoparticles in electroanalysis: A review.* Analytical and Bioanalytical Chemistry, 2006. **384**(3): p. 601-619.
144. Flint, S.H., J.D. Brooks, and P.J. Bremer, *Properties of the stainless steel substrate, influencing the adhesion of thermo-resistant streptococci.* Journal of Food Engineering, 2000. **43**(4): p. 235-242.
145. Whitehead, K.A. and J. Verran, *The effect of surface topography on the retention of microorganisms.* Food and bioproducts processing, 2006. **84**(4): p. 253-259.
146. Flexer, V., et al., *The nanostructure of three-dimensional scaffolds enhances the current density of microbial bioelectrochemical systems.* Energy and Environmental Science, 2013. **6**(4): p. 1291-1298.
147. He, Z., S.D. Minteer, and L.T. Angenent, *Electricity Generation from Artificial Wastewater Using an Upflow Microbial Fuel Cell.* Environmental Science & Technology, 2005. **39**(14): p. 5262-5267.
148. Ringeisen, B.R., et al., *High Power Density from a Miniature Microbial Fuel Cell Using Shewanella oneidensis DSP10.* Environmental Science & Technology, 2006. **40**(8): p. 2629-2634.
149. Franks, A.E., et al., *Novel strategy for three-dimensional real-time imaging of microbial fuel cell communities: monitoring the inhibitory effects of proton accumulation within the anode biofilm.* Energy & Environmental Science, 2009. **2**(1): p. 113-119.
150. Friedrich, J.M., et al., *Reticulated vitreous carbon as an electrode material.* Journal of Electroanalytical Chemistry, 2004. **561**(SUPPL. 1): p. 203-217.
151. Walcarius, A., et al., *Nanomaterials for bio-functionalized electrodes: recent trends.* Journal of Materials Chemistry B, 2013. **1**(38): p. 4878-4908.
152. Gutierrez, M.C., et al., *Biocompatible MWCNT scaffolds for immobilization and proliferation of E. coli.* Journal of Materials Chemistry, 2007. **17**(29): p. 2992-2995.
153. Mink, J.E., et al., *Vertically Grown Multiwalled Carbon Nanotube Anode and Nickel Silicide Integrated High Performance Microsized (1.25 μL) Microbial Fuel Cell.* Nano Letters, 2012. **12**(2): p. 791-795.
154. Xie, X., et al., *Nano-structured textiles as high-performance aqueous cathodes for microbial fuel cells.* Energy & Environmental Science, 2011. **4**(4): p. 1293-1297.
155. Chen, J., et al., *Direct growth of flexible carbon nanotube electrodes.* Advanced Materials, 2008. **20**(3): p. 566-570.
156. Ketep, S.F., et al., *Stainless steel foam increases the current produced by microbial bioanodes in bioelectrochemical systems.* Energy & Environmental Science, 2014. **7**(5): p. 1633-1637.
157. Freguia, S., et al., *Sequential anode–cathode configuration improves cathodic oxygen reduction and effluent quality of microbial fuel cells.* Water Research, 2008. **42**(6-7): p. 1387-1396.
158. An, S.J., et al., *Thin Film Fabrication and Simultaneous Anodic Reduction of Deposited Graphene Oxide Platelets by Electrophoretic Deposition.* The Journal of Physical Chemistry Letters, 2010. **1**(8): p. 1259-1263.
159. Friedrich, J.M., et al., *Reticulated vitreous carbon as an electrode material.* Journal of Electroanalytical Chemistry, 2004. **561**(0): p. 203-217.

160. Gapes, D. and J. Keller, *Analysis of biological wastewater treatment processes using multicomponent gas phase mass balancing.* Biotechnology and Bioengineering, 2001. **76**(4): p. 361-375.
161. Pratt, S., et al., *Development of a novel titration and off-gas analysis (TOGA) sensor for study of biological processes in wastewater treatment systems.* Biotechnology and Bioengineering, 2002. **81**(4): p. 482-495.
162. Manz, W., et al., *In situ identification of bacteria in drinking water and adjoining biofilms by hybridization with 16S and 23S rRNA-directed fluorescent oligonucleotide probes.* Applied and Environmental Microbiology, 1993. **59**(7): p. 2293-2298.
163. Amann, R.I., et al., *Combination of 16S rRNA-targeted oligonucleotide probes with flow cytometry for analyzing mixed microbial populations.* Applied and Environmental Microbiology, 1990. **56**(6): p. 1919-1925.
164. Daims, H., et al., *The domain-specific probe EUB338 is insufficient for the detection of all bacteria: Development and evaluation of a more comprehensive probe set.* Systematic and Applied Microbiology, 1999. **22**(3): p. 434-444.
165. Manz, W., et al., *Phylogenetic oligodeoxynucleotide probes for the major subclasses of proteobacteria: Problems and solutions.* Systematic and Applied Microbiology, 1992. **15**(4): p. 593-600.
166. Engelbrektson, A., et al., *Experimental factors affecting PCR-based estimates of microbial species richness and evenness.* ISME Journal, 2010. **4**(5): p. 642-647.
167. Engelbrektson, A., et al., *Experimental factors affecting PCR-based estimates of microbial species richness and evenness.* The ISME journal, 2010. **4**(5): p. 642-647.
168. Bolger, A.M., M. Lohse, and B. Usadel, *Trimmomatic: a flexible trimmer for Illumina sequence data.* Bioinformatics, 2014: p. btu170.
169. Masella, A.P., et al., *PANDAseq: paired-end assembler for illumina sequences.* BMC bioinformatics, 2012. **13**(1): p. 31.
170. Pearson, W.R., et al., *Comparison of DNA sequences with protein sequences.* Genomics, 1997. **46**(1): p. 24-36.
171. Caporaso, J.G., et al., *QIIME allows analysis of high-throughput community sequencing data.* Nature methods, 2010. **7**(5): p. 335-336.
172. Edgar, R.C., *Search and clustering orders of magnitude faster than BLAST.* Bioinformatics, 2010. **26**(19): p. 2460-2461.
173. McDonald, D., et al., *An improved Greengenes taxonomy with explicit ranks for ecological and evolutionary analyses of bacteria and archaea.* The ISME journal, 2012. **6**(3): p. 610-618.
174. Werner, J.J., et al., *Impact of training sets on classification of high-throughput bacterial 16s rRNA gene surveys.* The ISME journal, 2012. **6**(1): p. 94-103.
175. Way, C., *Standard methods for the examination of water and wastewater.* 2012.
176. Croese, E., et al., *Analysis of the microbial community of the biocathode of a hydrogen-producing microbial electrolysis cell.* Applied Microbiology and Biotechnology, 2011. **92**(5): p. 1083-1093.
177. Call, D.F., R.C. Wagner, and B.E. Logan, *Hydrogen Production by Geobacter Species and a Mixed Consortium in a Microbial Electrolysis Cell.* Applied and Environmental Microbiology, 2009. **75**(24): p. 7579-7587.
178. Kim, J.R., et al., *Electricity generation and microbial community analysis of alcohol powered microbial fuel cells.* Bioresource Technology, 2007. **98**(13): p. 2568-2577.
179. Yates, M.D., et al., *Convergent development of anodic bacterial communities in microbial fuel cells.* ISME Journal, 2012. **6**(11): p. 2002-2013.
180. Dolfing, J., et al., *Syntrophic Growth on Formate: a New Microbial Niche in Anoxic Environments.* Applied and Environmental Microbiology, 2008. **74**(19): p. 6126-6131.
181. Hedderich, R., *Energy-Converting [NiFe] Hydrogenases from Archaea and Extremophiles: Ancestors of Complex I.* Journal of Bioenergetics and Biomembranes, 2004. **36**(1): p. 65-75.
182. Stams, A.J.M. and C.M. Plugge, *Electron transfer in syntrophic communities of anaerobic bacteria and archaea.* Nature Reviews Microbiology, 2009. **7**(8): p. 568-577.
183. Geelhoed, J.S., H.V.M. Hamelers, and A.J.M. Stams, *Electricity-mediated biological hydrogen production.* Current Opinion in Microbiology, 2010. **13**(3): p. 307-315.
184. Butt, J.N., M. Filipiak, and W.R. Hagen, *Direct Electrochemistry of Megasphaera Elsdenii Iron Hydrogenase.* European Journal of Biochemistry, 1997. **245**(1): p. 116-122.
185. Woolerton, T.W. and K.A. Vincent, *Oxidation of dilute H2 and H2/O2 mixtures by hydrogenases and Pt.* Electrochimica Acta, 2009. **54**(22): p. 5011-5017.
186. Jeremiasse, A.W., H.V.M. Hamelers, and C.J.N. Buisman, *Microbial electrolysis cell with a microbial biocathode.* Bioelectrochemistry, 2010. **78**(1): p. 39-43.
187. Stephanopoulos, G., A.A. Aristidou, and J. Nielsen, *Metabolic engineering: principles and methodologies*. 1998: Academic press.

188. Zeng, R.J., et al., *Metabolic Model for Glycogen-Accumulating Organisms in Anaerobic/Aerobic Activated Sludge Systems.* Biotechnology and Bioengineering, 2003 a. **81**(1): p. 92-105.
189. Zeng, R.J., Z. Yuan, and J. Keller, *Enrichment of denitrifying glycogen-accumulating organisms in anaerobic/anoxic activated sludge system.* Biotechnology and Bioengineering, 2003 b. **81**(4): p. 397-404.
190. Villano, M., et al., *Electrochemically assisted methane production in a biofilm reactor.* Journal of Power Sources, 2011. **196**(22): p. 9467-9472.
191. Hu, H., Y. Fan, and H. Liu, *Hydrogen production using single-chamber membrane-free microbial electrolysis cells.* Water Research, 2008. **42**(15): p. 4172-4178.
192. Lee, H.-S., et al., *Fate of H2 in an Upflow Single-Chamber Microbial Electrolysis Cell Using a Metal-Catalyst-Free Cathode.* Environmental Science & Technology, 2009. **43**(20): p. 7971-7976.
193. Tartakovsky, B., et al., *High rate membrane-less microbial electrolysis cell for continuous hydrogen production.* International Journal of Hydrogen Energy, 2009. **34**(2): p. 672-677.
194. Nevin, K.P., et al., *Anode biofilm transcriptomics reveals outer surface components essential for high density current production in Geobacter sulfurreducens fuel cells.* PLoS ONE, 2009. **4**(5): p. 1-11.
195. Boccaccini, A.R. and I. Zhitomirsky, *Application of electrophoretic and electrolytic deposition techniques in ceramics processing.* Current Opinion in Solid State and Materials Science, 2002. **6**(3): p. 251-260.
196. Sarkar, P. and P.S. Nicholson, *Electrophoretic deposition (EPD): Mechanisms, kinetics, and application to ceramics.* Journal of the American Ceramic Society, 1996. **79**(8): p. 1987-2002.
197. Van Der Biest, O.O. and L.J. Vandeperre, *Electrophoretic deposition of materials*. Annual Review of Materials Science. Vol. 29. 1999. 327-352.
198. Choi, W.B., et al., *Electrophoresis deposition of carbon nanotubes for triode-type field emission display.* Applied Physics Letters, 2001. **78**(11): p. 1547-1549.
199. Chung, J., et al., *Toward Large-Scale Integration of Carbon Nanotubes.* Langmuir, 2004. **20**(8): p. 3011-3017.
200. Du, C. and N. Pan, *Supercapacitors using carbon nanotubes films by electrophoretic deposition.* Journal of Power Sources, 2006. **160**(2 SPEC. ISS.): p. 1487-1494.
201. Niu, C., et al., *High power electrochemical capacitors based on carbon nanotube electrodes.* Applied Physics Letters, 1997. **70**(11): p. 1480-1482.
202. Thomas, B.J.C., et al., *Electrophoretic deposition of carbon nanotubes on metallic surfaces*, in *Key Engineering Materials*. 2006. p. 141-146.
203. Ammam, M., *Electrophoretic deposition under modulated electric fields: a review.* RSC Advances, 2012. **2**(20): p. 7633-7646.
204. Higashi, M., K. Domen, and R. Abe, *Fabrication of efficient TaON and Ta3N5 photoanodes for water splitting under visible light irradiation.* Energy & Environmental Science, 2011. **4**(10): p. 4138-4147.
205. Thomas, B.J.C., A.R. Boccaccini, and M.S.P. Shaffer, *Multi-walled carbon nanotube coatings using Electrophoretic Deposition (EPD).* Journal of the American Ceramic Society, 2005. **88**(4): p. 980-982.
206. Boccaccini, A.R., et al., *Electrophoretic deposition of carbon nanotubes.* Carbon, 2006. **44**(15): p. 3149-3160.
207. Harnisch, F., et al., *Electrifying White Biotechnology: Engineering and Economic Potential of Electricity-Driven Bio-Production.* ChemSusChem, 2014: p. n/a-n/a.
208. Demler, M. and D. Weuster-Botz, *Reaction engineering analysis of hydrogenotrophic production of acetic acid by Acetobacterium woodii.* Biotechnology and Bioengineering, 2011. **108**(2): p. 470-474.
209. Xie, X., et al., *Graphene-sponges as high-performance low-cost anodes for microbial fuel cells.* Energy & Environmental Science, 2012. **5**(5): p. 6862-6866.
210. Freguia, S., et al., *Electron and Carbon Balances in Microbial Fuel Cells Reveal Temporary Bacterial Storage Behavior During Electricity Generation.* Environmental Science & Technology, 2007. **41**(8): p. 2915-2921.
211. Sleat, R., R.A. Mah, and R. Robinson, *Acetoanaerobium noterae gen. nov., sp. nov.: an Anaerobic Bacterium That Forms Acetate from H2 and CO2.* International Journal of Systematic Bacteriology, 1985. **35**(1): p. 10-15.
212. WILLEMS, A., et al., *Hydrogenophaga, a New Genus of Hydrogen-Oxidizing Bacteria That Includes Hydrogenophaga flava comb. nov. (Formerly Pseudomonas flava), Hydrogenophaga palleronii (Formerly Pseudomonas palleronii), Hydrogenophaga pseudoflava (Formerly Pseudomonas pseudoflava and "Pseudomonas carboxydoflava"), and Hydrogenophaga taeniospiralis (Formerly Pseudomonas taeniospiralis).* International Journal of Systematic Bacteriology, 1989. **39**(3): p. 319-333.
213. Kimura, Z.-i. and S. Okabe, *Hydrogenophaga electricum sp. nov., isolated from anodic biofilms of an acetate-fed microbial fuel cell.* The Journal of General and Applied Microbiology, 2013. **59**(4): p. 261-266.
214. Kimura, Z.I. and S. Okabe, *Acetate oxidation by syntrophic association between Geobacter sulfurreducens and a hydrogen-utilizing exoelectrogen.* ISME Journal, 2013. **7**(8): p. 1472-1482.
215. Lai, C.-Y., et al., *Nitrate Shaped the Selenate-Reducing Microbial Community in a Hydrogen-Based Biofilm Reactor.* Environmental Science & Technology, 2014. **48**(6): p. 3395-3402.

216. Park, H., Y.-J. Choi, and D. Pak, *Autohydrogenotrophic Denitrifying Microbial Community in a Glass Beads Biofilm Reactor.* Biotechnology Letters, 2005. **27**(13): p. 949-953.
217. Oren, A., *The Family Natranaerobiaceae.* The Prokaryotes: Firmicutes and Tenericutes, 2014: p. 261-266.
218. Yu, J., *Bio-based products from solar energy and carbon dioxide.* Trends in Biotechnology, 2014. **32**(1): p. 5-10.
219. Kim, B.S., et al., *Production of poly(3-hydroxybutyric acid) by fed-batch culture of Alcaligenes eutrophus with glucose concentration control.* Biotechnology and Bioengineering, 1994. **43**(9): p. 892-898.
220. Tanaka, K., et al., *Production of poly(D-3-hydroxybutyrate) from CO2, H2, and O2 by high cell density autotrophic cultivation of Alcaligenes eutrophus.* Biotechnology and Bioengineering, 1995. **45**(3): p. 268-275.
221. Beverskog, B. and I. Puigdomenech, *Revised Pourbaix Diagrams for Copper at 25 to 300°C.* Journal of The Electrochemical Society, 1997. **144**(10): p. 3476-3483.
222. Ahmed, J., et al., *Self-assembly of copper nanoparticles (cubes, rods and spherical nanostructures): Significant role of morphology on hydrogen and oxygen evolution efficiencies.* Solid State Sciences, 2011. **13**(5): p. 855-861.
223. Aslan, E., I.H. Patir, and M. Ersoz, *Cu Nanoparticles Electrodeposited at Liquid–Liquid Interfaces: A Highly Efficient Catalyst for the Hydrogen Evolution Reaction.* Chemistry – A European Journal, 2015: p. n/a-n/a.
224. Kumar, B., et al., *Enhanced hydrogen/oxygen evolution and stability of nanocrystalline (4-6 nm) copper particles.* Journal of Materials Chemistry A, 2013. **1**(15): p. 4728-4735.
225. Văduva, C.C., et al., *Catalytic enhancement of hydrogen evolution reaction on copper in the presence of benzylamine.* International Journal of Hydrogen Energy, 2011. **36**(12): p. 6994-7001.
226. Khodashenas, B. and H.R. Ghorbani, *Synthesis of copper nanoparticles: An overview of the various methods.* Korean Journal of Chemical Engineering, 2014. **31**(7): p. 1105-1109.
227. Ramanathan, R., et al., *Aqueous phase synthesis of copper nanoparticles: a link between heavy metal resistance and nanoparticle synthesis ability in bacterial systems.* Nanoscale, 2013. **5**(6): p. 2300-2306.
228. Rubilar, O., et al., *Biogenic nanoparticles: copper, copper oxides, copper sulphides, complex copper nanostructures and their applications.* Biotechnology Letters, 2013. **35**(9): p. 1365-1375.
229. Saif Hasan, S., et al., *Bacterial synthesis of copper/copper oxide nanoparticles.* Journal of nanoscience and nanotechnology, 2008. **8**(6): p. 3191-3196.
230. Salvadori, M.R., et al., *Intracellular biosynthesis and removal of copper nanoparticles by dead biomass of yeast isolated from the wastewater of a mine in the Brazilian Amazonia.* PLoS ONE, 2014. **9**(1): p. e87968.
231. Shantkriti, S. and P. Rani, *Biological synthesis of Copper nanoparticles using Pseudomonas fluorescens.* Int. J. Curr. Microbiol. App. Sci, 2014. **3**(9): p. 374-383.
232. Manuel, M.F., et al., *Hydrogen production in a microbial electrolysis cell with nickel-based gas diffusion cathodes.* Journal of Power Sources, 2010. **195**(17): p. 5514-5519.
233. Janicek, A., Y. Fan, and H. Liu, *Design of microbial fuel cells for practical application: a review and analysis of scale-up studies.* Biofuels, 2014. **5**(1): p. 79-92.
234. Rozendal, R.A., et al., *Towards practical implementation of bioelectrochemical wastewater treatment.* Trends in Biotechnology, 2008. **26**(8): p. 450-459.
235. www.alibaba.com, 2015.
236. Aresta, M. and A. Dibenedetto, *Utilisation of CO2 as a chemical feedstock: opportunities and challenges.* Dalton Transactions, 2007(28): p. 2975-2992.
237. Agency, U.S.E.P., *eGRID.* 2000.
238. Roth, J.F., *PRODUCTION OF ACETIC ACID.* Platinum Metals Review, 1975. **10**(1): p. 12-14.
239. Grande, C.A., *Biogas upgrading by pressure swing adsorption*. 2011: INTECH Open Access Publisher.
240. Van Eerten-Jansen, M.C.A.A., et al., *Microbial community analysis of a methane-producing biocathode in a bioelectrochemical system.* Archaea, 2013. **2013**.
241. Watanabe, R. and G. Robinson, *The European union emissions trading scheme (EU ETS).* Climate Policy, 2005. **5**(1): p. 10-14.
242. Carmo, M., et al., *A comprehensive review on PEM water electrolysis.* international journal of hydrogen energy, 2013. **38**(12): p. 4901-4934.
243. Lu, X. and C. Zhao, *Electrodeposition of hierarchically structured three-dimensional nickel–iron electrodes for efficient oxygen evolution at high current densities.* Nat Commun, 2015. **6**.
244. Dincă, M., Y. Surendranath, and D.G. Nocera, *Nickel-borate oxygen-evolving catalyst that functions under benign conditions.* Proceedings of the National Academy of Sciences, 2010. **107**(23): p. 10337-10341.
245. Esswein, A.J., et al., *Size-dependent activity of Co3O4 nanoparticle anodes for alkaline water electrolysis.* The Journal of Physical Chemistry C, 2009. **113**(33): p. 15068-15072.

246. Kanan, M.W. and D.G. Nocera, *In situ formation of an oxygen-evolving catalyst in neutral water containing phosphate and Co2+.* Science, 2008. **321**(5892): p. 1072-1075.
247. Leong, J.X., et al., *Ion exchange membranes as separators in microbial fuel cells for bioenergy conversion: A comprehensive review.* Renewable and Sustainable Energy Reviews, 2013. **28**(0): p. 575-587.